DOKTORI (PhD) ÉRTEKEZÉS

BALATON MIKLÓS GÁBOR

DOI: 10.18136/PE.2014.561

Pannon Egyetem

2014.

Pannon Egyetem
Vegyészmérnöki és Folyamatmérnöki Intézet
Folyamatmérnöki Intézeti Tanszék

Szakaszos gyártócella szimulációja és irányítása

DOKTORI (PhD) ÉRTEKEZÉS

Balaton Miklós Gábor

Konzulensek
Dr. Nagy Lajos, egyetemi docens
Dr. Szeifert Ferenc, egyetemi docens

Vegyészmérnöki- és Anyagtudományok Doktori Iskola
Pannon Egyetem
2014.

University of Pannonia
Institute of Chemical and Process Engineering
Institutional Department of Process Engineering

Simulation and control of batch processing units

PhD Thesis

Miklós Gábor Balaton

Supervisors
Lajos Nagy PhD, associate professor
Ferenc Szeifert PhD, associate professor

Doctoral School in Chemical Engineering and Material Sciences
University of Pannonia
2014.

SZAKASZOS GYÁRTÓCELLA SZIMULÁCIÓJA ÉS IRÁNYÍTÁSA

Értekezés doktori (PhD) fokozat elnyerése érdekében a
Pannon Egyetem Vegyészmérnöki- és Anyagtudományok
Doktori Iskolájához tartozóan.

Írta:
Balaton Miklós Gábor

Témavezetők: Dr. Nagy Lajos

Elfogadásra javaslom (igen / nem) …….
(aláírás)

Dr. Szeifert Ferenc

Elfogadásra javaslom (igen / nem) …….
(aláírás)

A jelölt a doktori szigorlaton .....%-ot ért el,

Az értekezést bírálóként elfogadásra javaslom:

Bíráló neve: …..... …..... igen /nem

…….
(aláírás)

Bíráló neve: …..... …..... igen /nem

…….
(aláírás)

A jelölt az értekezés nyilvános vitáján ….....%-ot ért el.

Veszprém, …….
a Bíráló Bizottság elnöke

A doktori (PhD) oklevél minősítése….....

……
Az EDHT elnöke

Köszönetnyilvánítás

Köszönetet mondani mindig egy felemelő érzés, mivel mindig valami lezárásaként tesszük, ami egyben egy új dolog kezdetét is jelenti. Nagy viszontagságok között készült el ez a dolgozat, többször is elbizonytalanodtam, hogy egyáltalán be tudom-e fejezni. Nagy áldozatokat kellett hoznom azért, hogy eljuthassak a köszönetnyilvánítás megírásáig, azaz a dolgozat befejezéséig. De végül sikerült.

Elsősorban témavezetőimnek Dr. Nagy Lajosnak és Dr. Szeifert Ferencnek szeretném megköszönni a rengeteg segítséget és szakmai útmutatást, amit kaptam tőlük az évek során. Valamint szeretném megköszönni a tanszéki kollektívának a számos építő jellegű szakmai vitát, amelyek nélkül nem tudtam volna ennyit fejlődni. A PhD-s csapatnak (Rádi György, Szabó László, Dobos László, Tóth Richárd, Egedy Attila, Bárkányi Ágnes, Borsos Ákos, Király András) is szeretném megköszönni a számos közös utazást és élményt, ami a PhD-s évek alatt megéltünk együtt.

Szeretném még megköszönni családomnak is az egyetemi éveim alatti támogatást, ami nélkül nem készült volna el ez a dolgozat sem.

Nagyon sok köszönettel tartozom minden barátomnak, ismerősömnek, aki tartotta bennem az erőt a nehéz időkben is, és bíztatott a dolgozat befejezésére.

Kivonat

A gyógyszer-, élelmiszer-, polimer- és finomvegyszer iparban a szakaszos (rugalmas) technológiai rendszerek gyakori eleme a keverővel ellátott fűthető-hűthető autokláv, amelyben a reagáltatáson túlmenően számos más művelet (desztilláció, extrakció, kristályosítás, stb.) is elvégezhető. Szakaszos reaktorok esetén a legfontosabb szabályozott jellemző a hőmérséklet, mivel a magas hozzáadott értékű termékek előállítása során a hőmérséklet elégtelen szabályozása esetén nem megfelelő termék keletkezhet, amely jelentős anyagi veszteséget okozhat, illetve a gyógyszeriparban felhasználhatatlan komponenst eredményezhet. Miközben az irányítási rendszer gyakorlati megvalósítását jól segíti az S88 szabvány, a különböző szintű irányítási algoritmusok kialakítását számos elméleti és gépészeti probléma nehezíti. A kutatás elsősorban a magasabb hierarchia szintek összetettebb irányítási problémáira irányul mint például az optimalizálás, ütemezés, stb. Ugyanakkor, az alacsonyabb szintek megoldatlan irányítástechnikai problémái a felsőbb hierarchia szintű megoldások realizálását lehetetlenné teszik.

Vegyipari gyártó rendszerek gépészeti tervezését és kivitelezését, különösen a mérőműszerek elhelyezését és beépítését gyakran a praktikusság és az esztétikai elvek vezérlik. Klasszikus szabályozó algoritmusok esetén (PID szabályozó) ezek a hibák viszonylag ritkán okozzák a szabályozás elégtelenségét, viszont magasabb szintű illetve modell alapú szabályozási algoritmusok esetén jelentős akadályokat jelenthetnek. A mérőműszerek és technológiai rendszer részletes vizsgálata és beállítása nélkül magasabb szintű irányítási algoritmusokkal nem érhető el jobb minőségű szabályozás (vagy csak rosszabb) a klasszikus megoldásokhoz képest.

Az iparban egyre inkább terjednek a három hőmérsékleti szinttel rendelkező hűtő-fűtő rendszerek, amelyek alkalmazása energiafelhasználás szempontból előnyös, viszont a köpeny hőmérsékletszabályozását bonyolultabbá teszik. A középső hőmérsékleti szint mind hűtő mind fűtő szerepet is betölthet a reaktor állapotától függően. A klasszikus két üzemmódot kezelő split-range megoldások nem alkalmasak ezen rendszer kezelésére, ezért új megoldás kidolgozására volt szükség.

Olyan split-range algoritmusok kerültek kidolgozásra, amelyek a klasszikus hőmérsékletszabályozási megoldásokhoz (PID) kapcsolhatóak. Az első split-range algoritmus során a köpeny és a belépő közeg hőmérsékletét figyelembe véve, valamint a köpeny recirkulációt mint keverő modellt felhasználva, a szabályozó különböző előre definiált karakterisztikák között vált, amivel elérhető, hogy a szabályozott objektum erősítésének előjele ne változzon. Ezzel megvalósítható, hogy mindhárom közeget megfelelően tudja kihasználni a köpenyhőmérséklet szabályozó.

A kutatás során egy második split-range algoritmus kifejlesztésére is sor került. A szerző különböző köpenymodellek felhasználásával két modell alapú split-range megoldást is kidolgozott. Mindkét megoldás esetén nemcsak a szabályozott objektum erősítésének előjele, hanem annak értéke is változatlanul tartható. A különböző split-range algoritmusok vizsgálata nem csak MATLAB környezetben végzett szimulációval történt, hanem a tanszéki laboratóriumban található félüzemi szakaszos gyártócellán végzett mérésekkel is.

Abstract

The heatable, coolable, and stirred autoclaves are common parts of batch technologies in the pharmaceutical-, food-, polymer- and fine-chemical industries. Beyond performing chemical reactions also several other operations can be performed in autoclaves as well (distillation, extraction, crystallization, etc.). In the case of batch reactors, the most important controlled variable is temperature, since in the manufacturing processes of high-value-added products, insufficient control might produce off-grade product that can cause significant financial loss, and in the pharmaceutical industry result in an unusable batch. While the practical implementation of the control system is supported by the S88 standard, the implementation of control algorithms at different hierarchy levels are encumbered by theoretical and mechanical problems. The scientific research mainly focuses on the more complex problems of the higher hierarchy levels, e.g., optimization, scheduling, etc. However, the unsolved control problems of the lower hierarchy levels make the realization of the higher hierarchy solutions impossible.

In the mechanical design and construction of chemical manufacturing systems, especially the location and implementation of measuring instruments are commonly driven by aesthetic and practical principles. When using classical control solutions (e.g., Proportional Integral Derivative (PID) controller), these errors rarely cause poor control performance; however, in the case of advanced and model-based control algorithms the control performance is significantly affected. Without the detailed analysis and tuning of the measuring instruments and the technology itself, better control performance cannot be achieved (or even worse) compared to classical control solutions.

In the industry an increasing number of heating/cooling systems utilizing three different temperature levels can be found, which are advantageous from an economic point of view; however, it makes the control more complicated. The medium temperature level can also be a heating or cooling media depending on the actual state of the reactor. The classical split-range solution handling two modes of operation are not suitable for such systems, thus the development of new solutions is needed.

Such split-range algorithms were developed that can be used together with classical control solutions (PID). The first split-range algorithm considers the actual temperature value of the jacket and the inlet thermal fluid. According to the mixer-based model describing the jacket recirculation loop, it switches between a set of predefined splitting characteristics with the aim to avoid the change in the sign of the gain of the controlled object. With this solution the adequate utilization of all three temperature levels by the jacket-temperature controller can be achieved.

A second split-range algorithm was also developed. To describe the jacket recirculation loop two modelling considerations were used. In both solutions not only the sign of the gain of the controlled object, but also the value of the gain is kept unchanged. The testing and analysis of the different split-range solutions were not only performed by MATLAB based simulation but also by test measurements on the pilot batch processing system, located in the laboratory of the department.

Auszug

Die beheizbare, kühlbare, mit einem Mixer ausgestattete Autoklaven sind häufig Bestandteil von Batch-Technologien in der Pharma-, Lebensmittel-, Polymer- und Feinchemie Industrie, in der zusätzlich zur Reaktion eine Anzahl von anderen Operationen (Destillation, Extraktion, Kristallisation, usw.) durchgeführt werden kann. Im Falle von Batch-Reaktoren der wichtigste Regelparameter ist die Reaktionstemperatur, weil die unzureichende Temperaturregelung in der Produktion vom Hochwertprodukten zu nicht-konformen Produkte führen kann, die Folge können erheblichen finanziellen Verlusten als auch Entstehung von nutzlosen Komponenten in der Pharmaindustrie sein. Während die praktische Implementierung des Produktionskontrollsystems vom S88-Standard unterstützt wird die Entwicklung von Regelalgorithmen wird von einen Reihe von theoretischen und mechanischen Problemen erschwert. Die Forschung konzentriert sich vor allem auf komplex Kontrollprobleme von höheren hierarchischen Ebenen wie Optimierung, Planung, usw., jedoch die ungelösten Probleme auf unteren Ebenen machen es unmöglich die höheren hierarchieebenen Lösungen zu realisieren.

Die mechanische Planung und Konstruktion von Produktionssystemen der chemischen Industrie insbesondere die Platzierung und Installation der Messinstrumente werden oft von Praktischer Anwendbarkeit und ästhetischen Prinzipien angetrieben. Im Falle der klassischen Regelalgorithmen (PID) diese Fehler verursachen nur selten unzureichende Regelung, jedoch sie können erhebliche Hindernisse bei übergeordneten und modellbasierten Regelalgorithmen darstellen. Im Vergleich zur klassischen Lösungen ohne eingehende Prüfung und Einstellung der Messinstrumente und Technology mit übergeordneten Regelalgorithmen kann keine bessere (oder noch schlimmer) Regelung erreicht werden.

Kühl-und Heizsysteme mit drei Temperaturstufen werden sich immer mehr in der Industrie verbreiten, was in Hinblick auf den Energieverbrauch vorteilhaft ist, jedoch die Manteltemperaturregelung kompliziert. Die mittlere Temperatur Ebene kann je nach dem Status des Reaktors sowohl Heiz- als auch Kühlmedien sein. Dieses System kann von klassischen zwei-mode Split-Range Lösungen nicht behandelt werden, deshalb war es notwendig neue Lösungen zu entwickeln.

Solche Split-Range Algorithmen wurden entwickelt, die mit den klassischen Temperaturregelung-Lösungen (PID) zu gleicher Zeit verwendbar sind. Es wird im ersten Split-Range Algorithmus unter Berücksichtigung der Mantel- und Zulauftemperatur sowie unter Einsatz vom Mantel Rezirkulation als Mischmodell zwischen verschiedene vordefinierte Regelcharakteristik umgeschaltet, um zu vermeiden, dass das Vorzeichen der Verstärkung des geregelten Objekts sich ändert. Mit dieser Lösung kann die angemessene Nutzung aller drei Temperaturen Ebene vom Manteltemperaturregler erreicht werden.

Während der Forschung wurde auch ein zweiter Split-Range Algorithmus entwickelt. Um die Mantel Rezirkulierungsschleife zu beschreiben zwei modellbasierte Split-Range Lösungen wurden ausgearbeitet. In beiden Lösungen wird nicht nur das Vorzeichen der Verstärkung des geregelten Objekts sondern auch ihr Zeitwert unverändert beibehalten. Der Test der verschiedenen Split-Range-Algorithmen wurde nicht nur in MATLAB simuliert sondern auch mit Messungen auf der Pilot Serienproduktion-Zelle im Lehrstuhllabor durchgeführt.

Table of Contents

List of Figures

List of Tables

Abbreviations

AD	Analogue digital
APC	Advanced Process Control
BFGS	Broyden–Fletcher–Goldfarb–Shanno
BRIEW	Batch Reactor Identification Excel Workbook
CAPD	Computer-Aided process design
CAPE	Computer-aided process engineering
CMA-ES	Covariant Matrix Adaptation Evolutionary Strategy
CSTR	Continuously Stirred Tank Reactor
DCS	Distributed Control System
DP	Decentralized Peripherals
EA	Evolutionary Algorithm
HMI	Human Machine Interface
HTL	High Temperature Level
ID	Inner Diameter
IP	Internet Protocol
LTL	Low Temperature Level
MIMO	Multiple Input, Multiple Output
MPC	Model Predictive Controller
MS	Microsoft
MSE	Mean Square Error
MTL	Medium Temperature Level
NLP	Nonlinear programming
OLE	Object Linking and Embedding
OPC	OLE for Process Control
OTS	Operator Training Simulator
PC	Personal Computer
PI	Proportional Integral
PID	Proportional Integral Derivative
PLC	Programmable Logic Controller
PWM	Pulse Width Modulation
QP	Quadratic Programming
SISO	Single Input, Single Output

SQP	Sequential Quadratic Programming
S-R	Split-range
TCP	Transmission Control Protocol
TEMA	Tubular Exchanger Manufacturers Association

Notations

a	Parameter
b	Parameter
c	Parameter
C_m	Cost of measurement or simulation test [HUF]
c_{mf}	Energy specific price of the temperature level [HUF/MJ]
C_{op}	Operating cost of the temperature level [HUF/h]
c_p^{feed1}	Specific heat of feed 1 [J/kgK]
c_p^{feed2}	Specific heat of feed 2 [J/kgK]
c_p^{mf}	Specific heat of the thermal fluid [J/kgK]
c_p^{rm}	Specific heat of the reaction mixture [J/kgK]
d	Parameter
e	Parameter
E_{cons}	Utility consumption [kW] or [m^3/h]
$e_{T_{jacket}^{in}}$	Control error for the temperature control of the jacket (slave loop) [°C]
$e_{T_{reactor}}$	Control error for the temperature control of the reactor (master loop) [°C]
f	Parameter
F_{feed1}	Feed 1 flow rate [m^3/h]
F_{feed2}	Feed 2 flow rate [m^3/h]
F_{max}	Maximal flow rate value of the introduced thermal fluid to the jacket recirculation loop [m^3/h]
F_{mf}	Flow rate of the introduced thermal fluid to the jacket recirculation loop [m^3/h]
F_{rec}	Flow rate of the jacket recirculation loop [m^3/h]
F_{rs}	Flow rate of the reaction simulation loop [m^3/h]

g	Parameter
K	Gain
K_C	Gain of the PID controller
K_{c_o}	Gain of the composite controlled object
K_{sl_o}	Gain of the slave loop object
m	Mode of operation {low, medium, high}
$m_{reactor}$	Reactor load [kg]
MV_{heater}	Manipulated variable of the electric heater [%]
$n_{agitator}$	Agitator speed [1/s]
P	Vector containing the possible steady-state temperatures
$\dot{Q}_{cal}$	Calibrating heat flow [W]
$\dot{Q}_{eff}$	Effective heating/cooling capacity [MJ/h]
$\dot{Q}_{feed1}$	Heat flow caused by feed 1 [W]
$\dot{Q}_{feed2}$	Heat flow caused by feed 2 [W]
$\dot{Q}_{heat\,loss}$	Heat loss heat flow of the reactor [W]
$\dot{Q}_{reaction}$	Reaction heat flow [W]
$\dot{Q}_{rs}$	Simulated reaction heat flow [W]
$\dot{Q}_{wall}$	Heat flow through the wall of the reactor [W]
s_m	Slope of the curve depending on the mode of operation
ΔT	Temperature difference [°C]
$T_{after\ heater}$	Temperature measured after the electric heater in the reaction heat simulation loop [°C]
$T_{ambient}$	Ambient temperature [°C]
TC_m	Master temperature controller
TC_{sl}	Slave temperature controller

T_{feed1}	Feed 1 temperature [°C]
T_{feed2}	Feed 2 temperature [°C]
T_{in}^{high}	Temperature of the introduced thermal fluid to the jacket recirculation loop in the case of the high temperature level [°C]
T_{in}^{low}	Temperature of the introduced thermal fluid to the jacket recirculation loop in the case of the low temperature level [°C]
T_{in}^{m}	Temperature of the introduced thermal fluid to the jacket recirculation loop [°C] $\{T_{in}^{low}, T_{in}^{med}, T_{in}^{high}\}$
T_{in}^{med}	Temperature of the introduced thermal fluid to the jacket recirculation loop in the case of the medium temperature level [°C]
$\overline{T}_{jacket}$	Average jacket temperature [°C]
T_{jacket}^{in}	Jacket inlet temperature [°C]
$T_{jacket}^{in\_max}$	Maximal possible steady-state jacket inlet temperature [°C]
$T_{jacket}^{in\_min}$	Minimal possible steady-state jacket inlet temperature [°C]
T_{jacket}^{out}	Measured jacket outlet temperature; jacket temperature in the case of lumped jacket model [°C]
T_{mf}^{high}	Temperature of the high temperature level monofluid thermoblock loop [°C]
T_{mf}^{low}	Temperature of the low temperature level monofluid thermoblock loop [°C]
T_{mf}^{med}	Temperature of the medium temperature level monofluid thermoblock loop [°C]
$T_{reactor}$	Reactor temperature [°C]
T_{s}^{high}	The maximal jacket inlet temperature in the case of the high temperature level [°C]
T_{s}^{low}	The maximal jacket inlet temperature in the case of the low temperature level [°C]
T_{s}^{m}	The maximal jacket inlet temperature at different modes of operation $\{T_{s}^{low}, T_{s}^{med}, T_{s}^{high}\}$ [°C]
T_{s}^{med}	The maximal jacket inlet temperature in the case of the medium temperature level [°C]
u_{slave}	Output of the slave loop controller [%]
u_{valve}	Set-point for the actuator of the control valve [%]
u_{slave}^{T}	Slave loop controller output on temperature basis [°C]
$UA_{heat\,loss}$	The product of the heat transfer coefficient and the heat transfer area for the heat loss [W/K]
UA_{wall}	The product of the heat transfer coefficient and the heat transfer area for the reactor wall [W/K]

V_{jacket}	Jacket volume [m^3]
$w_{T_{jacket}^{in}}$	Set-point for the temperature control of the jacket (slave loop) [°C]
$w_{T_{reactor}}$	Set-point for the temperature control of the reactor (master loop) [°C]
$y_{T_{jacket}^{in}}$	Controlled object output for the temperature control of the jacket (slave loop) [°C]
$y_{T_{reactor}}$	Controlled object output for the temperature control of the reactor (master loop) [°C]

Greek letters

α	Tuning parameter of the exponential filter
ρ_{rm}	Density of the reaction mixture [kg/m^3]
ρ_{feed1}	Feed 1 density [kg/m^3]
ρ_{feed2}	Feed 2 density [kg/m^3]
ρ_{mf}	Density of the thermal fluid [kg/m^3]
τ	Time constant [s]
τ_C	Tuning parameter in the case of the direct synthesis method [s]
τ_D	Derivative time constant of the PID controller [s]
τ_H	Dead time [s]
τ_I	Integrating time of the PID controller [s]
τ_r	Inverting time constant [s]

1. Review of scientific background

From an operating point of view the industrial production systems can be separated into the following two extremes [1]:

Commodity plants: These plants are custom-designed to produce large amounts of a small number of products. Usually the margins for the products from commodity plants are small; thus, the plants must be designed and operated with the highest possible efficiency. Energy costs are the issues with the highest impact in these kinds of plants.

In continuous technologies, a stationary one-to-one relationship exists between the mechanically fixed equipment network and the manufacturing process. This results in a temporal and spatial uniformity, which means that the continuous stream of raw materials are processed in a custom-designed processing plant with several different operations through conversion or separation equipment without interruption in time. These kinds of plants usually operate near some predefined operating points, and the time range of normal operating state (usually steady state) is larger by orders of magnitude then start-up or shutdown periods. Summary data such as hourly averages, daily averages, can mainly describe a continuous process.

Specialty plants: These plants are capable of producing from small to high amounts of a variety of products. Such plants are common in the manufacturing processes of high-value-added products such as in the fine-chemical, pharmaceutical, food, and polymer industries. As in the case of specialty plants the margins are usually high; therefore, high-value-added products are produced, thus issues such as energy costs are important but not as much as it is in commodity plants. As the production amounts might be relatively small, it is not economically feasible to dedicate processing equipment to manufacture only one product. This is one of the reasons why batch processing is utilized; hence, several products can be manufactured with the same process equipment. The key issue in such plants is to manufacture consistently each product in accordance with its specifications.

In batch systems, the connection of the recipe and the mechanically fixed equipment network represents a many-to-many relationship; this provides the flexibility of the batch systems, which leads to a multiproduct and multipurpose plant. The technological operations follow one another in a predefined order. The equipment is designed not only for producing a single product but also the same technological unit has to be capable for different operations or to produce different products. Consequently, significantly different conditions might be necessary, which demand high flexibility from both equipment and control. In these technologies the labour demand is significantly higher compared with continuous technologies. The intervention and manipulation of the operating staff is elemental in the operation. The technology is not operated near some predefined operating points but on an operating trajectory.

The process for making a given product is contained in the product recipe that is specific to the product. Such recipes normally state the following [2]:

- Raw material and amounts.
- Processing instructions: The order and conditions of different operations.

The above two categories represent the extremes in process configurations. The term semi-batch designates plants in which some processing is continuous but other processing is batch. Even processes that are considered to be continuous can have a modest amount of batch processing.

1.1. Batch processing units

In this chapter the main characteristics of batch production will be presented. The different jacket configurations commonly used in the industry for the heating/cooling purposes of the batch reactor will be described as well.

1.1.1. The characteristics of batch processing

The dominancy of batch-wise production usually originates from the laboratory level (R&D) and also influences pilot and plant scale production. Batch production can be characterized with diversity as well as with underdetermination and flexibility. The following characterisation describes the operation of batch reactors, related industrial problems, design, utilization of capacity, and production scheduling. [3]

Batch reactors are usually operated in the following ways:

- Batch operating mode: for slow and less exothermic chemical reactions
- Semi-batch operating mode: for fast and highly exothermic reactions
- The combination of the previous two, especially if a certain final concentration is required

The operating objectives are usually the following:

- Safety: The main risk is the runaway of the reactor caused by highly exothermic reaction.
- Product quality: Instead of high purity the goal is to reach the specified quality with low standard deviation. Reproducibility is highly important.
- Scale-up: Providing changes without pilot scale test.
- Productivity: The efficiency of the whole production should be considered instead of the individual steps.
- Flexibility: Accommodating to market demands.
- Economic efficiency: Can be described with operation time, costs, productivity, selectivity, etc.

From a process control point of view in batch production the following properties dominate:

- The change of dynamic properties in time
- Non-linearity: caused by chemical reactions and heat transfer
- Less-accurate models: caused by unknown reaction mechanisms
- Demand for special measurements: the measurement of individual components in the reaction mixture in time and space can be challenging or expensive. The measured physical quantities have wide ranges that can cause measurement inaccuracies.
- Operating between limits: the optimal operation is commonly the transition between limits.
- Frequent disturbances: mainly operating error, measurement failure, mixing problems etc. The reaction heat can be considered as a constantly changing load-type disturbance.
- Irreversible behaviour: during the production of a batch only a few correction possibilities are available.
- Limited correcting interventions: towards the end of the reaction the possibility of correcting interventions are highly limited.
- The recurrence of production: the information of the previous batch can be used for the actual one (run-to-run optimization).
- Time consuming processes: scheduling is essential. Calculations with high computational requirements can be performed (online optimisation)

In the pharmaceutical, fine-chemical, and food industries as well as in several technologies of the polymer industry [4], the high-value-added products are manufactured mainly in batch processing units, where the batch or fed-batch reactor is the main unit of the process. Due to the complexity of the reaction mixture and the difficulty of performing online composition measurements, control of the batch reactors is essentially treated as a temperature control problem [5]. The difficulties that arise in the temperature control of batch reactors are mainly caused by the discontinuous nature of operating modes and the multiple operations of the reactors. The controller has to work properly in the case of drastically changing, ramped, and constant set-points during the different modes of operation.

The temperature of the reaction mixture is usually controlled by heat exchange through the wall of the reactor with a heat-transfer fluid flowing inside the jacket surrounding the reactor. Therefore, the control performance mainly depends on the heating/cooling system associated with the reactor.

1.1.2. Different jacket configurations

The different jacket configurations applied in the industry can be separated according to the following considerations [6]:

- Single pass or recirculating flow
- Direct or indirect heating/cooling
- Mono- or multifluid

In the following paragraphs the different common jacket configurations will be described according to previous considerations.

Several different configurations of heating/cooling systems are cited in the literature and can be basically separated into two types: multifluid (90 percent of industrial applications [7]) and monofluid systems [6]. The multifluid systems are widely used in the industry, where water or brine (or alcohol solution) is used for cooling, and steam or hot water is used for heating purposes. During the temperature control, besides determining the adequate mode of operation and the flow rate of the heat transfer fluid, the changeover of fluid also has to be realised (usually an air purge is applied in the jacket), which results in discontinuities in the operation.

Several different types of jacket configurations can be found in the literature and in the industry that can contain indirect or direct heating/cooling, jacket recirculation loop, or single pass flow through [6]. The jacket configuration with a jacket recirculation loop and with direct heating/cooling is widely used in the industry both in the case of multi- and monofluid systems. Using systems with a jacket recirculation loop is advantageous because a high heat transfer coefficient can be achieved compared to the single pass configuration; local overheating/overcooling also can be avoided and the temperature gradient in the jacket can be reduced.

Multifluid systems typically dominate batch technologies; monofluid systems are not yet widely used, and only a few installations can be found in the industry. The slight industrial experience and academic research also make the spreading of monofluid systems more difficult. However, due to the potentials and advantages of monofluid systems (wide temperature range, lower maintenance cost, faster and smoother changes in the mode of operation, fast operation), they are becoming more widely used in industrial applications [8]. This move can be supported by more intensive academic research. Using a medium temperature level with low energy consumption (e.g., a temperature level controlled by cooling water) can reduce the usage of the heat-transfer fluids on the boundaries of the temperature range of the thermoblock. Thus, the energy consumption of the thermoblock can be reduced. However, this needs a jacket temperature controller that best utilizes the medium temperature level. Consequently, this research focuses on the development of such a controller.

Direct jacket heating/cooling without recirculation

One of the simplest possible jacket configurations can be seen in Figure 1.1, which is a single pass, multifluid, and direct heating/cooling system. It is mainly used for manually controlled reactors. The temperature control of the reactor is achieved by the control of the flow rate of the fluid entering directly into the

jacket. The achievable operating range is between -20 – 180 °C, which can be produced by steam heating and a cooling media like the mixture of water and ethylene-glycol.

This system has a quick response time that can result in unwanted effects. For example in the case of heating with steam, hot spots can develop, which can cause the formation of undesired side products and also heat shock of the reactor wall can occur. Similar effects can occur in cooling mode, when cool spots can develop that might cause the reaction mixture to crystallize on the wall of the reactor, degrading the heat transfer and causing unwanted effects in the reaction mixture. During the control of the reactor temperature, the flow rate of the heating/cooling media changes, also causing the Reynolds number to change in the jacket. At low Reynolds numbers the heat transfer coefficient significantly decreases causing the heat transfer to be inefficient. Low flow rates also increase the fouling effect.

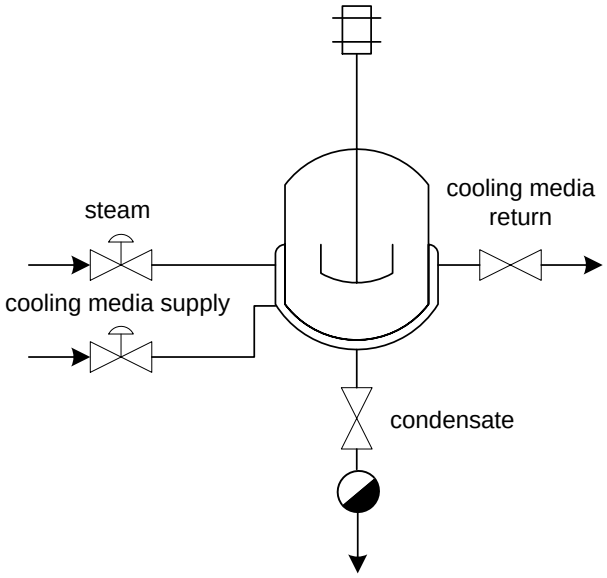

Figure 1.1: Direct heating/cooling without recirculation

Jacket configurations with recirculation

To avoid the previously described disadvantages of the single pass jacket configuration it is more preferred in the industry to implement a jacket recirculation loop. This solution provides constant, high flow rate in the jacket that ensures a high Reynolds number and also a high heat transfer coefficient. The hot and cool spots can be also avoided. According to the mode of heating/cooling direct and indirect heating/cooling can be separated.

Direct heating and direct cooling jacket configuration

In this configuration the heating/cooling media enters directly into the jacket recirculation loop. The temperature of the heating/cooling media is quasi constant as it is controlled before entering the recirculation loop. Beside the previously mentioned advantages in contrast with the single pass solution, this configuration has a quick response time compared with the hereinafter described indirect solutions. The reason of the quick response time is the lack of any heat

exchangers between the heating/cooling media and the jacket recirculation that might make the heat transfer slower.

The configuration in Figure 1.2 is a multifluid, direct system with jacket recirculation. If the cooling media is water, depending on the pressure of the system the available temperature range is 5 – 180 °C. This jacket configuration with jacket ejector and recirculation was developed by Ciba-Geigy AG. The lower limit of the temperature range can be extended by using the mixture of water and ethyl-alcohol. The automation of the system is quite complicated as the changeover between the heating and cooling media can cause unwanted effects especially if controlling exothermic reactions. The heating/cooling media can contaminate each other during changeovers, which can also cause corrosion problems.

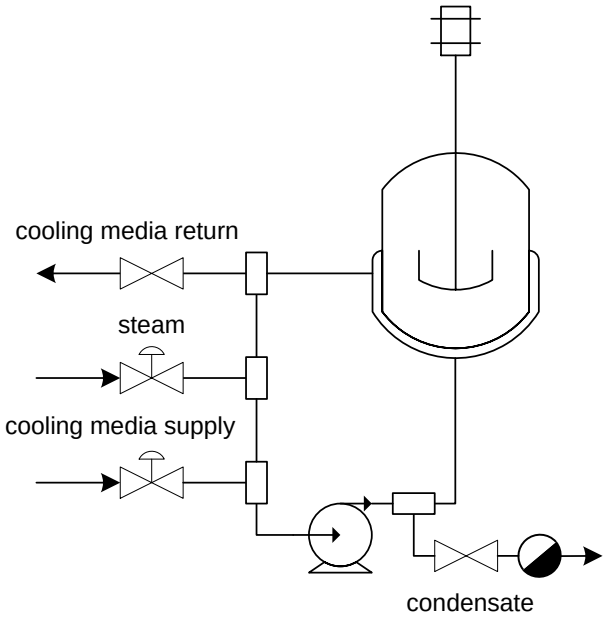

Figure 1.2: Direct heating and direct cooling jacket configuration

Indirect heating and direct cooling jacket configuration

The temperature range of the indirect heating and direct cooling configuration is -20 – 180 °C. This type of configuration can be seen in Figure 1.3, where the heating is commonly achieved through a plate heat exchanger and the cooling is performed by the direct injection of the cooling media into the jacket recirculation loop. The changeover of the different modes can be performed smoothly using a split-range controller. Due to the direct cooling media injection the response time of the system is significantly lower in cooling mode. The advantage of this system is that there is no contamination due to changeover of the different fluids as only one type of fluid can enter the jacket recirculation loop. To achieve high temperature range, the cooling media must satisfy the requirements for heating purposes as well, since it transfers the heat from the heating heat exchanger to the reactor.

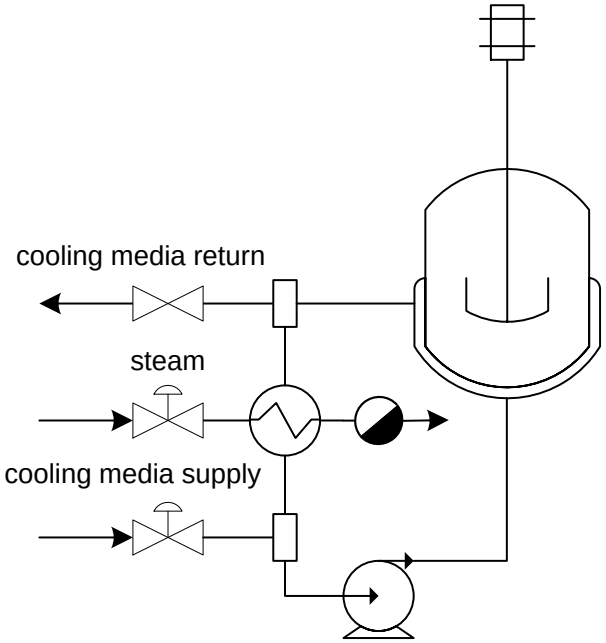

Figure 1.3: Indirect heating and direct cooling jacket configuration

Indirect heating and indirect cooling jacket configuration

The indirect heating and cooling of the jacket recirculation loop can be achieved by two heat exchangers, one for the heating and one for the cooling media. This type of configuration can be seen in Figure 1.4. The advantage of this solution is that a cheaper cooling media can be used as it does not need to satisfy strict specifications compared with the previously described configurations. Also a centralized heat block service can be used for this solution providing the heating/cooling media for several reactors. The temperature range of this solution can reach -20 – 220 °C.

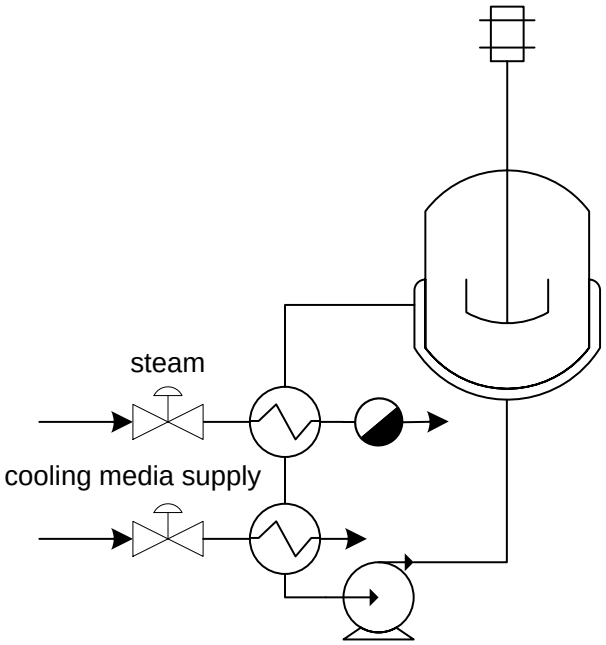

Figure 1.4: Indirect heating and indirect cooling jacket configuration

Monofluid heating/cooling configuration

A quite different solution from the previously described ones is the monofluid heating/cooling configuration. It is a direct heating/cooling solution that contains a jacket recirculation loop, and the media used for heating and cooling has the same material quality. The reason behind the naming convention monofluid is the quality of the used media, which differs only in its temperature and not in quality. The production of the different temperature levels can be achieved by an independent thermoblock, which might provide heating/cooling media for several reactors. The widest temperature range available in this configuration is -30 – 360 °C that highly depends on the quality of the selected thermal fluid and the operating pressure of the monofluid thermoblock [8], [9].

Beside the advantages of the jacket recirculation loop configuration this solution has also a low response time due to the direct thermal fluid injection. Also there is no changeover mechanism needed as the qualities of the different temperature levels are identical. This configuration has all the advantages of the direct and indirect solutions.

In a monofluid system where two temperature levels are used, the temperature control of the reactor can be achieved with a classical split-range controller. This control solution has several references in the literature and is identical to the ones used for the multifluid systems. However, more than two temperature levels can be used for the control of the reactor (also in the case of multifluid systems [10]) that require complex control mechanisms or advanced control solutions. Only a few publications are cited in the literature about systems containing a monofluid thermoblock with three different temperature levels and the split-range control for this configuration [7], [11], [12].

A solution connected with a monofluid thermoblock that contains three different temperature levels can be seen in Figure 1.5. The disadvantage of this configuration is that it needs the coordinated operation of the ball valves and the control valve to adjust the temperature of the jacket. The classical split-range solution is not capable to handle three temperature levels. However, this solution is more economic compared with solutions containing the two temperature levels. It is more economical to use a medium temperature level that has a low operation cost than using only the more expensive temperature levels at the boundaries of the available temperature range. For example if the medium temperature level is controlled by water, which has a significantly lower operating cost than refrigeration, it is more preferable to use this level for the cooling of the reactor if temperature of the reactor is higher than the medium temperature level. However, to gain the advantages of this three-levelled system a control solution is also necessary that can utilize all the three levels.

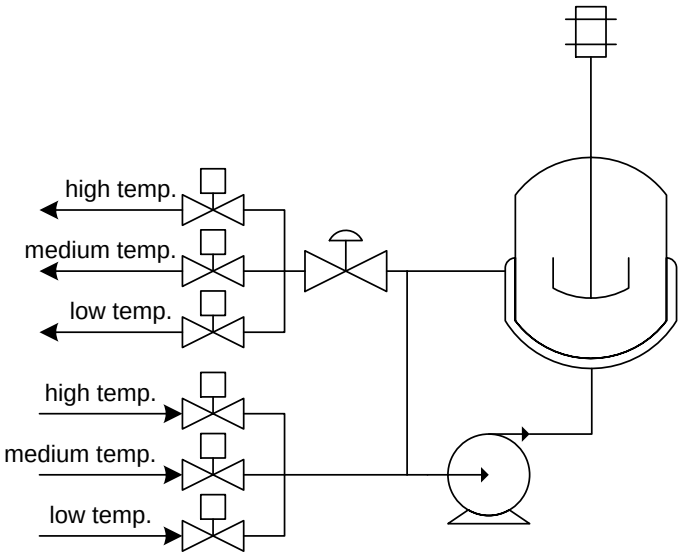

Figure 1.5: Monofluid heating/cooling jacket configuration

1.2. Chemical Process Simulation

Establishing a chemical engineer pool with high base knowledge significantly depends on the quality of the education in the universities. Instruction of chemical engineers should reflect the challenges they face in industry. Young chemical engineers are required to assimilate rapidly new and emerging technologies to react in a flexible manner to shorter production cycles and strict quality regulations [13]. A chemical engineer must have a working knowledge of mathematics, chemical and physical technology, biotechnology, materials science, and economics, which are the building blocks used by the design engineer. Additionally, competence in the use of the simulation tools allows process evaluation directly on an economic basis; controllability and operability can be assessed using dynamic simulation, while some simulation software automatically provides information to help determine the environmental impact of each of the product streams. Process simulators are an indivisible part of modern practice in chemical process design. Young engineers should have a well-structured knowledge relying on fundamentals as well as to have the balance between heuristic and computer-aided algorithmic approaches. The education should also reflect the current state-of-the-art in the integration of process design and process control. [14], [15], [16].

Chemical engineers have to make critical process and equipment design decisions in all stages of the process life-cycle, from the concept to the troubleshooting of an existing production process. In every stage different types of models with different information content are necessary to be used. This may range from the calculation of mass and energy balances of a single unit operation to the simulation and optimization of large flowsheets.

During the stages of a process life-cycle different models with different information content might be necessary [17]. In the phase of Research and Development (R&D) the form and accuracy of the models can first be quite simple, however it can become more detailed as work proceeds. The focus in R&D is in the phenomena: phase equilibrium, physical properties, chemical kinetics, mass and heat transfer, etc. For systematic approach the system is broken

into its components. The phenomena-related models then are combined into process unit models.

In the next step of the process life-cycle the conceptual design is performed. The optimal process structure and operating conditions are searched in this stage; the focus is on process synthesis and the full-scale plant. If the chemical components are well-known in the process, meaning usually that their properties and all related parameters can be found in databanks, models can be used to quickly check new process ideas. In distillation, design models are used to identify key and non-key components, the optimum distillation sequence, the number of ideal stages, feed stages, etc.

When a process reaches a step in its life-cycle where detailed engineering is applied, the focus is in technical solutions. Depending on the nature of the models, they can provide a description of how the system behaves in certain conditions, or they may be used to calculate detailed geometries of the equipment. When fine-tuned models are available the design of the new unit or process is easily optimized for yield or energy consumption.

The last phase in the life-cycle of the process is the operation stage. At this stage, models must include all relevant physical, chemical, and mechanical aspects. The model predictions are compared against actual plant measurements and tuned further to improve the accuracy of predictions. The focus at this stage is in guaranteeing optimal production. This is the stage where OTS (Operator Training Simulator) systems are applied. A detailed example can be found in the article of Zaldívar et al. [18], where the optimization of a batch reactor is achieved by using the simulator of the real process. Bradu et al. [19] describe the construction of an OTS system of a cryogenic plant that can be used for operator training, testing the control of the system, and plant optimization. Dynamic simulation has a very important role in such dynamic processes.

Today's process plants face all the real-world challenges to operational excellence; however, the stakes are much higher than ever before. The constantly changing nature of plants, and their internal and external environments, can threaten safe and profitable plant operations quickly. Uncontrolled upsets can cause start-up delays, production outages, severe equipment damage, and even catastrophic failures. The operational safety and excellence of the plant increasingly rely on well-trained, expert plant operators.

Dynamic Simulation and Operator Training Simulators have been available for a long time. However, over the last five years, improvements in technology (computers, software, and market understanding) have meant that the use of Dynamic Simulation and Operator Training Simulators has become a reality for many processes.

The primary OTS objectives are the following. The main objective is to keep the skilled workforce in spite of attrition by turnover or retirement, as it is one major prerequisite for a plant to operate safely and efficiently. The goal is to provide the plant operational staff with practical experience on how to operate complex plant process systems in various situations. Also an object of OTS systems is to assess the performance level of the trainees. [20]

High-tech automation is changing cognitive demands on operators, who are now required to:

- Supervise rather than directly monitor
- Make more cognitively complex decisions
- Deal with complex, mode-rich systems
- Increase need for cooperation and communication

An increasing number of chemical companies have recently decided to use OTS systems with the aim of training the operating staff on handling different plant failures, rarely used modes of operation, and measuring their skills. It is also an objective to support engineering tasks as well as testing new control methods and to perform safety tests without risk on the real system. [21], [22]

The main objectives of OTS use can be the following: [23]

- Practice procedures for plant start-up and shut-down situations
- Handling of utility system and process unit trips, turn-down, and other upsets
- Fault diagnosis, alarm handling, and corrective actions in case of process equipment malfunction during normal operation
- Practice steady-state operation
- Reduce start-up and shut-down times
- Increase safety
- Reduction in environmental concerns
- Increase unit up-time
- Increase operator awareness, skills, and readiness
- Assess operator competence

Optional functions of OTS systems:

- Testing and validation of operating procedures
- Testing and validation of control strategies and logic
- Debottlenecking
- Investigation of engineering solutions
- Sharing of incident and operating scenarios across shift teams
- Practicing energy efficient operation
- Understanding the operation of APCs
- APC limit handling and set-up

Computer-aided process design (CAPD) and simulation tools have been successfully used in chemical and oil industries since the early 1960s for the development and optimisation of integrated systems. Simulators used in these industries are designed to simulate continuous processes and their transient behaviour, mainly for process control purposes. Similar benefits can be achieved with the application of CAPD and simulation tools in other industries, such as

food processing, pharmaceutical, fine chemical, biochemical and polymer industries [24].

First principles process models play an important role in development, design, and control of chemical production processes. Currently two types of software tools are available for process modelling. The first category of advanced modelling tools is general-purpose equation-oriented environments, i.e. model editors. Process models are represented only by their mathematical system equations. For example MATLAB can be classified with this type. This is one of the reasons why MATLAB is preferred by academic researchers. This software provides only an advanced mathematical solver environment for mainly ordinary and differential equations; however only a few and mainly general purpose built-in models are available. The possibility to implement user-defined models opens a wide range of applicability; however it has its own programming language that needs to be learned in advance. MATLAB also has a quite large number of toolboxes that can be additionally purchased, which provide specialized models for the different fields of science. The most important information for chemical process simulation, the thermodynamic data of chemical compounds are not available in these types of simulators.

The second group offers modular software components for the solution of very specific simulation problems. These tools are highly specialized and do allow expansion to new situations only with limitations. However, most of these software provide a wide range of built-in models and a database containing thermodynamic data of the most frequently used chemical compounds. [25]

Process simulators for continuous processes have been used in the petrochemical industry since the early 1960s. From the available simulators, Aspen Plus (Aspen Technology, Inc.), ChemCAD (Chemstations, Inc.), HYSYS (Hyprotech, Ltd./AEA Engineering Software – now Aspen Technology, Inc.), UniSim Design (Honeywell International Inc.), Petro-SIM (KBC Advanced Technologies Plc.) and PRO/II (Simulation Sciences, Inc. – now Invensys Inc.) are the most widely used.

The time-dependent behaviour of batch processes makes the development of process simulators more challenging. The first process simulator expressly for batch processes called “Batches” was commercialised in the mid-1980s by Batch Process Technologies (West Lafayette, IN). All of the built-in models are dynamic and simulation involves the integration of differential equations over time. In the mid-1990s, Aspen Technology (Burlington, MA) introduced its recipe-driven simulation software called Batch Plus, which was mainly aimed at the pharmaceutical industry. Around the same time, Intelligen, Inc. (Scotch Plains, NJ) also introduced SuperPro Designer [26].

With the aim of performing detailed batch reactor simulation, commercially available products such as ProSim BatchReactor (ProSim SA) are also available. They provide detailed customisation of the reactor unit [27]. Identification (KinIdent), detailed simulation of chemical reactions (KinSim) and the simulation of autoclaves (AuSim) are also available in a software suit developed in the University of Pannonia [28].

In OTS applications, the entire plant is to be simulated; however, with the detailed reactor simulation software, the simulation of the auxiliary units might be

more difficult than using general purpose process simulators like UniSim Design. The most advantageous solution would be the connection of these software.

In this research, the process model of the batch processing unit is implemented in Honeywell's UniSim Design Suite, which is developed from HYSYS (Aspen Technology, Inc.) software. It offers steady-state and dynamic simulation, design, performance monitoring, optimisation, and business planning for the oil and gas production, gas processing, petroleum refining, and chemical industries [29]. Honeywell's UniSim Design simulation software was chosen for more detailed investigation and for use in building a batch processing unit. It is commercially available boxed software widely used in OTS applications. UniSim Design also has a high quality support for academic use.

UniSim Design uses lumped models for all of the unit operations, because the distributed parameter models require additional calculation capacity and time. The units with a given volume are divided into several sub-volumes, which are considered to be lumped. The reaction rate, temperature, and compositions are constant through each sub-volume, varying only with time. With this method, the entire volume is calculated like a distributed parameter model.

In dynamic mode, UniSim Design uses a pressure-flow solver that contains two basic equations. They define most of the pressure-flow network, and these equations only contain pressure and flow as variables. Resistance equations define flow between pressure hold-ups; volume balance equations define the material balance at pressure hold-ups [30].

"One Model, Many Uses": The single model concept enables the user to build one model of the process and migrate it through the various stages of the life-cycle. During the design stage, a model can be used for conceptual design, real process design, detailed engineering design, and finally, for operability studies. Once the asset has been built, the same model can be used for the improvement of operations, operator training, safety studies, and asset optimisation. In addition to delivering simulation capabilities that support the lifecycle, UniSim Design also serves as the platform for modelling across the entire range of the chemical and hydrocarbon processing industries. [17], [30].

One of the biggest limitations of flowsheeting simulators is that in the case of tank reactors, lumped models are generally used for the inner side of the reactor. However, inside the tank reactors found in the industry, the physical properties (especially temperature) have distribution. From the aspect of the heat transfer, lumped models are only valid if the reaction mixture is well mixed and a high inner wall heat transfer coefficient can be achieved. The other main disturbance is the effect of the reaction, which can change the viscosity, heat capacity, density, heat transfer coefficient, etc., of the reaction mixture in time. These effects can seriously affect the accuracy of these models.

1.3. Temperature control of batch reactors

In continuous technologies, a stationary one-to-one relationship exists between the mechanically fixed equipment network and the manufacturing process. This results in a temporal and spatial uniformity. Therefore, the model of the technology is mostly steady-state.

In case of batch systems, the connection of the recipe and the mechanically fixed equipment network represents a many-to-many relationship; this provides the flexibility of the batch systems: multiproduct and multipurpose plant.

The consequence of the discontinuous behaviour is that the significance of the setting and the shutdown transients are comparable with the "steady-state" operation. Thus, the qualitative requirements of the control are also to be extended to transient states. There is no steady-state operation in the traditional sense. Consequently, systems with variable parameters are to be handled, which sets special requirements for the controllers.

The difficulties that arise in the temperature control of batch reactors are mainly caused by the discontinuous nature of the operating modes and the multiple functions of the reactors. The controller has to work properly in case of drastically changing, ramped and constant set-points during the different modes of operations. A batch production in a batch reactor can be separated to the following phases [10]:

- Heating phase: Preheating of the reaction mixture to the desired temperature
- Reaction phase: The temperature is usually maintained constant
- Cooling phase: Cooling the reaction mixture to avoid by-product formation.

1.3.1. Classical control algorithms

In industrial applications, the temperature control of batch reactors is usually carried out with PID controllers in a cascade structure [31], [32]. Hence, the disturbances affecting the jacket can be eliminated and the constraints regarding the jacket can be defined. The cascade control of the reactor temperature can be seen in Figure 1.6. According to Author's experience, the quality of the slave control loop (jacket temperature control) fundamentally restricts the quality of complex control solutions; hence, the analysis of this loop is the focus of this research.

For the appropriate operation of the cascade controller, the inner (slave) loop has to be more dynamic (at least three or four times quicker) than the outer (master) loop, and both controllers have to be properly tuned. The controlled variable of the master loop is the temperature of the reactor, and the manipulated variable is the set point of the slave loop. The controlled object of the master loop can be described with a first-order plus dead time transfer function, which can be used in the PID design algorithms cited in the literature.

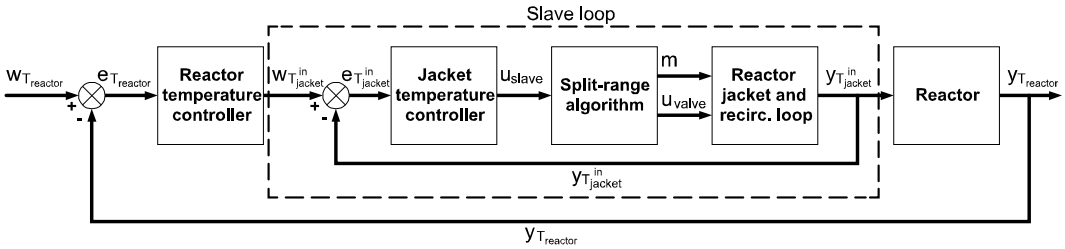

Figure 1.6. Cascade control of the reactor temperature

In the case of the jacket, usually two measurement points are available: the jacket inlet and outlet temperature. Thus, different possibilities exist for choosing the controlled variable: the jacket inlet, jacket outlet, and their average

temperature. The best choice for the controlled variable of the jacket temperature control is the jacket inlet temperature, because it results in simpler dynamics, and constraints related to the jacket can be simply handled. This configuration can be seen in Figure 1.7.

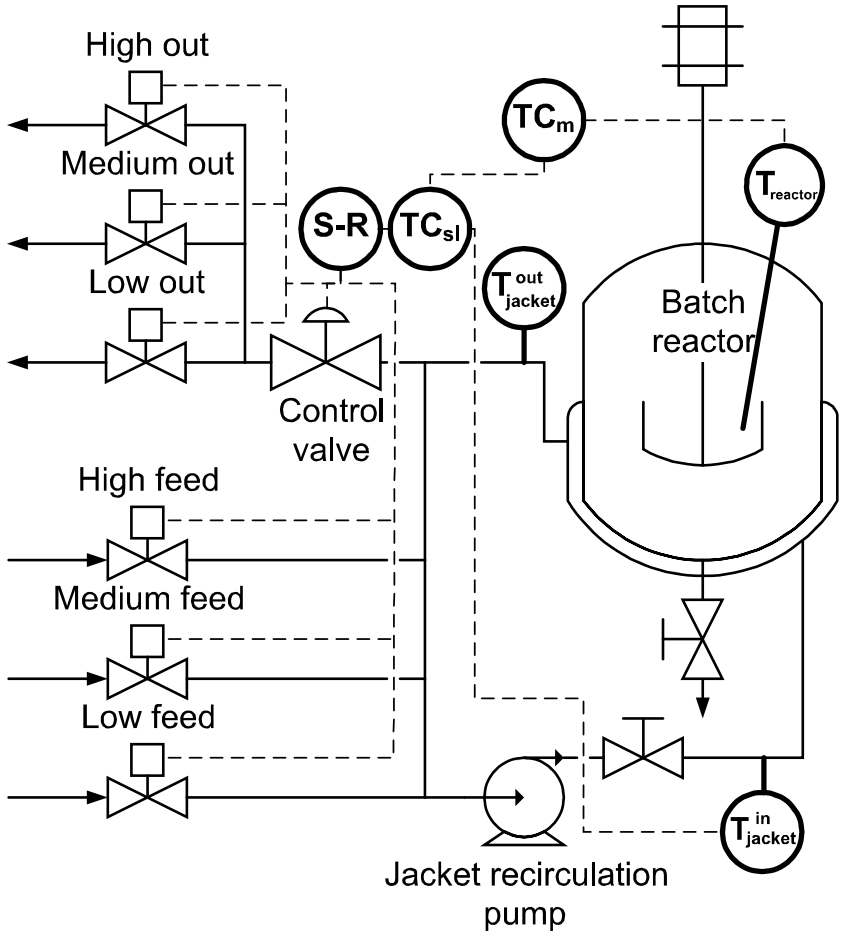

Figure 1.7. The temperature control configuration of the batch reactor

In industrial control engineering, a split-range controller is preferred in the slave loop of the cascade control to operate two actuators with different effects at the same time. Mostly proportional splitting is used in the case of two modes of operation [33]. In terms of the PID controller, the two actuators can be considered one manipulated variable and the split-range algorithm as part of the controlled system. The main role of the split-range algorithm is to ensure that the sign of the gain of the controlled object remains unchanged. For this purpose, the split-range algorithm in Figure 1.8 is the simplest and most widely used solution in the industry.

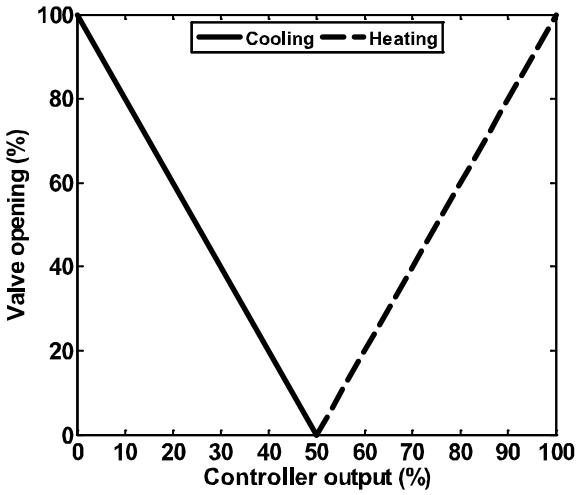

Figure 1.8. Split-range algorithm for two modes of operation

Using three different temperature levels as modes of operation, the control becomes more complicated; keeping the sign of the gain of the controlled object unchanged is not as trivial as in the case of two modes of operation. However, due to the aforementioned advantages of systems with three different temperature levels, the research efforts on controllers handling such systems are becoming more important. In the literature, only a few papers can be found that deal with controllers used in systems with three different modes of operation, and most of them present advanced control solutions such as model predictive control. In the article of Madár et al., the importance of the slave loop is emphasized; however the test system differs from the one used in this research, as it contained a multifluid thermoblock [10]. In another important related article Bouhenchir et al. used a test system that contained a monofluid thermoblock; however their research focused on the control of the reactor, and the slave loop was not analysed [34].

The aim of this research is to find a solution that uses the model of the controlled object and can be implemented in the conventional cascade temperature control structure of batch reactors (using PID controllers) without restructuring or using advanced control solutions.

1.3.2. Advanced control algorithms

Despite the approximately three decades of industrial use and the intense academic research to support the spreading of model-based (mainly predictive) control solutions, PI and PID feedback controllers remain the typical control solution in the chemical industry [35]. The main reason of the dominance is the role of the PID controllers in the classical control techniques, the major position in education, the wide availability even with its modifications in industrial DCS systems, and last but not least the efficiency of their use. Additionally, other model-based techniques can result in a PID controller depending on the model of the controlled object; therefore they can be implemented as a PID controller [36]. The varying operating points cause the efficiency of PID controllers to decrease, which can be enhanced by adaptive techniques. From the basic adaptive techniques in control theory, in the case of batch technologies gain scheduling is most commonly used. As the recipe is known, the different PID parameters for the varying operating parameters can be implemented in advance and modified in

function of time or some other process variable. In this case the adaption is actually a feedforward that does not affect the stability of the entire controlled system. Stability only depends on the specific PID parameters [37]. Not only predefined PID parameters can be used; in addition, fuzzy or neural network techniques can be applied to calculate the actual desired PID parameters using some of the process variables [38], [39].

Both in continuous and batch technologies, self-tuning adaptive controllers are widely used [31], [40], [41]. According to this technique the online identification of a presumed process model (mainly first order plus dead time transfer function) is performed. The varying of the operating point can be taken into consideration by a forgetting factor. With the results of the online identification the process model is corrected, and this can be used in a PID parameter designing technique to determine the actual parameters.

The so-called Dual-Mode controllers and their different modifications are also widely used in the industry. This type of controller minimizes the control error by using maximal heating capacity during the heating-up period until the temperature of the reactor reaches the set-point. Only thereafter is the controller turned on, which is responsible for controlling the temperature of the reactor (mainly PID controller). [42], [43]

Despite the previously mentioned industrial trends the research of model-based control algorithms are important in such objects where PID controllers are less efficient. The development of model-based algorithms is becoming more intense due to the growing possibilities in computer technology, and the model of the technology is turning to be the focus of the analysis.

The main problem of feedback controllers is the time delay between the actual manipulation and the resulting effect on the output of the process, especially in the case of high order systems with dead time. A slight change on the output can cause significant manipulation that can eventually lead to instability. The mathematical model of the object can provide the opportunity to predict the entire effect of a manipulation on the output and to determine the optimal manipulation. The Model Predictive Controller (MPC) determines the future discrete-time manipulations by solving an optimal control problem on the prediction horizon. The first future manipulation is realized, and the calculations are performed at every sample time. Solving the optimal control problem is actually the producing of the process model inverse [34]. MPC controllers have been used in industrial applications for more than three decades, and an increasing number of products are available to support the design of MPC controllers (e.g., Honeywell's Profit Design Studio [44]). These controllers can be used efficiently mainly for MIMO (Multiple Input, Multiple Output) problems and are generally placed above basic controllers in a cascade structure. For simple SISO (Single Input, Single Output) problems the performance of MPC is comparable to PID controllers; however, the computational requirements and the implementation costs are significantly higher.

Creating the adequate model of the controlled object has an important role in applications using model-based control algorithms. Several types of models are available for modelling purposes. Most common, black-box models are used, such as the classical input-output, state-space, and neural network models [43], [45], [46]. Beside the deterministic and stochastic versions that have been previously

mentioned, fuzzy models are applied more frequently [46], [47]. In industrial MPC applications most commonly impulse and step response function-based convolution models are used, which can be determined from experiments (step-test). Therefore, it is more difficult to use MPC for batch systems.

The difference between the real process and the model can be considered in model-based control solutions by the feedback of the modelling error. The previously mentioned adaptive techniques also can be used. Additionally, further possibilities are available in batch technologies to improve control. When producing batches with the same or similar recipes, the process data of the previous batches can be used for the actual ones in a run-to-run optimization [3].

The increasing quality demands for the control of batch reactors require such model-based controllers that transcend the classical PID solutions. Simultaneously, the process control systems are becoming more open for these types of new algorithms.

2. The pilot batch processing unit

In the case of manufacturing processes the mechanical constructions as well as the quality of the measuring instruments significantly influence the performance of the control system. An improperly built-in thermometer or an undersized pump can cause the control system to perform poorly. This effect has even more relevance in the case of systems that have quick dynamic responses, amplifying the importance of quick responses.

The best process control techniques can only help the operation of the technologies to retrieve the maximal profit from the actual construction. The change in the technology always has a bigger impact compared with the best available control. However, without proper control in complex systems the desired results can be difficult to achieve, and especially, maintain.

2.1. Configuration and construction of the system

In the laboratory of the Department of Process Engineering, a batch processing unit (Figure 2.1) containing a 30-liter reactor with a conventional jacket can be found. The pilot unit was built in the 1980s for educational and also research purposes. The main part of the batch processing unit, namely the reactor, was provided by a pharmaceutical company, and the temperature of the reactor was controlled with two media; steam for heating and water for cooling. The auxiliary parts of the processing unit (feeding and weighing tanks, vapour product condenser, product collectors) were constructed by the staff of the department and were also the part of the original construction. The control system of the original construction was designed and manufactured by the department as well as the control algorithms.

According to the advantages described in Chapter 1.1.2, the pharmaceutical companies are starting to implement monofluid heating/cooling systems. In 2007 the upgrading of the batch processing unit was started with the aim to prepare the system for the new control challenges of the industry generated by the monofluid heating/cooling systems. The pilot batch processing unit is a very important and useful tool for testing new control algorithms and investigating phenomena occurring in the industry. According to these considerations, the heating/cooling system of the batch processing unit was changed from the classical steam/water construction to the new, and in the industry increasingly spreading monofluid heating/cooling system.

The flowsheet of the pilot unit can be seen in Figure 2.1. The 30-litre batch reactor has a conventional jacket that has a jacket recirculation loop with direct heating/cooling. This kind of configuration has several advantages, such as quick response time, high dispersion of the heating/cooling media in the recirculation loop (which avoids hotspots and freezing in the reactor), and results in less corrosion due to fluid changes.

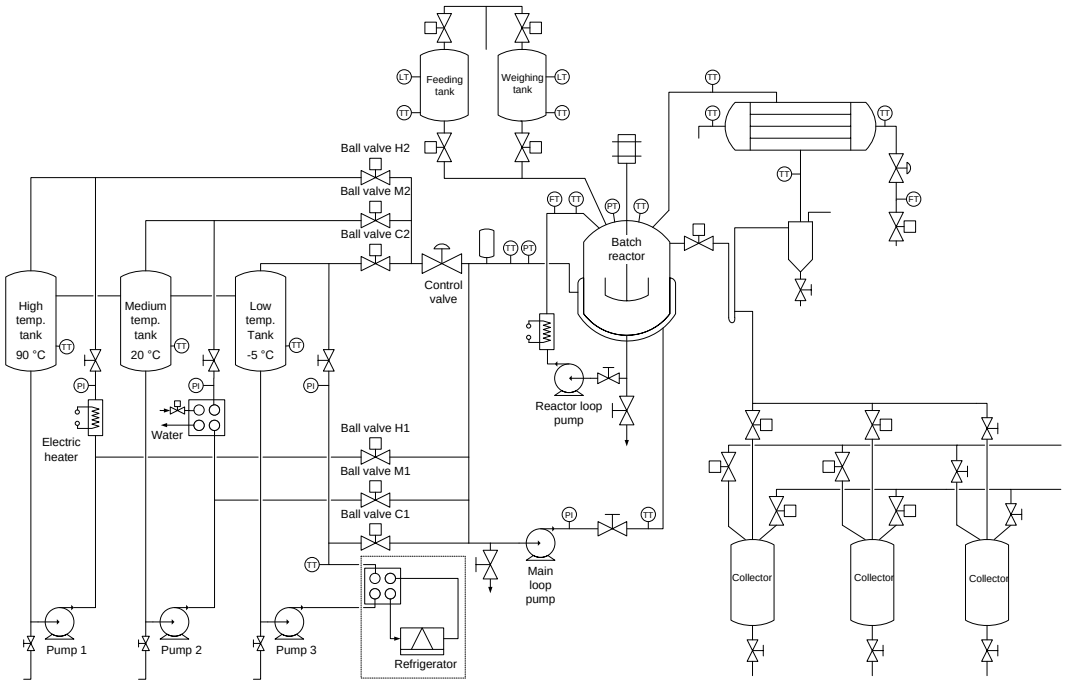

Figure 2.1. Flowsheet of the batch processing unit

The thermoblock is filled with the mixture of water and ethylene glycol to provide higher temperature range than pure water. The thermal fluid contains 34.6 vol% glycol that consist of mainly ethylene glycol and some propylene glycol. The exact rate of propylene glycol is unknown; however it is under 10 vol%. The addition of propylene glycol was necessary to keep the maximal allowed limit of ethylene-glycol in the space of its room. In the models and calculations the thermal fluid was considered as a pure ethylene glycol water mixture, as the small amount of propylene glycol does not affect the properties of the mixture significantly. The temperature-dependent specific heat and density of the thermal fluid can be seen in Figure 2.2. Temperature has a significant effect on these parameters that can affect heat transfer. These values were calculated using Peng-Robinson method in UniSim Design and were also controlled by data from literature.

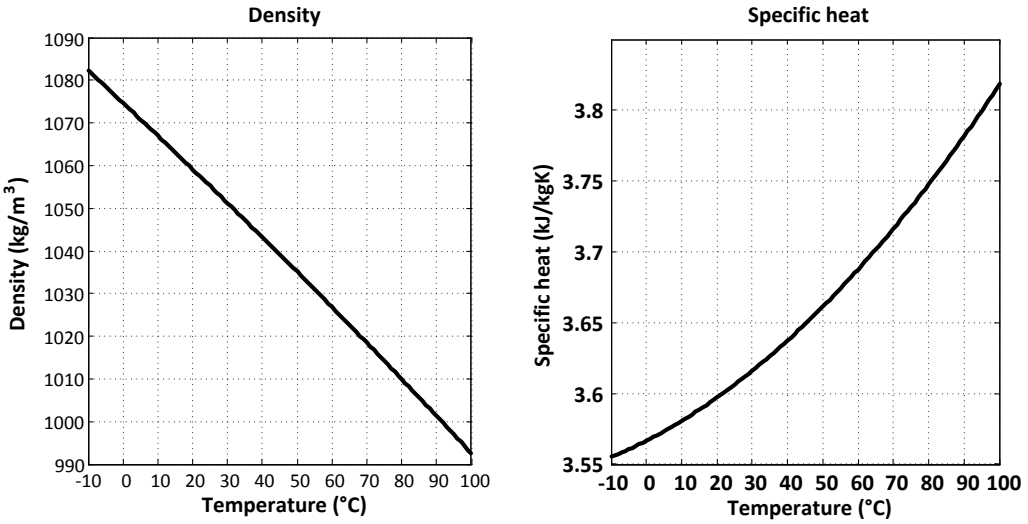

Figure 2.2. The temperature dependence of the thermal fluid

The monofluid thermoblock (Figure 2.3) contains three similar loops at three different temperature levels. The highest can be controlled by an electric heater, the medium by tap water through a plate heat exchanger, and the lowest by a refrigerator. Every loop has a 100-liter buffer tank, and one pump per loop provides the appropriate circulation. The buffer tanks are also connected with spillway pipes preventing them from filling up totally. The monofluid loops operate separately and have independent temperature control. In the case of the lowest temperature level, where the desired temperature can be achieved by a refrigerator, it is controlled by an on/off controller that switches the refrigerator. The temperature control of the medium temperature level, where the temperature is adjusted by tap water through a plate heat exchanger, is also performed by an on/off controller switching the tap water with a solenoid valve.

The temperature control of the high temperature level is different from the previously mentioned ones. This loop contains two electric heaters (6 kW/ heater) with three filaments per heater. These six filaments are separated into three groups, where one group contains one filament from each electric heater. Two filament groups are controlled by digital outputs, i.e. they are turned on/off. The third group is controlled by an analogue output and PWM signal generator with the aim to adjust the power of these filaments quasi linearly. According to this configuration, which can be seen in Figure 2.4, the whole power range of the electric heaters can be covered with analogue manipulation.

Also, each monofluid thermoblock loop contains a manometer for indicating the pressure gauge and a throttle valve for adjusting the flow rate. The manual throttle valves are only for setting up the system. Their position defines the flow rates also in standalone recirculation and when a certain loop is opened on the jacket recirculation loop.

Figure 2.3: The monofluid thermoblock

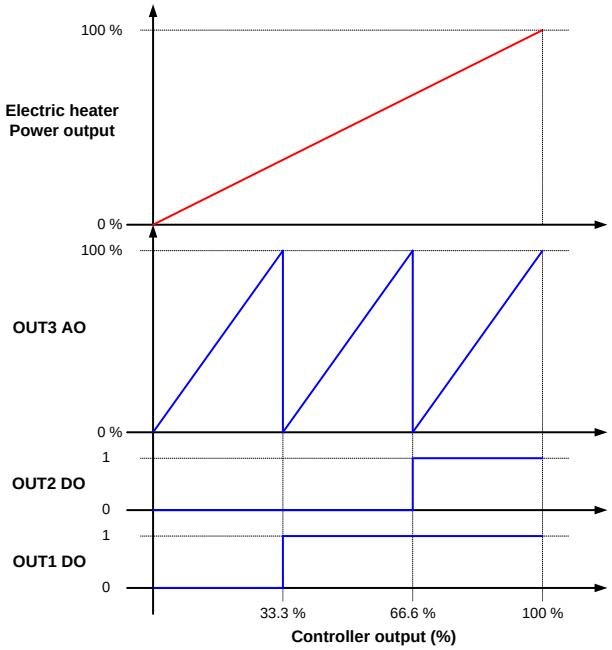

Figure 2.4: The control logic of the electric heaters

The temperature of the reactor can be manipulated by the coordinated operation of the ball valves connecting the monofluid thermoblock with the jacket recirculation loop (temperature level of monofluid) and the control valve (flow rate of monofluid). The control valve located at the returning pipe section from the jacket recirculation to the monofluid thermoblock has the purpose to control the flow rate of the introduced thermal fluid.

A photo taken from the monofluid thermoblock can be seen in Figure 2.3, where the previously mentioned equipment can be identified. On the top the three buffer tanks can be seen and on the bottom the three circulation pumps. The electric heaters are situated on the middle left with aluminium and rockwool insulation. Next to them on the right the plate heat exchanger can be found. The refrigerator responsible for maintaining the temperature of the lowest temperature level cannot be seen in the picture, as it is located outside the building. Only the connecting pipelines can be seen in the bottom right corner of the picture. All the tanks and pipes are insulated to avoid heat loss.

The batch processing unit also contains a feeding and a weighing tank, a condenser for vapour product condensation, product collector tanks, and a recycle loop for the thermal simulation of chemical reactions. The picture of the batch reactor and the auxiliary equipment can be seen in Figure 2.5.

Figure 2.5: The batch reactor, feeding and weighing tanks, vapour product condenser, and product collectors

The control system of the batch processing unit changed several times during the years. After implementing the new monofluid thermoblock the control scheme was constructed as it can be seen in Figure 2.6. The measuring and manipulating instruments were connected to a Remote I/O module (ADAM 5000 TCP), which could be accessed via Ethernet using ModBus TCP protocol. The data from the system was accessible through ModBus TCP/IP OPC server. The basic control and the Human Machine Interface (HMI) were implemented in AdamView HMI software and the advanced control in MATLAB / Simulink, which is a flexible and powerful software for developing control algorithms and performing complex calculations.

The control of the auxiliary parts of the system was available only from a different PC at this intermediate time; thus, the control system was unsuitable to perform the temperature control and the recipe control at the same time.

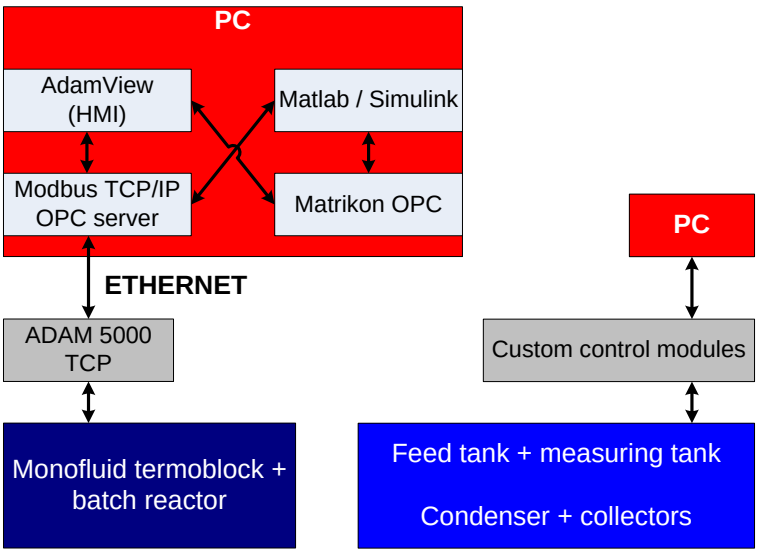

Figure 2.6: The control scheme of the batch processing unit (before 2010)

In 2010 the development of the control system began to have an integrated control system that is similar to the ones used in the industry. The parts of the new control system were provided by Siemens, and the engineering work was performed by a partner of the department called Batch Control Ltd.

After the development a Siemens PCS7 process control system was implemented, which is connected to several remote I/O units through a Profibus DP network. The new structure of the control system can be seen in Figure 2.7. The measuring instruments and actuators are connected to the remote I/O units through appropriate interface modules. The Siemens PCS7 system provides not just the temperature control of the reactor and the monofluid thermoblock but also the control of the auxiliary parts and the higher level control: recipe control. When the Siemens PCS7 is in use, the components in Figure 2.7 above the Siemens Soft-PLC are not available. This configuration was also provided with an industrial standard HMI.

Another configuration is also available for development purposes. Beside the Siemens PCS7, the control of the batch processing unit can be achieved using third-party software connected through a Siemens OPC server. In this configuration the Siemens PCS7 is not available; however the components in Figure 2.7 above the Siemens Soft-PLC are available. The control is partly implemented in the Genie DAQ HMI software and the main part in MATLAB and Simulink. This configuration simplifies the implementation and testing of the new control algorithm on the pilot system.

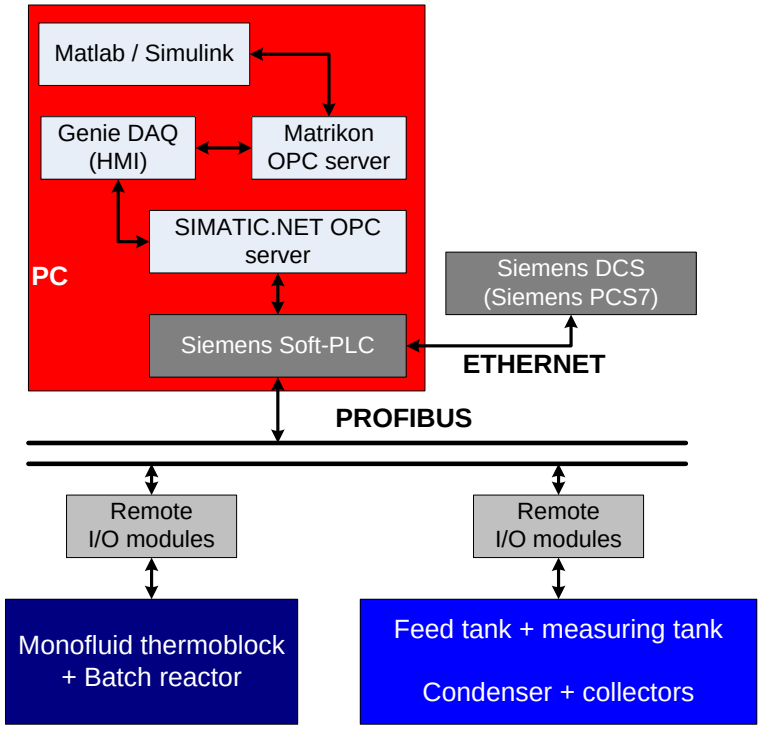

Figure 2.7: The control scheme of the batch processing unit (after 2010)

2.2. Thermometers

One of the most challenging tasks during the development of the pilot system was the adequate installation of the thermometers. Some unexpected results led to a change in the configuration of the system several times over the years. Most of the described phenomena should not cause any problem in the classical PID-based control of the reactor; however, if advanced and model-based control solutions are used, the previously ignored effects can have serious effect on the quality of the control. In this chapter the changes made in the system caused by thermometers will be described.

Location of the thermometers

According to the first configuration after the compilation of the monofluid thermoblock, which can be seen in Figure 2.8, the hereinafter described problem occurred. The inlet temperature to the jacket recirculation of the monofluid thermoblock loops is not known. Temperature measurement is only available in the buffer tanks. The temperature of the inlet fluid differs from this, since the equipment responsible for manipulating the temperature of the loop is before the intersection and not installed on the returning pipe section.

For advanced control solutions especially in the case of model-based control, high quality basic instrumentation is essential for good control performance. As the inlet temperatures of the monofluid loops were unknown exactly, it could not be used as an input for model-based temperature control of the batch reactor. The inlet temperature could only be estimated; however, that brought uncertainty to the calculations.

Due to the previously mentioned installation failure the configuration was changed in 2009 according to Figure 2.9. In the previous configuration the

monofluid thermoblock loops had independent connections to the jacket recirculation loop. This part was changed; all the monofluid loop inlets were connected together to a common pipe section. In the common pipe section a thermometer was installed to measure the inlet temperature of the monofluid thermblock loop in use. This thermometer was a resistance thermometer and had an industrial standard thermowell. For this purpose a very fast thermometer was needed due to the quick temperature changes in the common pipe section, when the change of monofluid loops was performed. But unfortunately it seemed to have too high response time. The change of the temperature in the pipe section happens in under a second, due to the low residence time (Pipe length: ~60 cm, ID: 28 mm, Volume: ~0.35 litre); however, the time constant of the thermometer was over ten seconds. Thus, the advantage of the reconstruction of the connection section could not be utilized.

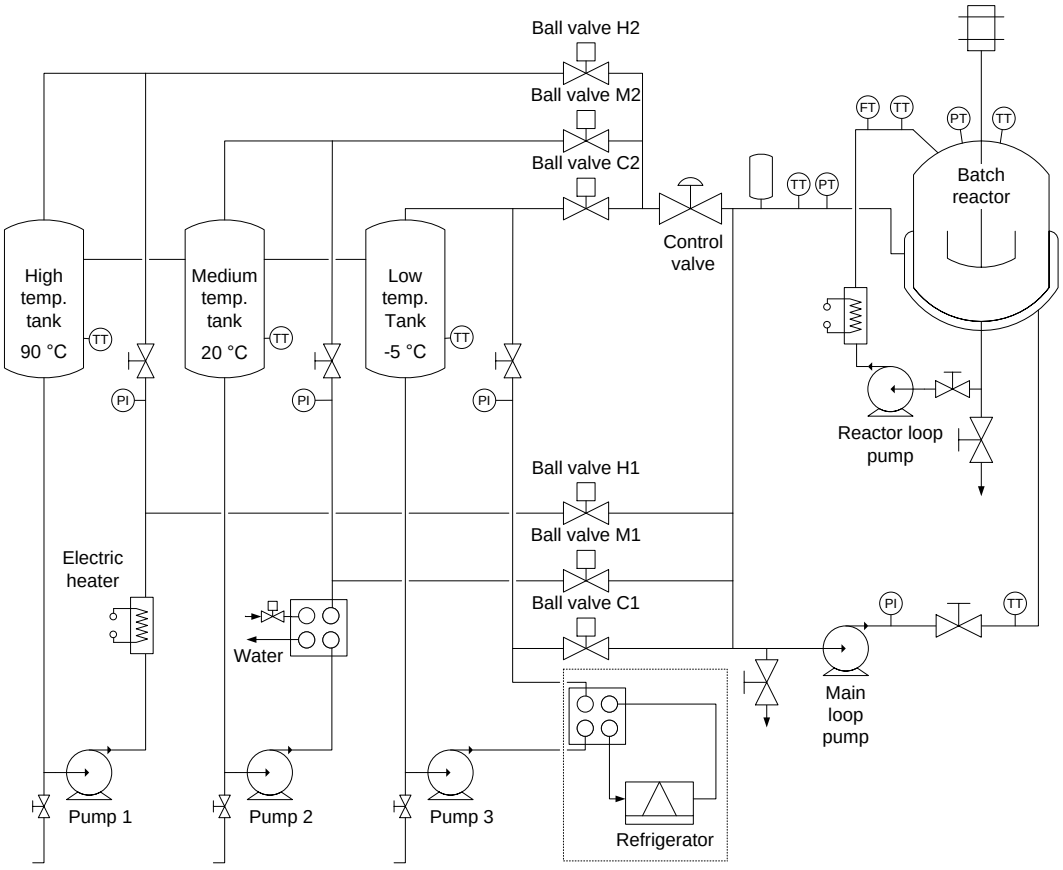

Figure 2.8: Flowsheet of the pilot-plant-size batch processing unit, – the original configuration (2007-2009)

Two additional phenomena also occurred due to this new configuration. When changing temperature level, the remaining fluid in the common pipe section was pushed in the jacket recirculation loop as a plug flow, slightly delaying the effect of the temperature-level change. This phenomenon was not noticeable in the previous configuration since there was no common pipe section.

The other phenomenon occurred when the control valve was operating at low percentage (~0-5%), i.e., only a slight amount of fluid was introduced to the jacket recirculation loop. The recirculating fluid in the jacket recirculation loop back mixed with the fluid in the common pipe section, causing the thermometer to measure a different value from the actual temperature that enters the jacket

recirculation loop. Also, the heat transfer with the wall of the common pipe section caused similar inaccuracy. As it happened in one of the test measurements, this phenomenon caused the model-based controller not to switch from heating to cooling. This might cause reactor runaway if exothermic reaction would have been performed. Therefore, the inlet temperature measured in this configuration could not be used for reliable calculations. Thus, further configuration change was needed.

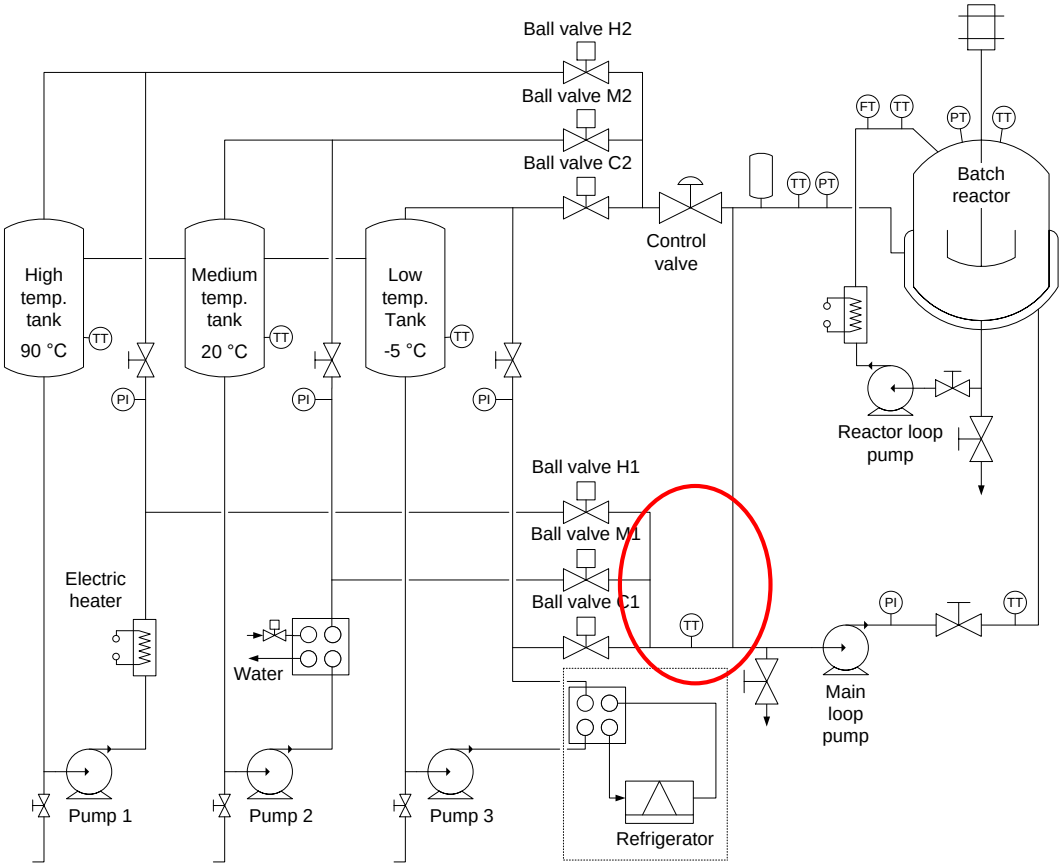

Figure 2.9 Flowsheet of the pilot-plant-size batch processing unit, – after the first modification (2009-2010)

As can be seen in Figure 2.10 several modifications were performed on the pilot system in 2010. The common pipe section with the thermometer measuring the temperature of the actually introduced fluid was removed. This section was modified as it was in the previous configuration; each monofluid loop was connected independently into the jacket recirculation loop. However, with this modification the actual inlet temperature of the monofluid loops remained unmeasured. Therefore, the equipment responsible for modifying the temperature of the monofluid loops were moved. In the case of the high and medium temperature level the electric heaters and the plate heat exchanger was moved after the intersection. According to this modification these monofluid loops are only heated or cooled on the recirculating stream; hence, the inlet temperature of the monofluid loops are quasi equal to the one measured in the buffer tank. This inlet temperature can only be modified in the pipe sections from the buffer tank to the jacket recirculation loop by the recirculating pump and by the heat loss on the pipes.

In the case of the low temperature level this modification could not be performed due to limitations. The refrigerator has a minimum flow rate interlock at 1 m^3/h for the throughput of the plate heat exchanger. If modifying the configuration of this loop the same way as the other two, the capacity of the pump would not be enough to fulfil the flow rate interlock when the low temperature level is switched to the jacket recirculation loop. For this reason the refrigerator remained in the original configuration; however, the disassembled thermometer from the previous common pipe section was installed in the outlet stream of the refrigerator. With this configuration the actual inlet temperature of the lowest temperature level could be measured.

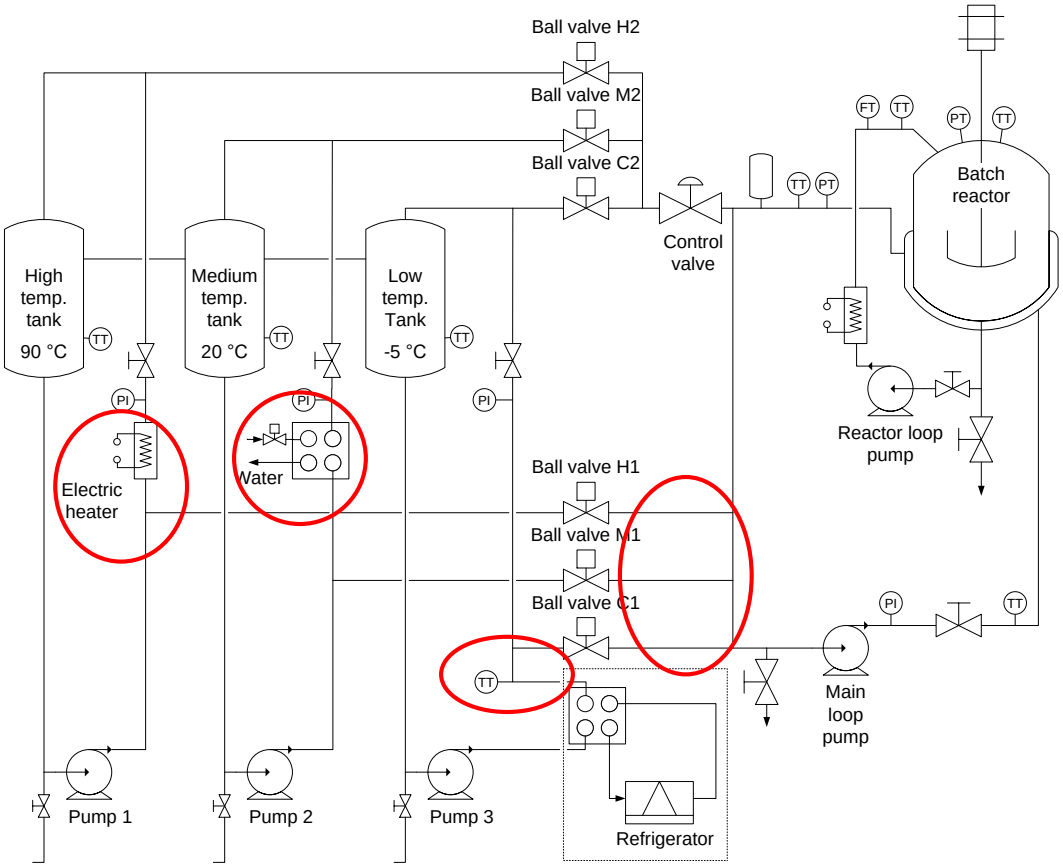

Figure 2.10: Flowsheet of the pilot-plant-size batch processing unit, – after the final modification (2010-present day)

After several changes during the years the final configuration was achieved that can be seen in Figure 2.1 and also in Figure 2.10. With this configuration the inlet temperature of the monofluid loops to the jacket recirculation loop can be measured without any high-impact unmeasured disturbance, which is essential for model-based control algorithms.

Thermometer installation directions

Not only the location of the thermometers and the configuration of the system are important but the installation of the thermometers has a high impact on the quality of the control. In the case of cascade reactor temperature control, the control quality of the slave loop, i.e., the control of the jacket temperature, mainly restricts the quality of the reactor temperature control. Thus, good control quality should be achieved in the slave loop. For the measurement of the jacket

temperature usually two thermometers are available, one in the inlet and one in the outlet of the jacket. These thermometers provide the only information about the temperature of the circulating fluid; thus, their measured data must be analysed if used for advanced control algorithms.

According to Egedy at al. [48] the installation direction of the thermometer has a great impact on the heat transfer between the fluid and the thermowell of the thermometer. This should be a trivial assumption; however, according to the experience in industrial configurations, the installation direction of the thermometers depends mainly on aesthetic, space saving, and wiring considerations. If the thermometers are installed in a preconfigured location into a pipe bend, as it can be seen in Figure 2.11, it can be performed two ways. It can be installed in the pipe bend in countercurrent a), or concurrent directions b). The proper way to install the thermometers is the countercurrent direction [Figure 2.11 a)], as the heat transfer is higher, which is caused by higher Nusselt number. When it is installed in concurrent flow direction, the heat transfer coefficient is lower due to wave detachments and blind spots caused by turbulent flow. This causes higher response time for the thermometer.

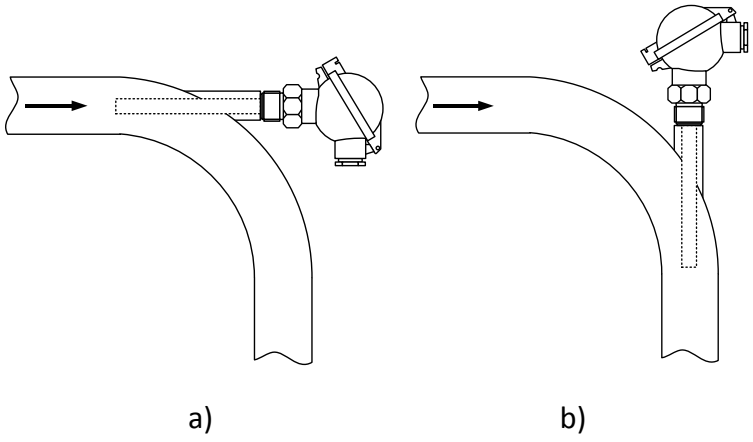

Figure 2.11. Different thermometer installations in a pipe bend

After the implementation of the new monofluid thermoblock in the pilot batch processing unit in 2007, the inlet and outlet thermometers of the jacket were installed in the same direction as can be seen in Figure 2.12 a), since it was easier to wire. However, in these two pipe sections the flow of the thermal fluid is contrary. This means that one of two installations must be incorrect. The thermometer for the jacket inlet temperature can be seen in Figure 2.12 a) as the rear one. The thermal fluid is flowing from the left side, from the recirculation pump, thus the thermometer is installed flow concurrent way. This incorrect installation was noticed and proven via measurements. When changing the temperature of the jacket recirculation loop significantly by switching to maximal heating or cooling capacity, after the dead time that is caused by the volume of the jacket, the jacket outlet temperature was changing quicker than the inlet. This also caused the jacket inlet and outlet temperatures to cross, which produced an impossible state. As can be seen in Figure 2.13, in the case of heating, the jacket outlet temperature was higher than the inlet in spite of the reactor temperature that was cooler than both of them. This phenomenon was caused by the incorrect installation of the jacket inlet thermometer that caused higher response time.

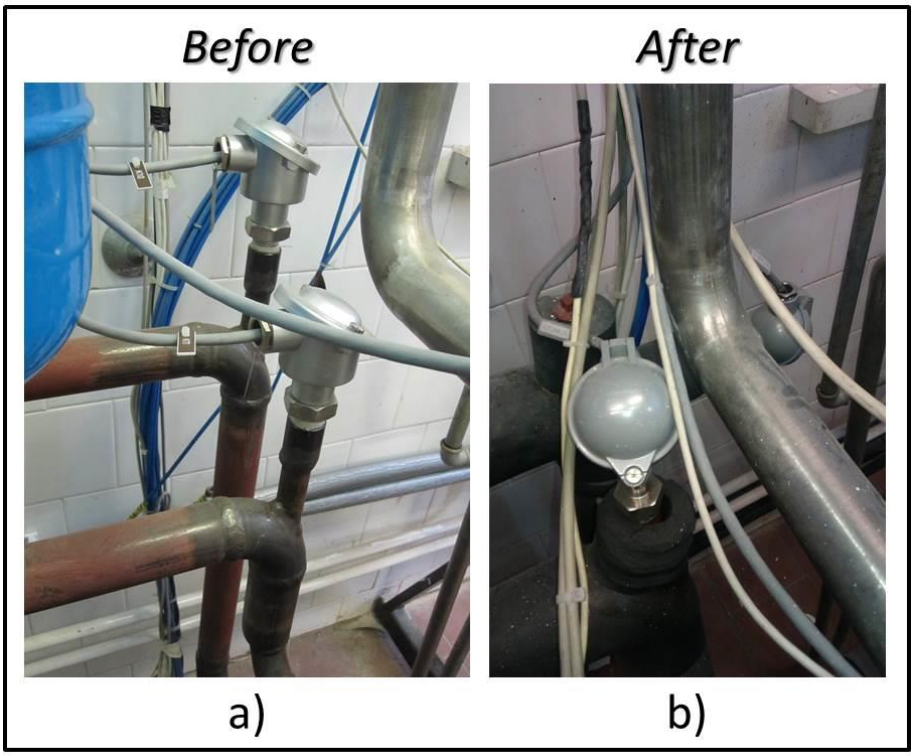

Figure 2.12: The change of the direction in the case of the jacket inlet and outlet thermometers

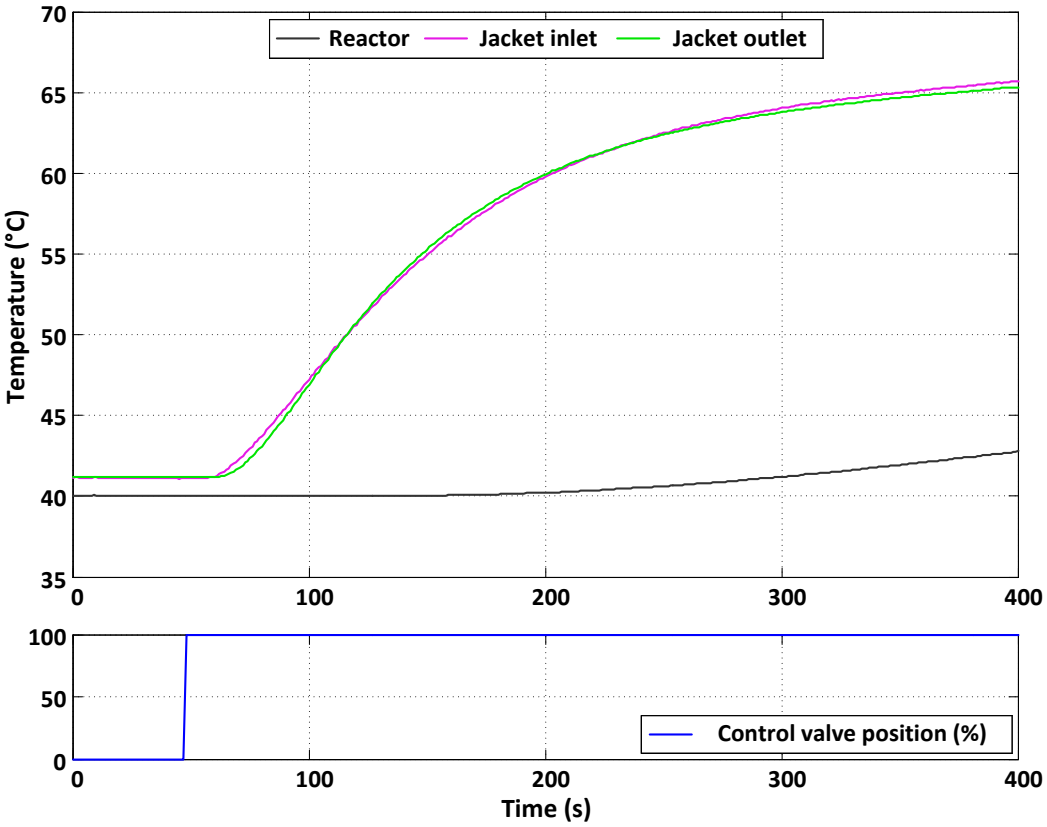

Figure 2.13. The effect of the incorrect installation of the jacket inlet and outlet thermometers

After it has been proved that the incorrect installation causes the unexpected behaviour of the jacket inlet temperature, the pipe bend was inverted to meet the configuration in Figure 2.11 a). After the change, the new configuration can be seen in Figure 2.12 b). Test measurements have proved that the improper installation was responsible for this incorrect behaviour as this phenomenon was not experienced since.

The response time of the thermometers

In the case of dynamic systems, measuring instruments with low response time are necessary to achieve high control performance. To achieve high control performance in the temperature control of the batch reactor, also the temperature controller of the jacket has to perform well. The jacket recirculation loop has a high flow rate (~ 4200 l/h) with low volume (pipes: ~30 litres; reactor jacket: ~ 20 litres) that results in low residence time. Thus, the time constant of this system is very low, which also needs measuring instruments with low response times. The response time of the measuring instrument must always be lower than the time constant of the measured system.

The measuring chain consists of several components as it can be seen in Figure 2.14, thus the response time and accuracy of the measuring instruments depend on several factors. In the case of thermometers the response time depends on the construction, wall thickness and material of the thermowell, and also on the type of the sensor. The accuracy is mainly defined by the thermometer sensor; however the wiring and the compensation also affect the quality of the signal. The accuracy of the recorded digital value as the result of the measurement significantly depends on the resolution and configuration of the A/D (analogue/digital) converter and also on the format of the recorded numeric value. In the pilot batch system the Siemens analogue input card allows different measuring ranges to be configured. The narrowest range that can be configured is -25 °C – 100 °C. The resolution of the A/D converter is 12 bits, which results in an accuracy of 0.03 °C. This limitation can be significant in the case of precise and sensitive reactor temperature control, and also some set point values are impossible to reach (for example: 40.00 °C). In the cascade temperature control when the controlled variable is close to the set point, the random numeric value changes caused by the resolution of the A/D converter can result in a movement in the manipulated variable of the master loop, which simultaneously alters the set-point of the slave loop. Depending on the gain of the controllers this can end in an unnecessary operating mode change.

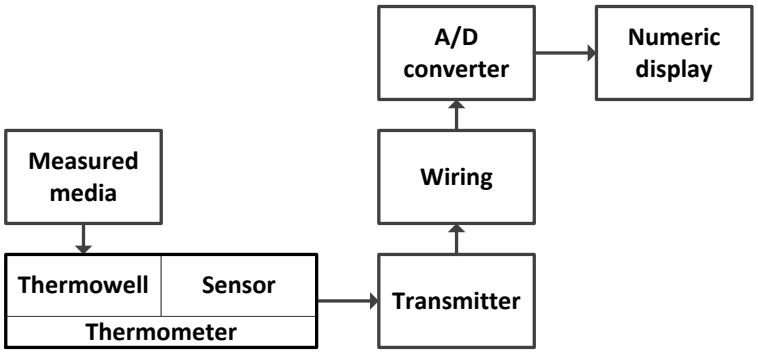

Figure 2.14: The temperature measuring chain

According to previous consideration, to achieve good control performance it is necessary to know at least the approximate response time of the thermometers. To determine the response time, test measurements were performed, where the measuring instruments were disassembled. Several water-filled containers were prepared with different temperatures. The analysed thermometers were tied together with the aim to move them from each container to another at the same time. One of the containers that is a jacketed glass vessel was heated by a thermostat, and the disassembled thermometers can be seen in Figure 2.15. This way the exact time constant cannot be determined as the flow conditions differ from the configuration where the instruments are installed. However, the relative time constants and also the offsets can be determined.

In the first test measurement the two thermometers of the jacket recirculation loop, namely the thermometers for the jacket inlet and outlet temperatures, were analysed. These instruments with industrial thermowell can be seen in Figure 2.16 b) – the jacket inlet, and in Figure 2.16 c) – the jacket outlet thermometer. Another thermometer can also be seen in Figure 2.16 a), which is a special, low response time instrument with low thermowell wall thickness around the temperature sensor. This instrument was planned to replace the other ones.

Figure 2.15: Test configuration for comparing the dynamics of the different thermometers

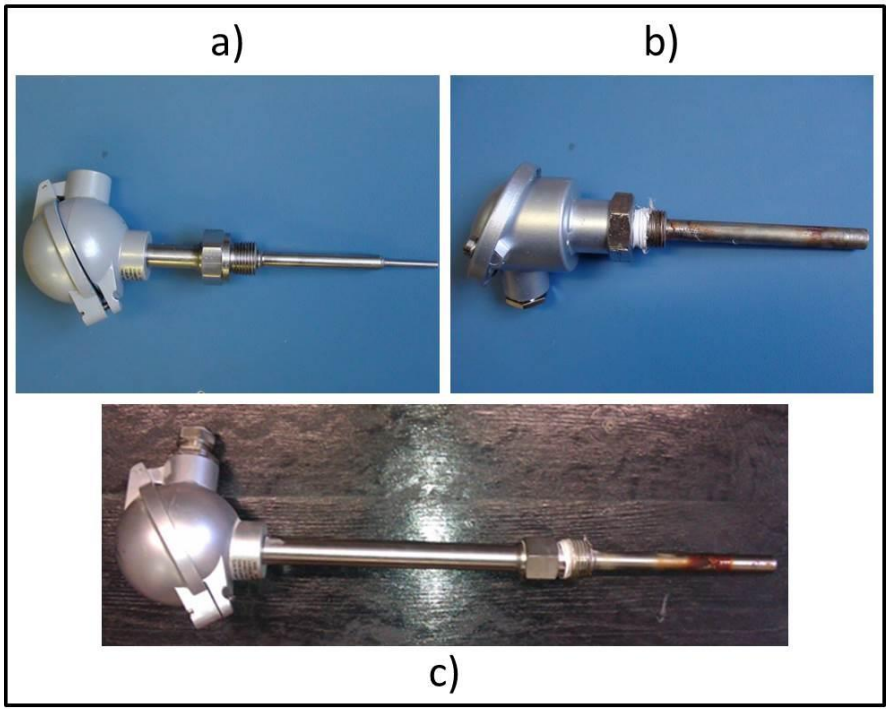

Figure 2.16: The tested thermometers

The results of the first test measurement can be seen in Figure 2.17. Three containers were used with three different temperatures. The container containing the fluid with the lowest temperature was the jacketed glass vessel that can be seen on Figure 2.15. The set-point of the thermostat controlling its temperature was 5 °C. The highest temperature was achieved by the available high temperature water network of the laboratory. The medium measured temperature was water on ambient temperature.

As it can be seen in Figure 2.17 there are significant differences between the time constants of the three tested thermometers. The curve highlighted with green represents the measured values of the jacket inlet thermometer that can be seen in Figure 2.16 c); the red curve represents the measured values of the jacket outlet thermometer in Figure 2.16 b). The curve highlighted with blue is the new, special thermometer with low thermowell wall thickness. It has much lower time constant than the other ones (~10 s). The jacket inlet thermometer has a time constant ~ 100 s, and the jacket outlet thermometer about 30 s.

After this test measurement it was proved that the response time of the thermometers are not sufficient to measure the dynamic changes of the jacket recirculation loop. Therefore, the thermometers were changed to the new, special thermometers with low thermowell wall thickness.

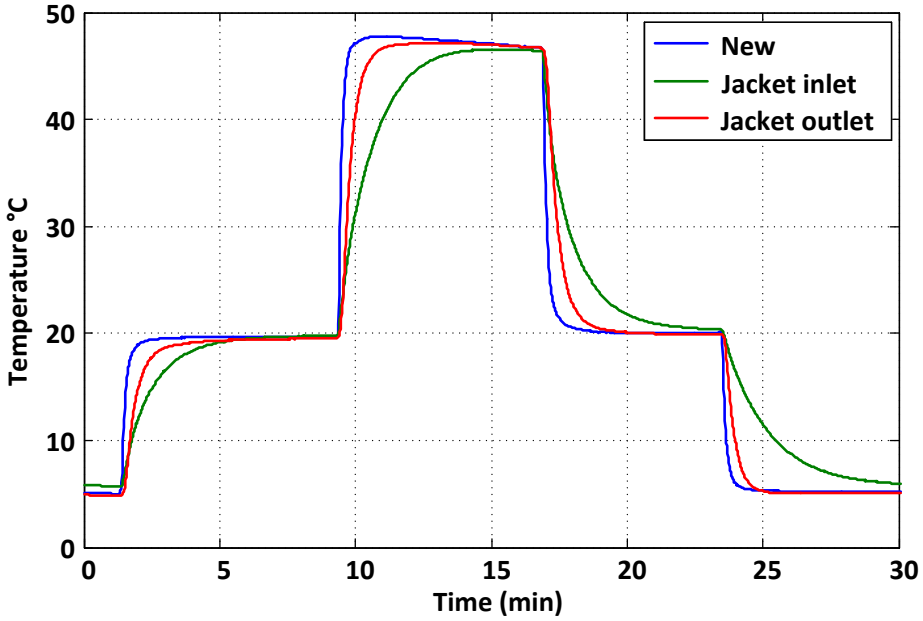

Figure 2.17: The difference in dynamic behaviour of the tested thermometers

The details of the new thermometers can be seen in Table 2.1. The sensors also had a ceramic coating, as well as the other temperature sensors in the system. Unfortunately the details of the reactor thermometer were not available; however it was known that the sensor was a ceramic coated Pt100 resistance temperature sensor with four wire compensation.

Table 2.1.
Details of the jacket thermometers

Resistance type	Pt100
Sensor accuracy class	A
Number of sensors	single
Number of wires	4
Measuring range	-50 – 400 °C
Thermowell material	1.4301 stainless steel

According to the idea of the previous test measurement another similar test was performed with the new jacket inlet and outlet thermometers and the reactor thermometer. The aim of this test measurement was to identify the relative offsets, time constants, and dead times of the instruments. The test measurement was carried out in the tempered, jacketed glass container, and it was divided into two subtests. First the temperature was increased with 5 °C stepping, and then decreased the same way as can be seen in Figure 2.18. The dynamic behaviour can be seen in Figure 2.19, where the thermometers were moved from a tempered 90 °C container to a vessel containing water at ambient temperature. The identification of the dynamic parameters was performed by the least squares method using a first order plus dead time model. The resulting dynamic parameters can be found in Table 2.2. The jacket inlet and outlet thermometers

have similar time constant and dead time values, but the thermometer of the reactor has a significant difference, which is mainly caused by the high wall thickness of the thermowell.

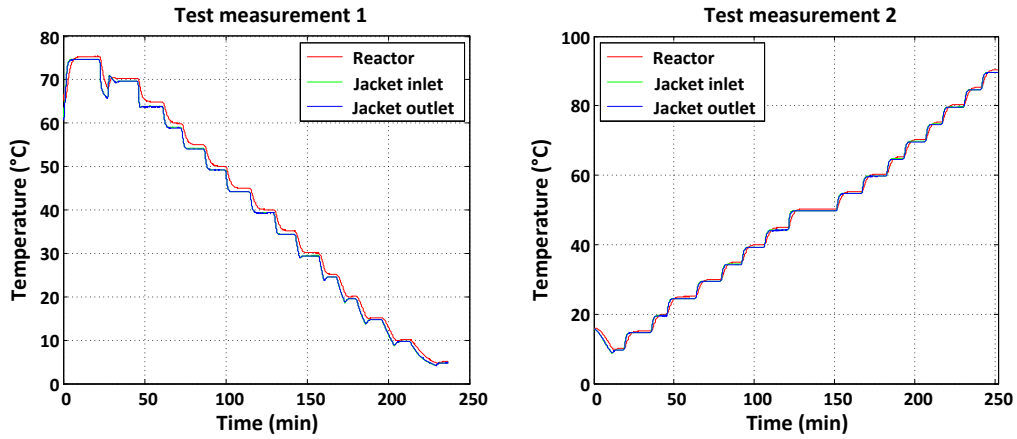

Figure 2.18: The test measurements to identify the relative offsets, time constants, and dead times of the thermometers

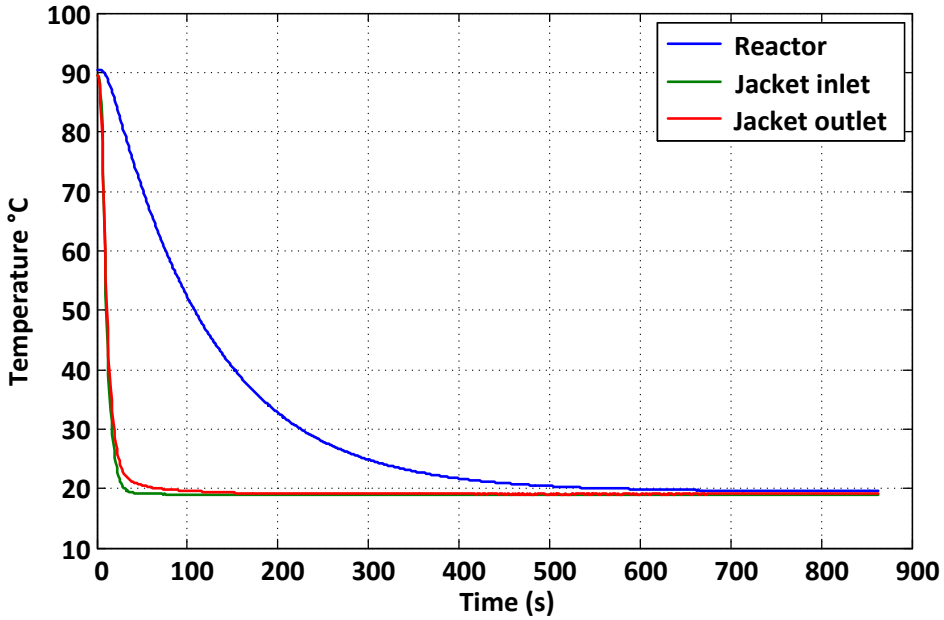

Figure 2.19: The dynamic behaviour of the final thermometers

Table 2.2.
The time constant and dead time values of the final thermometers

	$T_{reactor}$	T^{in}_{jacket}	T^{out}_{jacket}
Time constant (s)	112	6.1	8.1
Dead time (s)	13	5.3	4.5

The relative offset between the measured values of the thermometers were also determined from the first test measurement. A base thermometer was chosen, namely the jacket outlet thermometer, from which the offset will be originated. According to the measurement data, the offset seemed to be temperature

dependent and also nonlinear. Power function was chosen to describe the temperature-dependent offset as it can be seen in Equation (2.1). The temperature differences calculated from the measured data and the fitted curve can be seen in Figure 2.20 for both the reactor and jacket inlet thermometer. The resulting parameters can be found in Table 2.3.

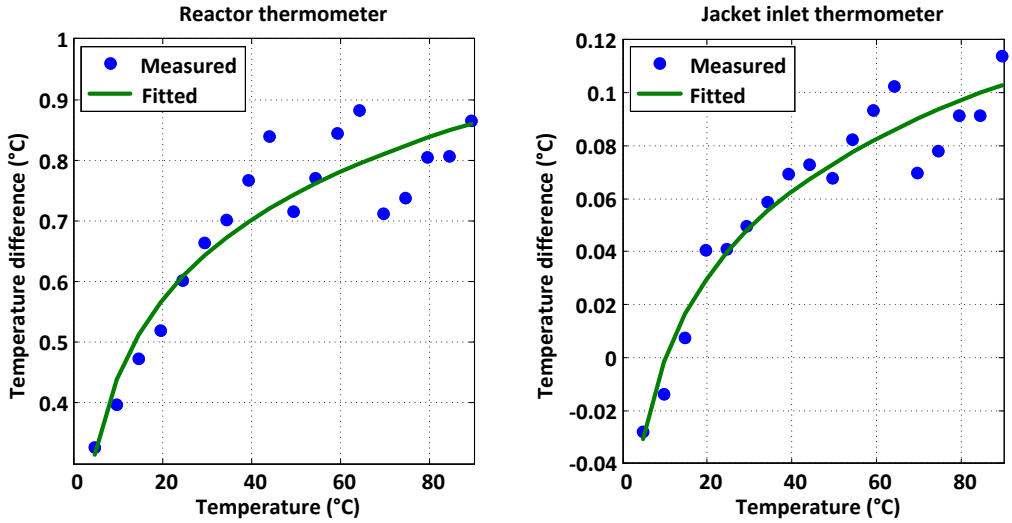

Figure 2.20: The temperature-dependent offset compared to the jacket outlet thermometer

$$\Delta T = a \cdot T^{b} + c \tag{2.1}$$

Table 2.3.
The parameters to calculate the temperature-dependent offset

	a	b	c
Reactor thermometer	3.20	0.0500	-3.15
Jacket inlet thermometer	0.40	0.0872	-0.49

It can be concluded that the thermometer of the reactor has a significantly different dynamic behaviour, namely higher response time compared with the other two tested ones. This can be explained with different thermowell construction of the thermometers. This information can be useful in the design of the reactor temperature controller to know that the measured reactor temperature only represents a value delayed with the response time. It is especially important in dynamic highly exothermic/endothermic reactions, where the temperature of the reaction mixture might change quickly. The thermometer of the reactor also shows significant offset compared to the other tested ones. It is essential to build this offset in the model-based controller of the reactor to make the model more accurate. It is also important if our objective is to calculate accurate heat flow through the wall of the reactor to estimate reaction heat flow.

2.3. Setting the system

One of the most important prerequisites before starting to use the system is to know the flow rates in all pipe sections in all modes of operation. It is also a very important input in creating the simulator of the system.

There were no online flow measuring instruments installed in the system, thus the actual flow rates are not available for control. However, in the case of such closed loops as in the pilot batch processing unit and the monofluid thermoblock, where the composition of the thermal fluid is constant, an accurately tuned system will maintain its state for a longer time period. Only fouling and pump efficiency reduction can result in flow rate decreasing. Consequently, the hydrostatic characteristics of the system containing all the independent manipulators that affect the flow rate of the system can be used to calculate the actual flow rates. These valves can be seen in Figure 2.21 highlighted with red.

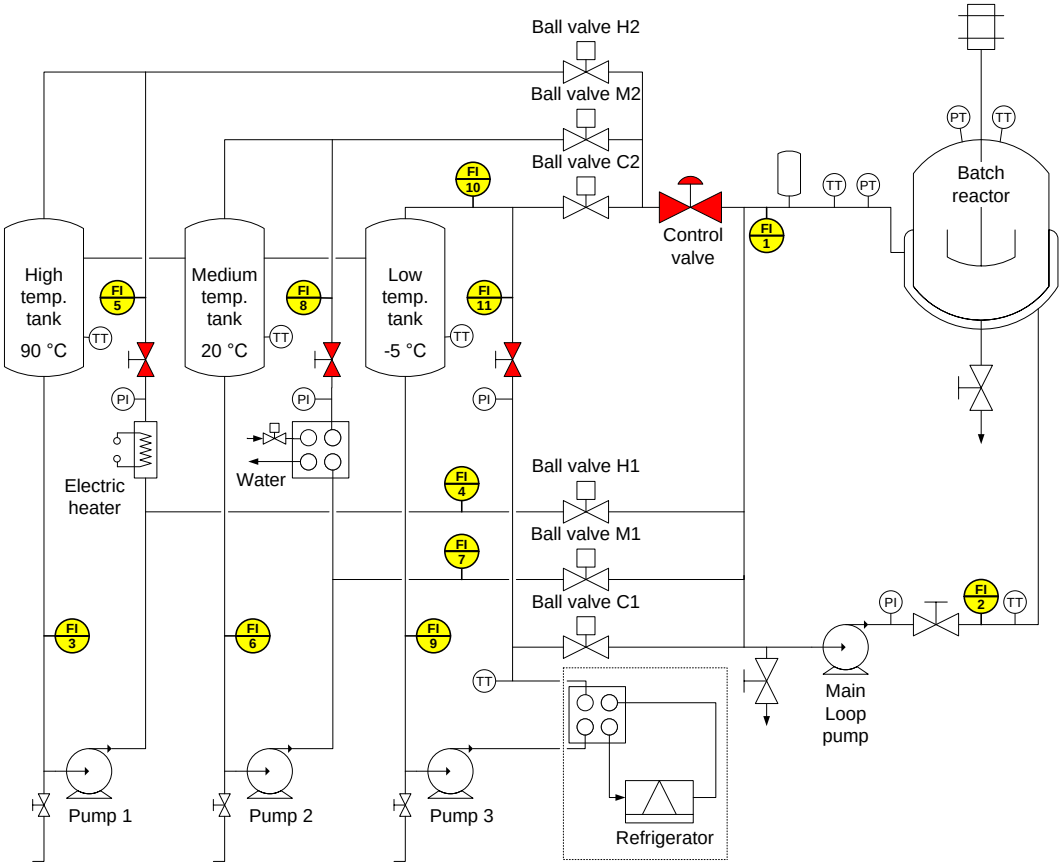

Figure 2.21: The measuring points and valves used for recording the hydrostatic characteristics of the system

The measurement of the hydrostatic characteristic of the system was performed with a mobile ultrasonic flow meter that can be seen in Figure 2.22. The instrument has a measuring accuracy (flow velocity) of ±1.6%. The ultrasonic transducers can be attached on the outer side of the pipes. The measuring points were determined regarding certain criteria to avoid measurement disturbances. For example it is necessary to place the transducers at a distance more than 10 times the pipe diameter from a pipe elbow. These measuring locations can be seen in Figure 2.21 highlighted in yellow. All of the monofluid thermoblock loops have three measuring places, one for the outlet of the buffer tank, one for the recirculation stream, and one for the inlet to the jacket recirculation loop. The flow rate of the jacket recirculation loop has also two measuring points, one for the jacket inlet and one for the jacket outlet flow rate. Unfortunately it was not possible to establish a measuring location between the outlet and inlet point of the monofluid thermoblock, because this pipe section is too short and the basic criteria for the placing of the transducers would not be satisfied.

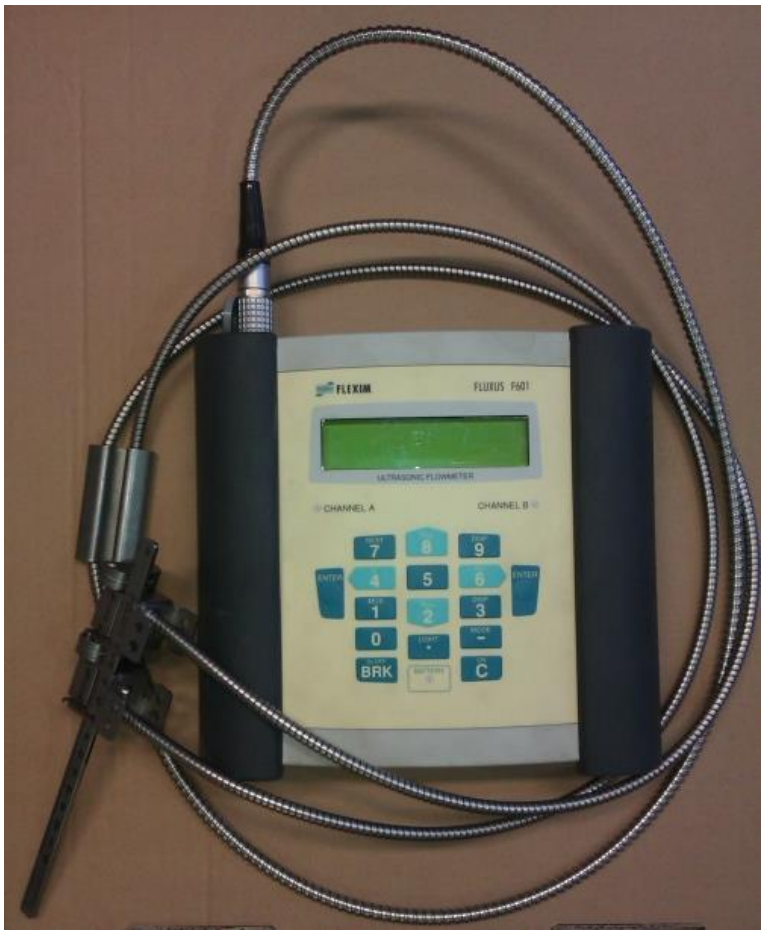

Figure 2.22: The FLEXIM FLUXUS F601 ultrasonic flow meter

Using the ultrasonic flow meter, only one measuring point can be measured at a time as it has only one pair of transducers. The measurement data is stored in the memory of the instrument and can be seen in its display. However, there is the option to connect it to a computer via a serial cable using RS232 port. With this solution the data can be transferred to a computer after the measurement (offline) or it can be visualized online on a display and also stored. GeniDAQ HMI software was used to visualize the data of the ultrasonic flow meter and to perform changes on the batch processing unit during the measurement.

Two types of manipulators can be found in the system that affects the flow rate. These equipment are highlighted with red in Figure 2.21. A throttle valve is available in every monofluid thermoblock loop that can be only manipulated manually. It has the role to determine the recirculation flow rate of the monofluid loop. The other manipulator is the control valve at the outlet of the jacket recirculation loop. This has the role to control the inlet amount of the thermal fluid from the monofluid thermoblock.

Every throttle valve are the same type; however, they have different turn numbers to fully open. They are also oversized, which causes a significant effect on the flow rate only in the first third of the range. This is the reason why the measuring positions of the throttle valves are unevenly distributed in the range. The number of turns to fully open and the number of measuring positions can be seen in detail in Table 2.4.

Table 2.4.
The number of turns to fully open and the number of measuring positions in the case of the throttle valves

	Number of turns to fully open	Number of measuring positions
High-temperature loop	7 1/5	8
Medium-temperature loop	6	8
Low-temperature loop	5	7

In the case of the control valve, evenly distributed measuring positions were used with 10 percent stepping, as the type of the valve is linear.

The ultrasonic flow meter can be installed only at one measuring point at a time, thus, the test measurement was performed as the following schedule. Each monofluid thermoblock loop was analysed separately, because only their own throttle valve and the control valve has an effect on their hydrostatic characteristics. From an operating point of view these loops are independent and also can be considered as three different modes of operation, as they are never switched on the jacket recirculation loop at the same time. The throttle valve was turned to the predefined measuring position, the ultrasonic flow meter was mounted on the first measuring point, and the control valve was stepped from 0 percent to 100 percent with 10 percent stepping. The control valve was stepped only after a certain waiting time to reach steady state of the flow rate measurement. The stepping was performed from GenieDAQ software automatically. After a test at a measuring point was finished, the ultrasonic transducers were moved to the next measuring point. For every monofluid loop their three measuring points were used.

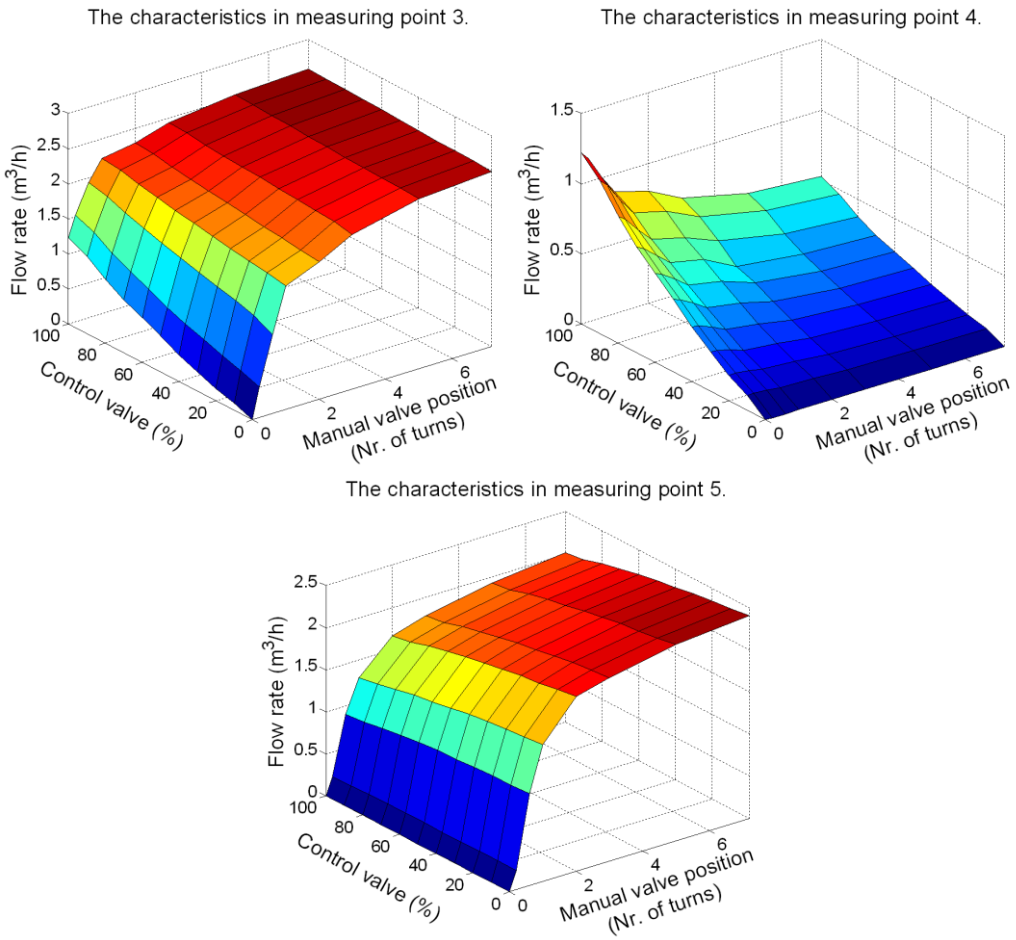

Figure 2.23: The hydrostatic characteristics in measuring point 3 – 5

The hydrostatic characteristics of the high-temperature loop can be seen in Figure 2.23, where it is unequivocally shown that the throttle valve is oversized.

After performing the test measurements for all the three monofluid thermoblock loops and analysing the results of the characteristics, the operating points had to be chosen. The following assumptions were to be made:

- Equal inlet flow rate to the jacket recirculation loop for all three thermoblock loops (easier handling in control)
- Minimum throughput of 1 m^3/h at the plate heat exchanger of the refrigerator must be achieved at any position (flow rate interlock)
- Maintain sufficient flow rate on the electric heaters at all positions to avoid boiling of the thermal fluid

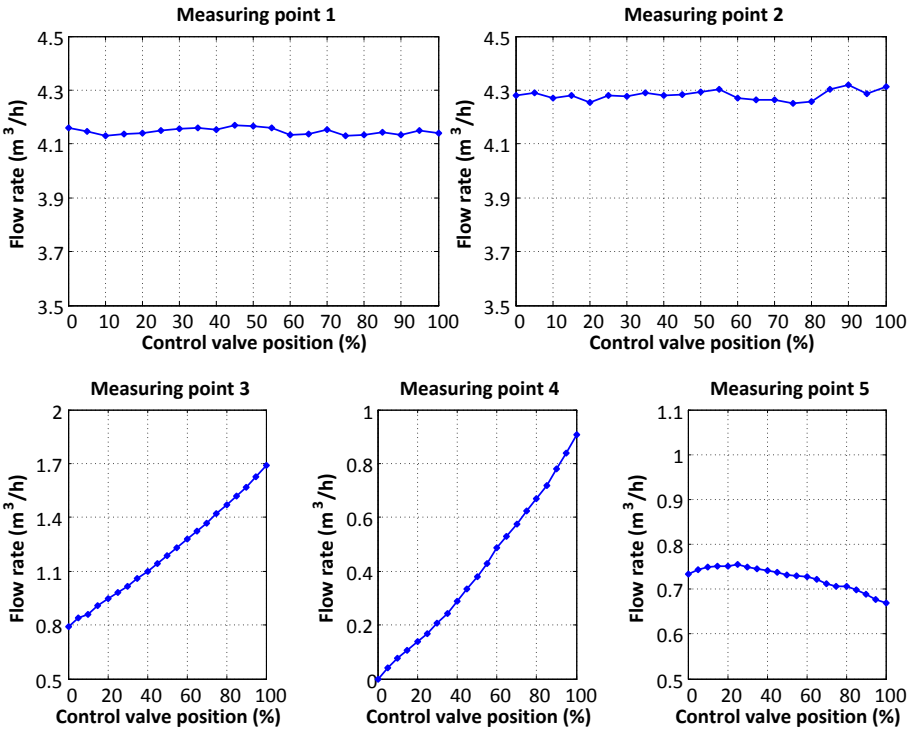

Figure 2.24: Hydrostatic characteristics at the tuned operating point for the high-temperature loop

After choosing the adequate position of the throttle valve to achieve the previously mentioned assumptions, another test measurement was performed on the system with the finalised configuration. The throttle valve was not adjusted, only the control valve, but with higher resolution (5% stepping), and not only the measuring points of the monofluid thermoblocks were used but also the measuring points of the jacket recirculation loop.

In the case of the high-temperature loop the results can be seen in Figure 2.24. The difference between the values of measuring point 1 and 2 can be explained with the error caused by the different pipe size and type compared with the other measuring points. The pipes of the recirculation loop have higher inner surface roughness that can cause higher measuring disturbances. The achieved maximal inlet flow rate to the jacket recirculation loop is 0.9 m^3/h in measuring point 4, which can be seen in Figure 2.24.

The results of the test measurement for the medium-temperature loop can be seen in Figure 2.25. Similar flow rate values were achieved compared with the high-temperature loop, which means that the plate heat exchanger and the electric heaters have similar hydrostatic resistances.

The results of the test measurement in the case of the low-temperature loop can be seen in Figure 2.26. This loop has a different pump with higher dynamic head, thus, the characteristic is different from the other two loops. The assumption for this loop was to have at least 1 m^3/h throughput at the plate heat exchanger at all positions. As it can be seen in Figure 2.26 this criterion was achieved in measuring point 9.

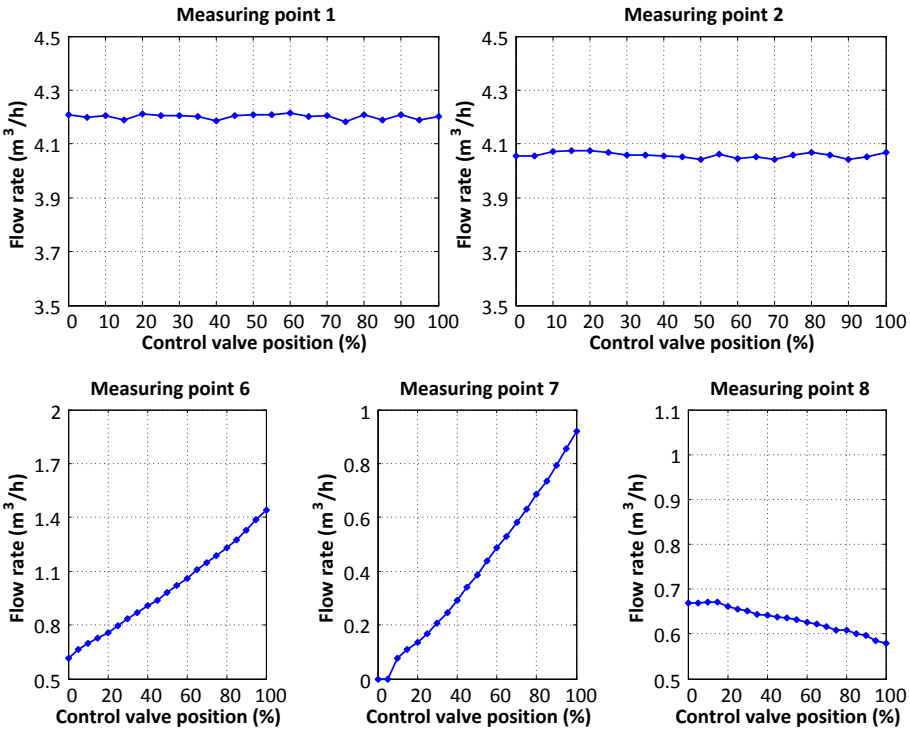

Figure 2.25: Hydrostatic characteristics at the tuned operating point for the medium-temperature loop

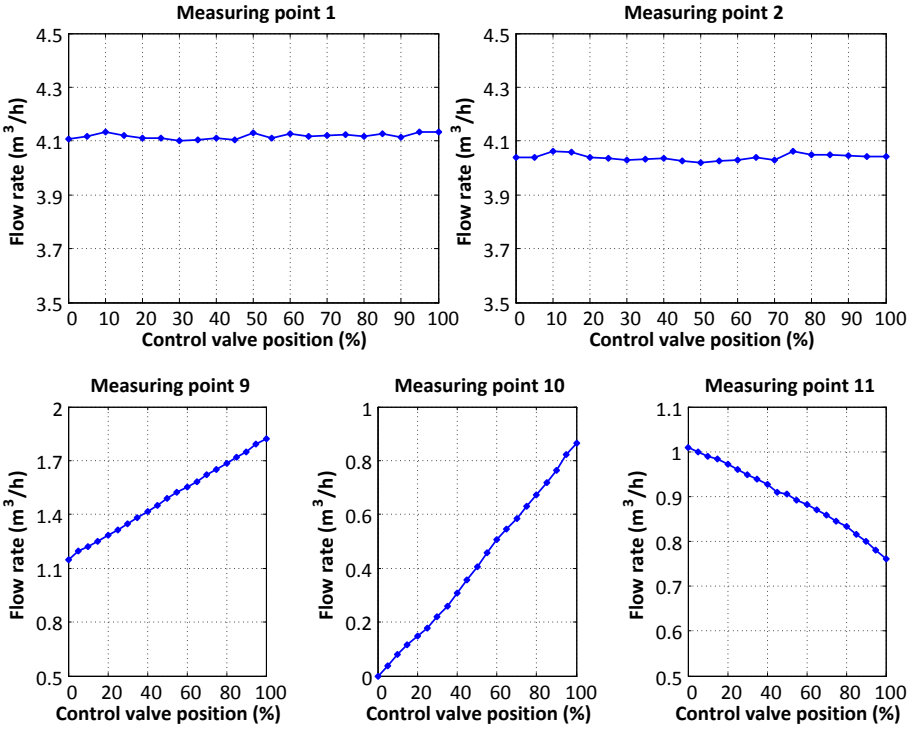

Figure 2.26: Hydrostatic characteristics at the tuned operating point for the low-temperature loop

The tuned operating points have to be reviewed at least every year due to fouling and pump efficiency reduction.

2.4. Reaction heat simulation

One of the most important effects on the heat balance of the reactor is the reaction heat. When developing new control algorithms for the control of the reactor temperature the most important effect cannot be excluded. The classical way to incorporate the effect of the reaction is to perform the chemical reaction. However, this is only an economic way when it is performed in small scale, like in a 1 litre laboratory reactor. In the case of pilot-plant-size reactors, as it is in our case, using real chemicals would highly increase the costs of the research. Additionally, the laboratory does not need extra authorisation as no chemicals, only water and thermal fluid, are used. This is the reason why we decided to implement an additional loop to the reactor with the aim to simulate the heat of the reaction physically. This extra loop contains a pump to provide the circulation, a flow meter, a thermometer, and an electric heater to introduce the exothermic heat to the fluid. The flowsheet of this loop can be seen in Figure 2.27.

Before starting to use this reaction heat simulating loop, first the heat flow in function of the control input of the heater had to be identified. This electric heater has the same structure as the ones in the monofluid thermoblock. Therefore, it has three filaments; two of them are connected to digital outputs and the third is controlled by an analogue output card through a PWM signal generator. The control of the whole electric heater can be seen in Figure 2.4.

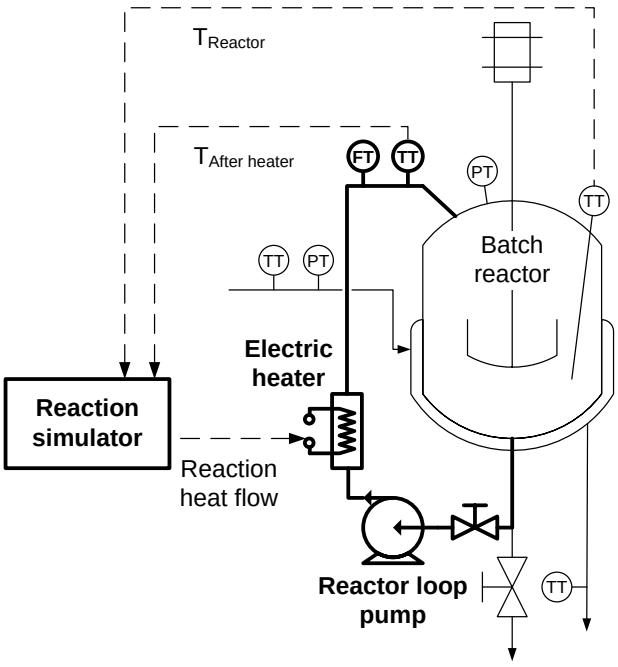

Figure 2.27: Flowsheet of the reaction heat physical simulation loop

There are two ways to determine the introduced heat to the fluid. The electric power can be measured that is consumed from the electric grid, and after identifying the efficiency of the heater the introduced heat flow can be calculated. The other way is to calculate it from the temperature difference that is caused by the electric heater. To calculate the temperature difference, the temperature before and after the heater must be available. The temperature of the reactor can be

considered as the value before the heater as in the case of well stirred reactors there are only slight temperature differences in the bulk fluid. The temperature after the heater is measured with a resistance thermometer installed in a pipe elbow. Also the flow rate of the fluid is needed, which is measured with a flow meter after the heater. The properties of the fluid is known, thus the heat flow can be calculated according to Equation (2.2).

$$\dot{Q}_{rs} = F_{rs} \cdot \rho_{rm} \cdot c_p^{rm} \cdot \left(T_{after\ heater} - T_{reactor}\right) \tag{2.2}$$

The heat flow of the electric heater is expected to be linear depending on the manipulated variable. The heat generated on the resistance filaments is introduced to the fluid with high efficiency as there is no heat loss possible around the filament. Heat loss is only probable on the surface of the electric heater; however, it is well insulated, thus it can be ignored. According to Figure 2.4, where the control of the electric heater can be seen, the analogue output controlled filament ensures the electric heater to operate quasi linearly. The filament is controlled by a PWM signal generator, which turns the filament on/off in a given time (pulse) depending on the input analogue signal value. The pulse time must be selected to avoid oscillation of the temperature after the heater, i.e., it must be lower than the response time of the filament and the thermometer.

A test measurement (Figure 2.32) was performed to determine the heat flow introduced by the electric heater depending on the manipulated variable. The resulting characteristics can be seen in Figure 2.28, which are significantly different from the expected. This high difference can be explained with the different behaviour of the two thermometers that are used for the heat-flow calculation. A test measurement (Figure 2.29) was performed to determine the static and also the dynamic differences of the two thermometers. The temperature of the reactor was modified through its jacket in the whole operating range, the circulation pump was providing the flow in the reaction heat simulation loop, and the electric heater was turned off. As the circulation pump introduces only a small amount of heat, which can be ignored, theoretically the temperature of the reactor must be equal to the temperature measured after the heater in steady state and only dead time can be the difference in transient state. As it can be seen in Figure 2.29 not only dynamic but also static difference occurs between the two measured temperatures. It can be explained with the different constructions and the different flow characteristics around the two instruments. The thermometer for measuring the reactor temperature has a high wall thickness that causes high response time. The thermometer in the ½" pipe elbow after the heater has no industrial thermowell. The resistance sensor with a ceramic coating is directly installed in a preconfigured small pipe in the elbow that has a low wall thickness. This construction results in a low response time.

In steady state the static difference between the measured temperatures are always below 1 °C, which is a slight difference. However, when using the temperature difference for calculations this can cause significant error. A small difference in the material of the sensors can cause this difference, which can be corrected by recalibration or by offsetting its value.

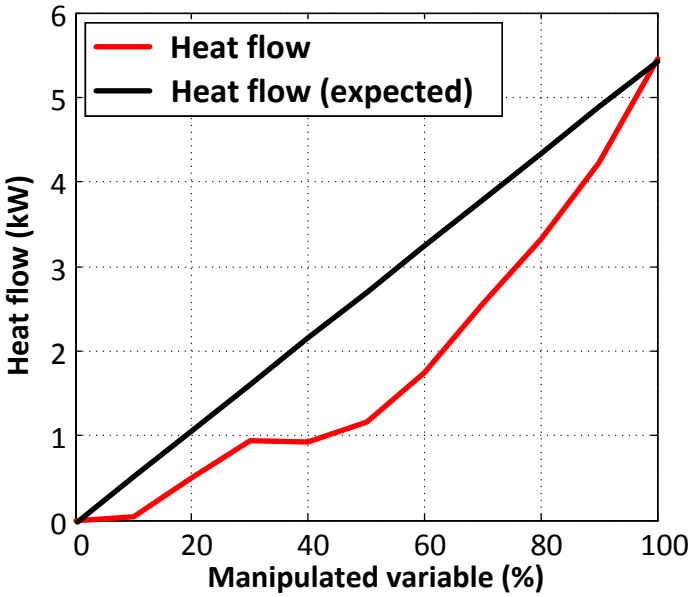

Figure 2.28: The expected and calculated (from raw data) heat flow characteristics of the electric heater

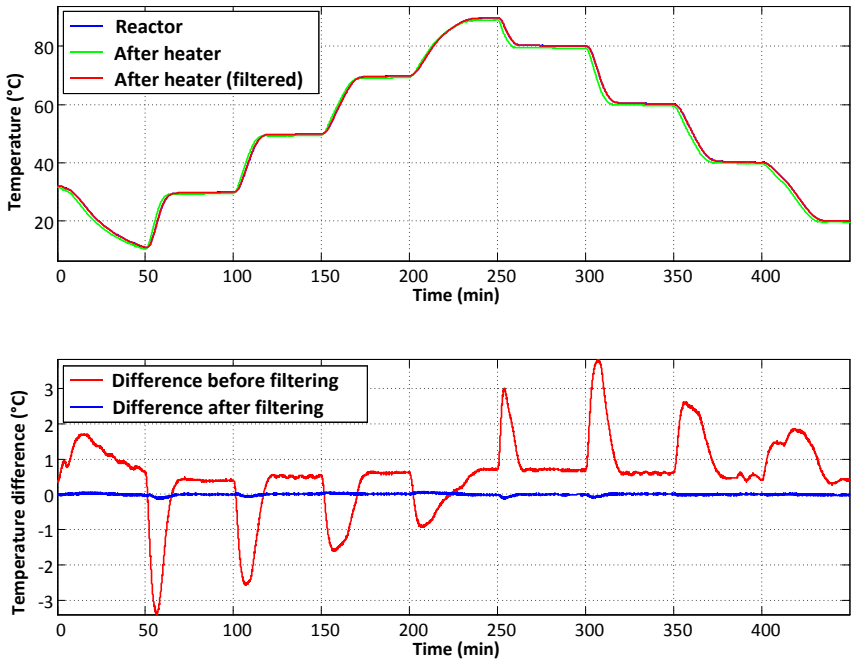

Figure 2.29: Measurement for identifying the parameters of the temperature-dependent offset and the first-order exponential filter

To achieve more accurate heat flow calculations both thermometers have to have the same dynamic and steady-state behaviour. There are two possible ways to achieve the same dynamic behaviour. The thermometer with higher response time can be modified to be faster; however this is very difficult to perform and the disturbance would be amplified. The other way is to slow down the thermometer with low response time to meet the dynamics of the thermometer with high response time. This can be performed easily by filtering; however the accuracy

will be lower for the calculated heat flow in transient states. The offset between the two thermometers could be achieved by adding a constant value to either of them; however as it can be seen in Figure 2.29 this difference is not only a constant value, but depends on the actual temperature. Therefore, the offset was described by a second order function that can be seen in Equation (2.3). Accordingly, the modifications effectuated on the temperature value of the thermometer after the heater can be seen in Figure 2.30. The raw value is modified first by adding a temperature-dependent bias; then it is filtered by a first order exponential filter.

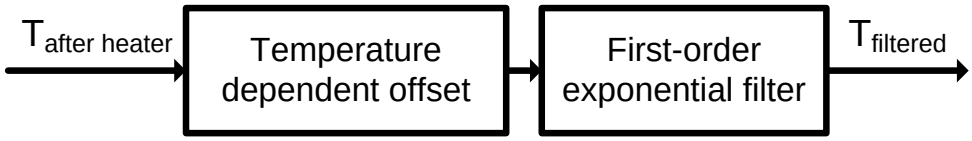

Figure 2.30: The modules for compensating the measured raw temperature signal of the thermometer after the heater

The equation for calculating the temperature-dependent offset:

$$Offset = a \cdot T_{reactor}^2 + b \cdot T_{reactor} + bias \qquad (2.3)$$

The data of the test measurement in Figure 2.29 was used to identify the parameters of the temperature-dependent offset and the tuning parameter of the exponential filter. The identification was performed with numerical optimisation using MATLAB/Simulink. The parameters of the second order equation describing the temperature-dependent offset can be seen in Table 2.5. The bias values depending on the actual temperature can be seen in Figure 2.31.

For the tuning parameter of the exponential filter the following value was identified:

$$\alpha = 0.0098$$

Table 2.5: The parameters of the temperature-dependent offset

Parameter	Value
a	$2.48 \cdot 10^{-5}$
b	0.0026
bias	0.3184

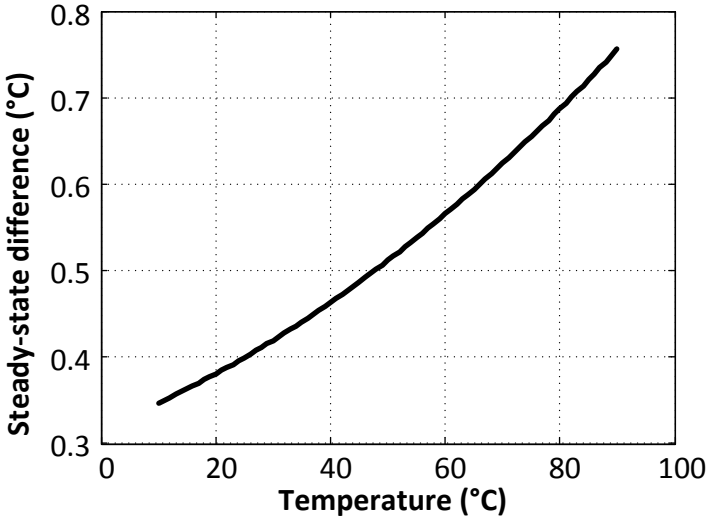

Figure 2.31: The temperature-dependent offset between the $T_{reactor}$ and $T_{after\ heater}$

After implementing the offset and filter on the temperature measurement after the electric heater, another test measurement was performed to record the heat flow characteristic of the heater. The manipulated variable of the electric heater was modified first from 0-100% increasingly then decreasingly to 0% with 10% stepping. The time of the steps was chosen to achieve steady state in all steps. The results of this test measurement can be seen in Figure 2.32, where also the raw temperature values and raw calculated heat flow can be seen. The raw values compared with the treated ones show significant differences, which can be also noticed in the resulting heater characteristic curve in Figure 2.33.

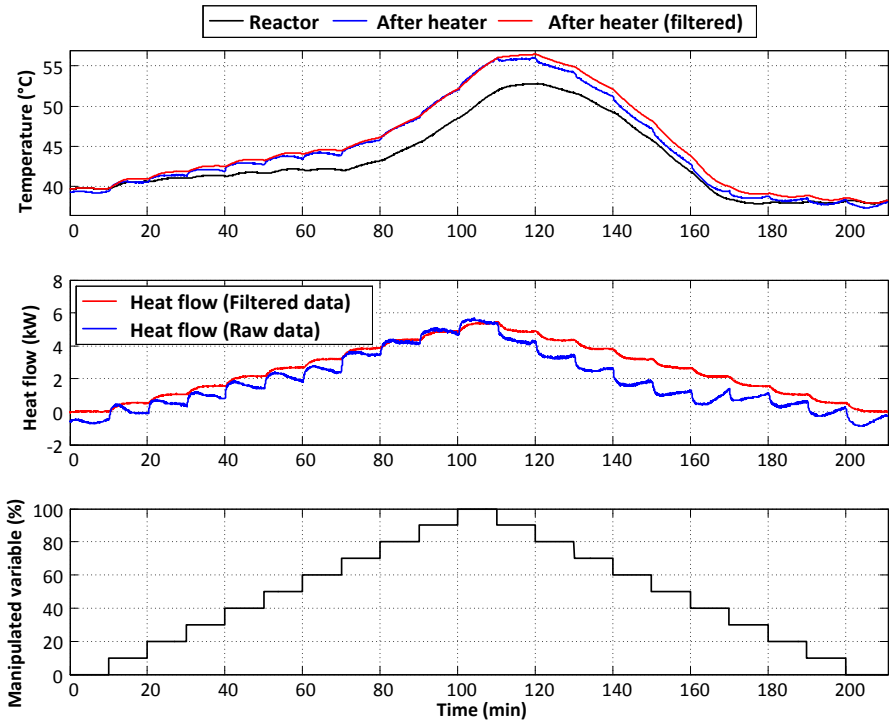

Figure 2.32: Measurement for recording the output heat flow of the electric heater

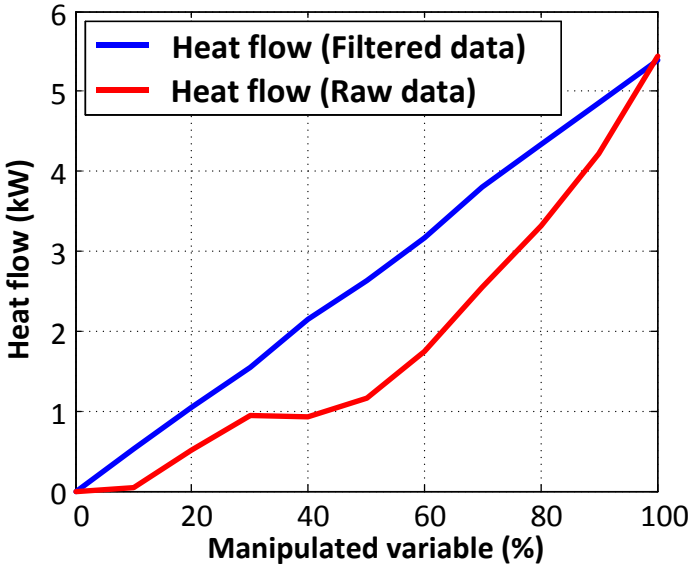

Figure 2.33: The heat flow characteristics of the electric heater calculated from both the raw and filtered data

The heat flow characteristic by filtering the temperature signal after the heater can be seen in Figure 2.33. This correlation between the manipulated variable of the electric heater and the generated heat flow can be expressed with a simple linear equation (Equation (2.4)).

$$\dot{Q}_{rs} = 0.05 \cdot MV_{heater} \tag{2.4}$$

3. Simulation models with different levels of detail

In the modelling of batch systems different levels of detail can be achieved. For distinct purposes different levels of detail might be sufficient. The higher detailed the model the more time and effort are needed for the design, identification and solving. However, the provided results can be more accurate compared with simple models. The problem for which the model is used determines the level of detail. For example if the task is to perform a rough order of magnitude estimation on the dynamics of the batch reactor it is unnecessary and inefficient to use highly detailed models (boxed process simulators); mass and heat balance equations with constant parameters and several simplifications are sufficient for the precision of these estimations. These types of models can support the estimation of the dynamics of batch reactors, and they can be useful in the design; in addition with some slight extension and a more detailed model the operation of the reactor can be supported.

The expectations for models used in controllers are quite different from other purposes. The main requirement for these types of models is to keep them as simple as possible, i.e., ignore all the phenomena that have minor impact on the output. Therefore, the models are easier to handle; need less calculation capacity, which is highly important in model-based controllers; and the implementation is simpler and takes less engineering hours.

According to these considerations, models with different levels of detail were developed for different purposes. In the following chapters two reactor models will be presented. The first model was created with the aim to support quick engineering calculations and reactor temperature controller retuning using the model of the reactor and measurement data. Therefore, some effects were ignored in the model (for example, the heat capacity of the reactor wall).

The second simulation model was created in a boxed simulation software allowing in-detail modelling of the reactor, including the calculation of temperature-dependent media properties, pressure gradient, hydrostatic pressure, heat loss, and additional calculations. A detailed heat transfer coefficient calculation will be also presented in this solution.

Compared to these two modelling solutions the models used in the split-range algorithms in Chapter 4 are much simpler. As the models for controller use have different requisites, all the possible effects were ignored.

3.1. Simplified reactor model

A user-friendly application was created in Microsoft Excel and MATLAB with the aim to support the hereinbefore-mentioned purposes in a widely used and known software environment. In this chapter the MS Excel-based application and the implemented models will be described.

If the aim is to perform quick and rough-order calculations, in most cases simple mass and heat-balance models are sufficient for this purpose, which contain several simplifications regarding reactor geometrics, temperature dependency of fluid properties, fluid viscosity, ideal mixing, and other considerations. One of the essential balance equations is the mass balance of the

reactor mixture, which is the base of the model (3.1). The reactor has two possible feed streams and no output streams.

$$\frac{dm_{reactor}}{dt} = F_{feed1} \cdot \rho_{feed1} + F_{feed2} \cdot \rho_{feed2} \tag{3.1}$$

In this model as one of the simplifications, the jacket of the reactor is handled as a single heat transfer area with the same temperature on every point of its surface. No temperature distribution or residence time was considered. Accordingly, the temperature of the jacket can be calculated by Equation (3.2).

$$\overline{T}_{jacket} = \frac{T_{jacket}^{in} + T_{jacket}^{out}}{2} \tag{3.2}$$

The heat balance of the reactor consists of five elements that can be seen in Equation (3.3), where the temperature change of the reactor is already expressed. These elements are namely the heat flow between the wall of the reactor and the reaction mixture (Equation (3.4)), the heat loss (Equation (3.5)), the two feed streams (Equation (3.6) and (3.7)) and the calibrating heat flow ($\dot{Q}_{cal}$).

$$\frac{dT_{reactor}}{dt} = \frac{\dot{Q}_{wall} + \dot{Q}_{heat\,loss} + \dot{Q}_{feed1} + \dot{Q}_{feed2} + \dot{Q}_{cal}}{m_{reactor} \cdot c_p^{rm}} \tag{3.3}$$

$$\dot{Q}_{wall} = UA_{wall} \cdot \left(\overline{T}_{jacket} - T_{reactor}\right) \tag{3.4}$$

$$\dot{Q}_{heat\,loss} = UA_{heat\,loss} \cdot \left(T_{ambient} - T_{reactor}\right) \tag{3.5}$$

$$\dot{Q}_{feed1} = c_p^{feed1} \cdot F_{feed1} \cdot \rho_{feed1} \cdot \left(T_{feed1} - T_{reactor}\right) \tag{3.6}$$

$$\dot{Q}_{feed2} = c_p^{feed2} \cdot F_{feed2} \cdot \rho_{feed2} \cdot \left(T_{feed2} - T_{reactor}\right) \tag{3.7}$$

The variable UA_{wall} is responsible for describing the heat transfer between the wall of the reactor and the reaction mixture. It is the product of the heat transfer coefficient and the heat transfer area. It is calculated by Equation (3.8), and as it can be seen, it depends on the reactor temperature and the speed of the agitator.

$$UA_{wall} = a + b \cdot T_{reactor} + c \cdot n_{agitator} \tag{3.8}$$

The variable $UA_{heat\,loss}$ is responsible for describing the heat transfer between the reactor body and the environment. It is also the product of a heat transfer coefficient and the heat transfer area of this phenomenon. It only depends on the temperature of the reactor and can be calculated by Equation (3.9).

$$UA_{heat\,loss} = d + e \cdot T_{reactor} \tag{3.9}$$

The specific heat of the reaction mixture can also depend on the temperature of the reactor, thus, it can be calculated by Equation (3.10).

$$c_p^{rm} = f + g \cdot T_{reactor} \tag{3.10}$$

The application

A user-friendly application was developed with the aim to provide industrial engineers with an easy-to-use tool for the identification of batch reactor parameters, which can be used as well as in design and operation. The application is based on the previously described reactor model. It has several functions generated mainly by industrial demands. The logo of the application can be seen in Figure 3.1, where its name BRIEW is an acronym for Batch Reactor Identification Excel Workbook.

The application can be used in the case of a reactor configuration alike in Figure 3.2, which is suitable for most of the reactors in the industry. It is mandatory to have jacket inlet, outlet and reactor temperature measurement in the analysed system; the measurement of feed temperatures and flow rates as well as the agitator speed are optional.

The application has the following functionalities:

- Offline identification of the thermal parameters of a batch reactor using measurement data
- Calculating PID parameters for the temperature controller of the reactor using the previously identified thermal parameters
- Heating-up simulation
- Offline reaction heat flow calculation

Figure 3.1: The logo of the batch reactor thermal parameter identifying application

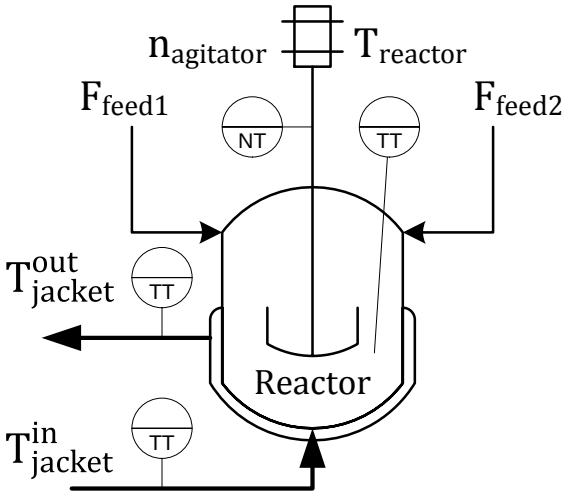

Figure 3.2: The batch reactor configuration feasible for BRIEW

Identification of the thermal parameters

The first and most important functionality of BRIEW is the offline identification of the thermal parameters from measurement data. The following time-dependent data is necessary to accomplish the identification:

- Reactor temperature
- Jacket inlet temperature
- Jacket outlet temperature
- Agitator speed
- Feed 1 flow rate
- Feed 2 flow rate
- Calibration heater state
- Ambient temperature

However, to provide a more universal solution that can be used in the case of different reactor configurations, some of the time-dependent data can be ignored or set constant. Thus, if one of the necessary measurements is not available in the analysed technology the identification can be still performed but at the cost of accuracy. These are the following:

- Agitator speed: can be set to a constant value
- Feed 1 flow rate: can be set to zero or to a constant value
- Feed 2 flow rate: can be set to zero or to a constant value
- Calibration heater: can be set to on/off in the entire time range
- Ambient temperature: can be set to a constant value

The worksheet called “Data_assignment” has the purpose to navigate the collecting of necessary time-dependent data for the identification process. The measurement data can be selected from the “Data” worksheet that contains raw data, the previously mentioned settings can be performed and also the time range used for the identification can be selected. This worksheet can be seen in Figure 3.3.

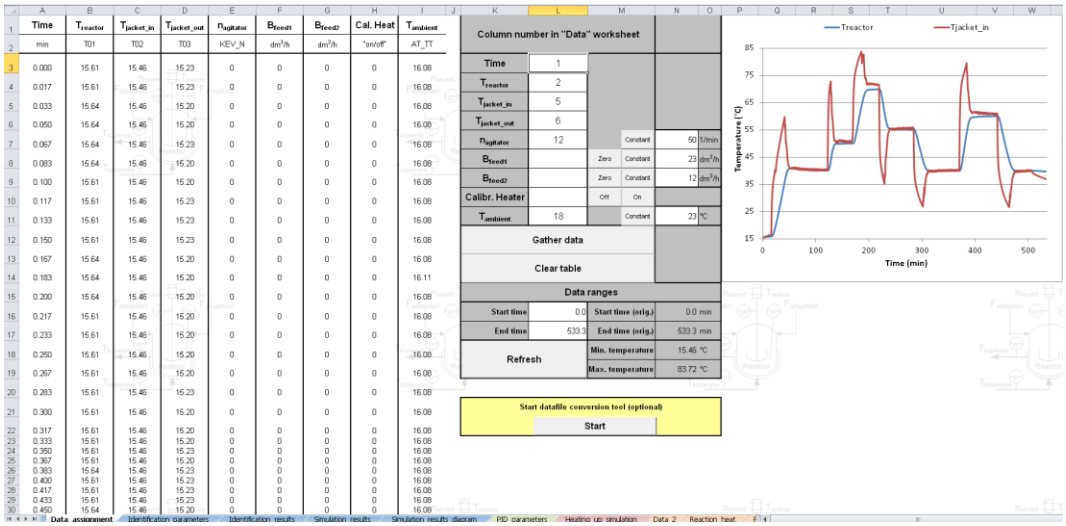

Figure 3.3: The worksheet for composing the required data

The next step in setting up the identification can be found in the worksheet called “Identification_parameters”. The dependencies of the variables UA_{wall}, $UA_{heatloss}$, and the specific heat of the reaction mixture can be defined. Also the parameters to be identified can be chosen here, as there might be some information available from previous measurements, specification datasheets, or from literature. The initial value for each parameter is also to be defined as it might affect the optimization algorithm, or in the case of a variable that is out of the scope of the identification, the initial value will be used in the calculations. The conditions of the used measurement are also needed to be defined in this worksheet, namely the initial reactor load weight, temperature, density, specific heat values of the feed streams, and the heat flow of the calibrating heater. Of course if the flow rates of the feed streams were set to zero or the calibrating heater was off in the whole time range then defining these conditions are unnecessary.

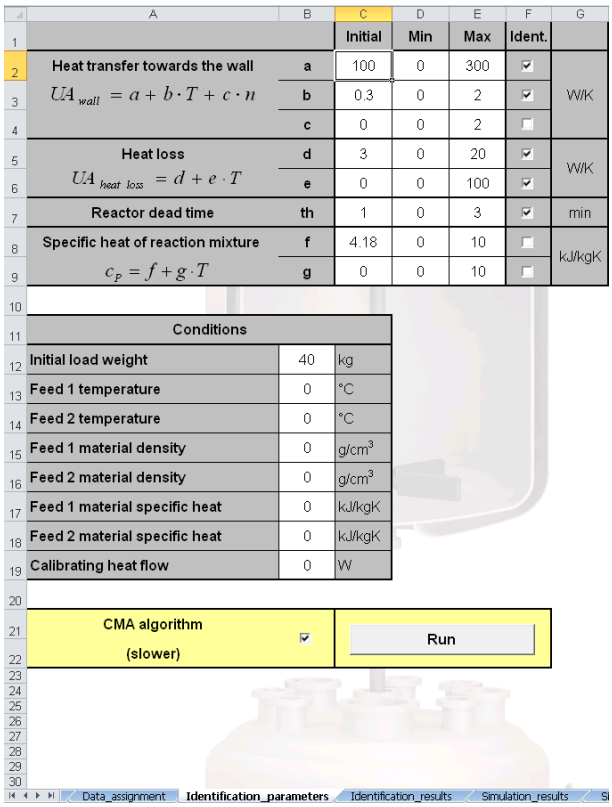

		Initial	Min	Max	Ident.	
Heat transfer towards the wall $UA_{wall} = a + b \cdot T + c \cdot n$	a	100	0	300	☑	W/K
	b	0.3	0	2	☑	
	c	0	0	2	☐	
Heat loss $UA_{heat\ loss} = d + e \cdot T$	d	3	0	20	☑	W/K
	e	0	0	100	☑	
Reactor dead time	th	1	0	3	☑	min
Specific heat of reaction mixture $c_P = f + g \cdot T$	f	4.18	0	10	☐	kJ/kgK
	g	0	0	10	☐	

Conditions		
Initial load weight	40	kg
Feed 1 temperature	0	°C
Feed 2 temperature	0	°C
Feed 1 material density	0	g/cm^3
Feed 2 material density	0	g/cm^3
Feed 1 material specific heat	0	kJ/kgK
Feed 2 material specific heat	0	kJ/kgK
Calibrating heat flow	0	W

CMA algorithm (slower) ☑ Run

Data_assignment | Identification_parameters | Identification_results | Simulation_results

Figure 3.4: The worksheet for choosing the desired equations, limits of the parameters, and the conditions of the used measurement

Two optimization algorithms are available to minimize the value of the objective function and to find the desired parameters. The default solver algorithm in this application uses a constrained local NLP (Nonlinear programming) solver from MATLAB Optimization toolbox (fmincon). This solver uses a sequential quadratic programming (SQP) method where a quadratic programming (QP) sub-problem is solved in each iteration, which makes the complex optimization problem simpler. SQP methods are stabilized by a monotone line search procedure subject to a suitable merit function. An estimate of the Hessian of the Lagrangian is updated in each iteration using the BFGS formula (BRIEW). The main limitation of this algorithm is that it might give local solutions. This is the reason why defining the initial values for the parameters to be identified are an important step in the identification process.

To overcome this limitation another optimization algorithm was implemented in the application, namely an Evolutionary Algorithm (EA), the Covariant Matrix Adaptation Evolutionary Strategy (CMA-ES) was implemented. The EA is an optimization method that is based on the natural selection and survival of the fittest as it works in the real world. EAs consistently perform well approximating solutions to all types of problems since they do not make any assumption about the underlying fitness landscape. Accordingly this makes EAs applicable in different fields of science [49]. Learning the covariance matrix in the CMA-ES can improve the performance on ill-conditioned and/or non-separable problems by orders of magnitude. In contrast to most other evolutionary algorithms, the CMA-ES is, from the users' perspective, quasi parameter free. However, the population size can be adjusted by the user in order to change the characteristic search behaviour. [50], [51], [52]

Applying this algorithm, the probability of finding a global minimum of the objective function is significantly higher. However the solving time of the same problem is higher compared to the SQP algorithm.

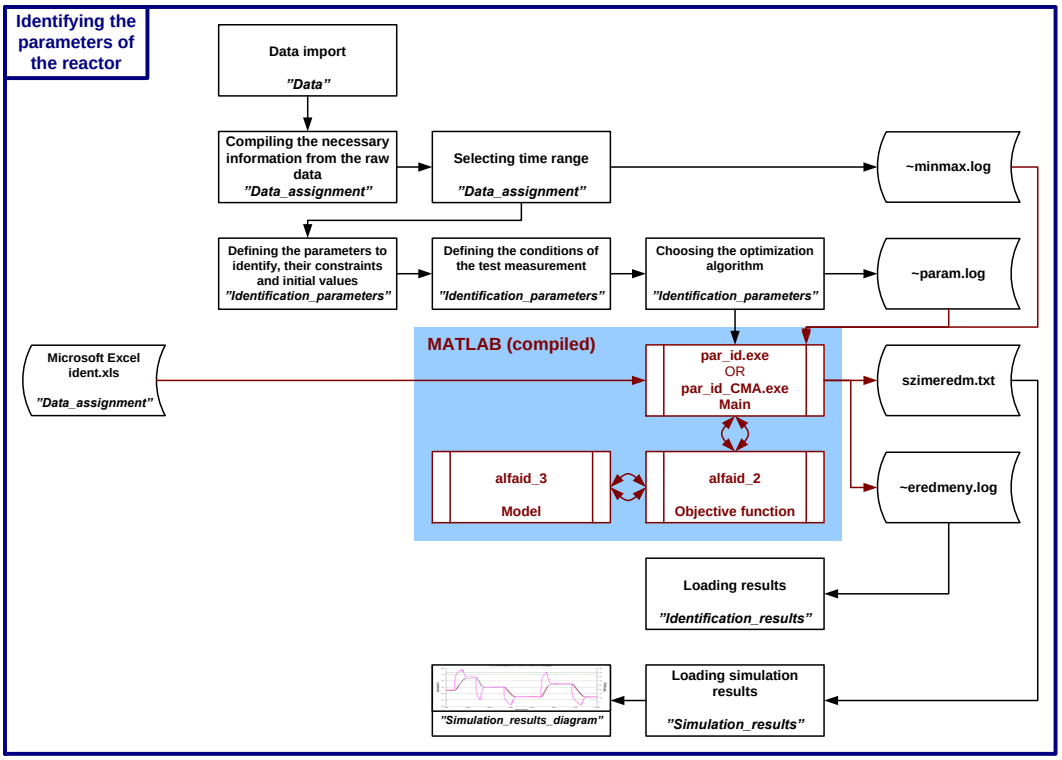

Figure 3.5: The flowsheet of the thermal parameter identification

The flowsheet of the reactor thermal parameter identification process can be seen in Figure 3.5. Three worksheets are used for data assignment, defining conditions and parameters of the identification. The optimization algorithm is implemented in MATLAB, which is available for the MS Excel workbook in a C++ compiled executable format, thus no MATLAB installation is needed to use this application. The MS Excel workbook communicates with the MATLAB executable through text files. Three worksheets have the purpose to present the results of the identification. The resulting thermal parameters are available on the worksheet "Identification_results", which has two versions depending on the initial settings of the identification. If the variable UA_{wall} is set to depend only on reactor temperature, the worksheets can be seen in Figure 3.6, where a two dimensional diagram shows the results. If the agitator dependency is also included then the result can only be visualized on a three-dimensional diagram as it can be seen in Figure 3.7. In both cases the results are also available in a table format.

In worksheet "Simulation_results" (Figure 3.8) the results of a simulation can be found; the simulation was performed with the previously described model and the resulting thermal parameters using the measurement data for identification. The results include the change of the reactor load weight and also the reactor temperature as the results of the two differential equations included in the reactor model.

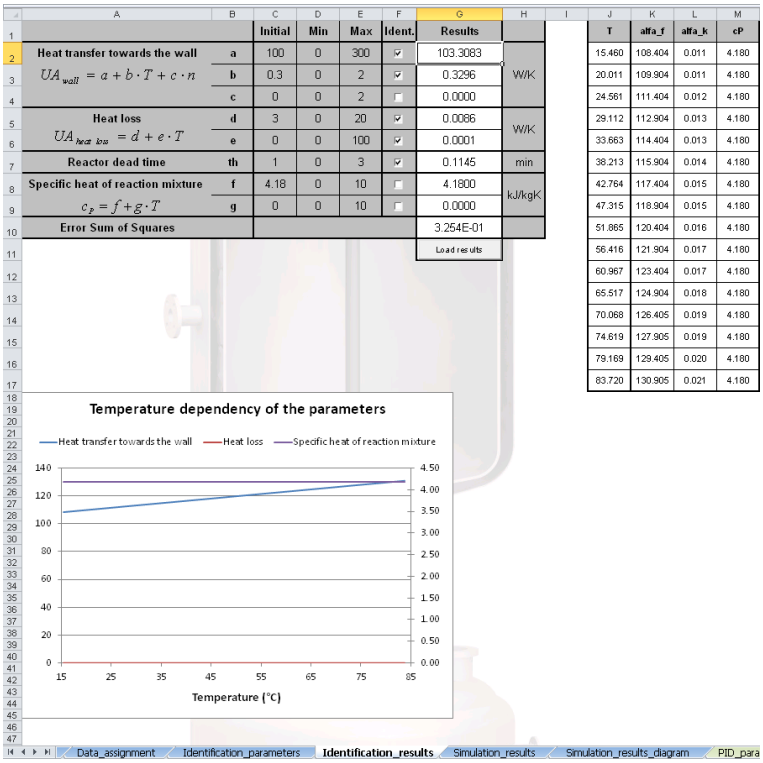

Figure 3.6: The worksheet showing the results of the identification with temperature dependency only

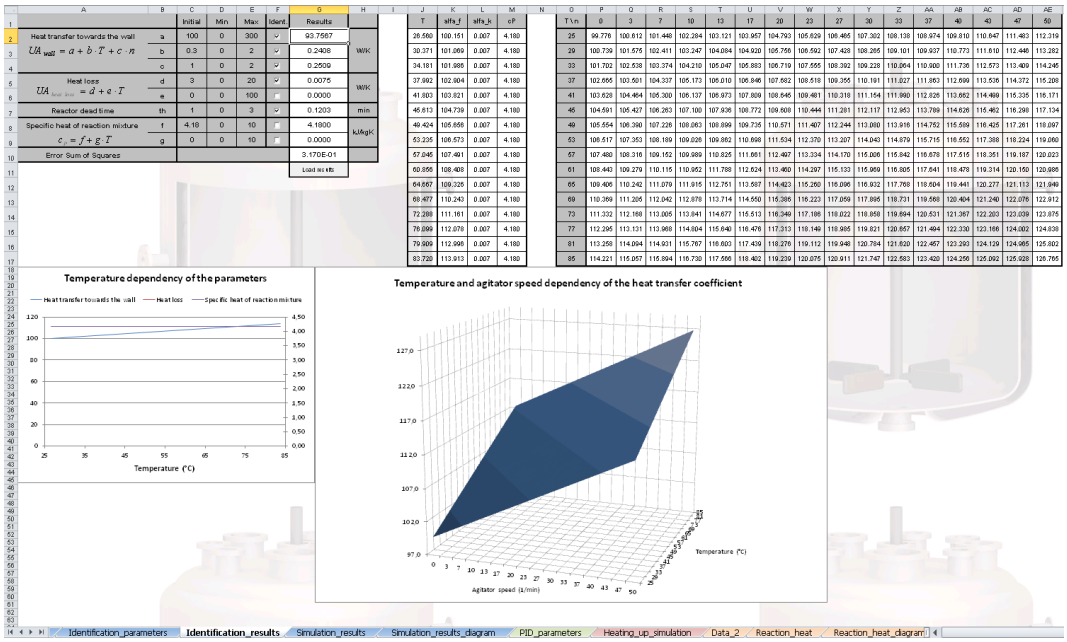

Figure 3.7: The worksheet showing the results of the identification with temperature and agitator speed dependency

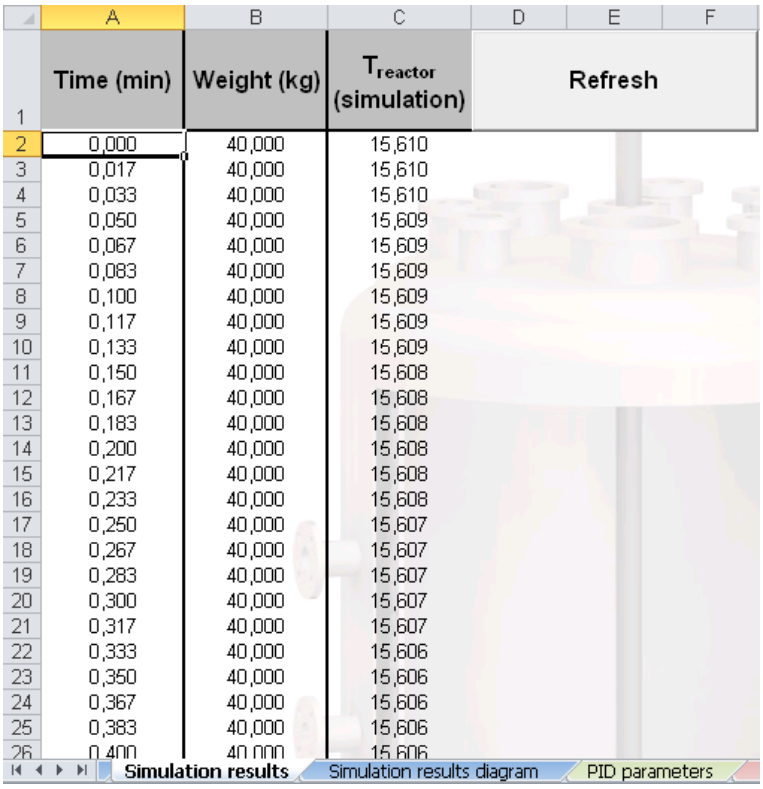

	A	B	C	D	E	F
1	Time (min)	Weight (kg)	$T_{reactor}$ (simulation)	Refresh		
2	0,000	40,000	15,610			
3	0,017	40,000	15,610			
4	0,033	40,000	15,610			
5	0,050	40,000	15,609			
6	0,067	40,000	15,609			
7	0,083	40,000	15,609			
8	0,100	40,000	15,609			
9	0,117	40,000	15,609			
10	0,133	40,000	15,609			
11	0,150	40,000	15,608			
12	0,167	40,000	15,608			
13	0,183	40,000	15,608			
14	0,200	40,000	15,608			
15	0,217	40,000	15,608			
16	0,233	40,000	15,608			
17	0,250	40,000	15,607			
18	0,267	40,000	15,607			
19	0,283	40,000	15,607			
20	0,300	40,000	15,607			
21	0,317	40,000	15,607			
22	0,333	40,000	15,606			
23	0,350	40,000	15,606			
24	0,367	40,000	15,606			
25	0,383	40,000	15,606			
26	0,400	40,000	15,606			

Figure 3.8: The worksheet for the simulation results

PID controller design

The other major functionality of the application is to calculate the PID parameters of the reactor temperature controller using the previously identified reactor model. From the results of the identification the transfer function between the jacket and reactor temperate can be determined. This can be the input for a PID design algorithm to determine the controller parameters. In this application the direct synthesis method is used.

This functionality is available in the "PID_parameters" worksheet (Figure 3.9), where basically the parameters of the first order plus dead time transfer function can be calculated, which are the base of several PID design algorithms. Three additional values are also necessary to calculate the PID parameters, which are the following:

- Characteristic temperature: The temperature where the controller should work most efficiently.
- Characteristic agitator speed: A characteristic agitator speed.
- Characteristic load weight: The load of the reactor where the controller should perform the most efficiently.

The characteristic values are necessary especially when the heat transfer coefficients depend on the temperature of the reactor and the agitator speed and also when operating the reactor in fed-batch mode, since the optimal PID parameters would change depending on the state of the reactor.

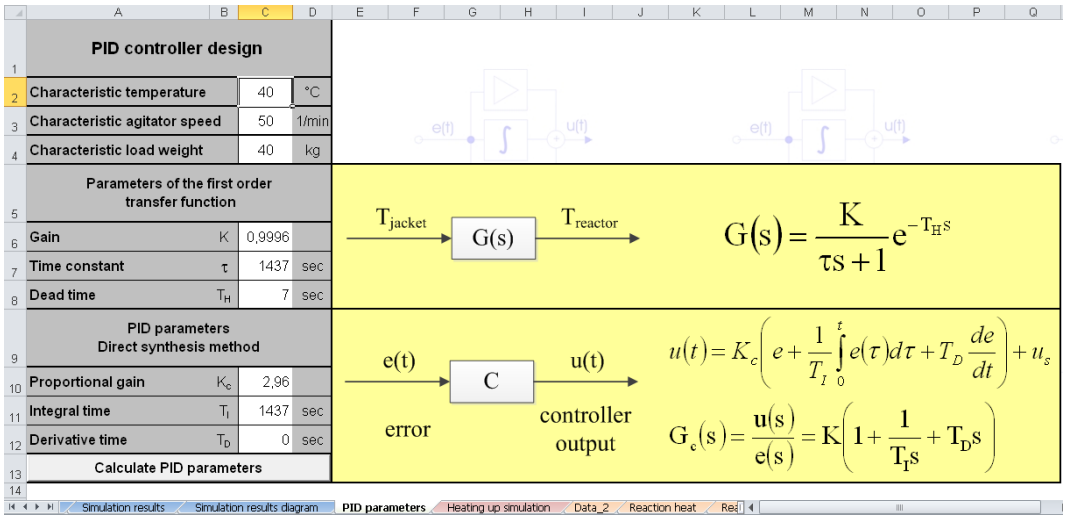

Figure 3.9: The worksheet for calculating PID parameters

The parameters of the first order plus dead time transfer function (Equation (3.11)) are calculated according to Equation (3.12) and (3.13). The determination of the reactor dead time is performed during the previous identification process.

$$G(s) = \frac{K}{\tau \cdot s + 1} \tag{3.11}$$

$$K = \frac{UA_{wall}}{UA_{wall} + UA_{heat\,loss}} \tag{3.12}$$

$$\tau = \frac{m_{reactor} \cdot c_p^{rm}}{UA_{wall} + UA_{heat\,loss}} \tag{3.13}$$

The PID parameters are calculated with the following equations using the direct synthesis method:

$$K_C = \frac{1}{K} \cdot \frac{\tau}{\tau_C + \tau_H} \text{ , where } \tau_C = \frac{\tau}{3} \tag{3.14}$$

$$\tau_I = \tau \tag{3.15}$$

$$\tau_D = 0 \tag{3.16}$$

Heating-up simulation

Beside the two main functionalities described previously, two additional functions are also available in the application. After opening the Excel workbook a pop-up window appears where the two optional functions can be turned on, as can be seen in Figure 3.10.

The reactor heating-up simulation can be a useful tool in analysing operational problems or in the design of recipes. The heating-up simulation can be performed using the previously identified parameters or with user-defined thermal parameters. This can provide quick information about the heating-up time of the reactor in given conditions.

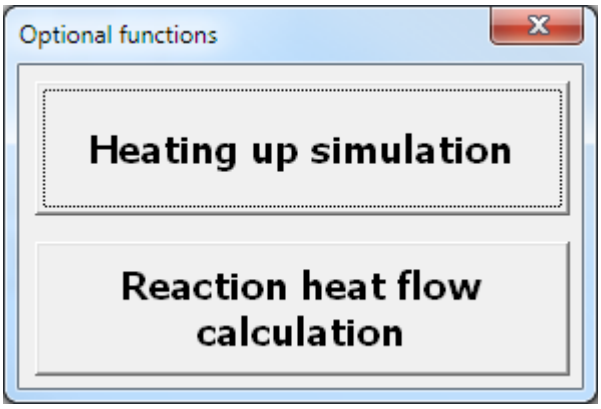

Figure 3.10: Pop-up window for choosing optional functions

The flowsheet of the heating-up simulation can be seen in Figure 3.11. It also uses a C++ compiled executable file that was created in MATLAB, and communicates with Excel through text files. For the simulation of the reactor it uses the same model that was described previously.

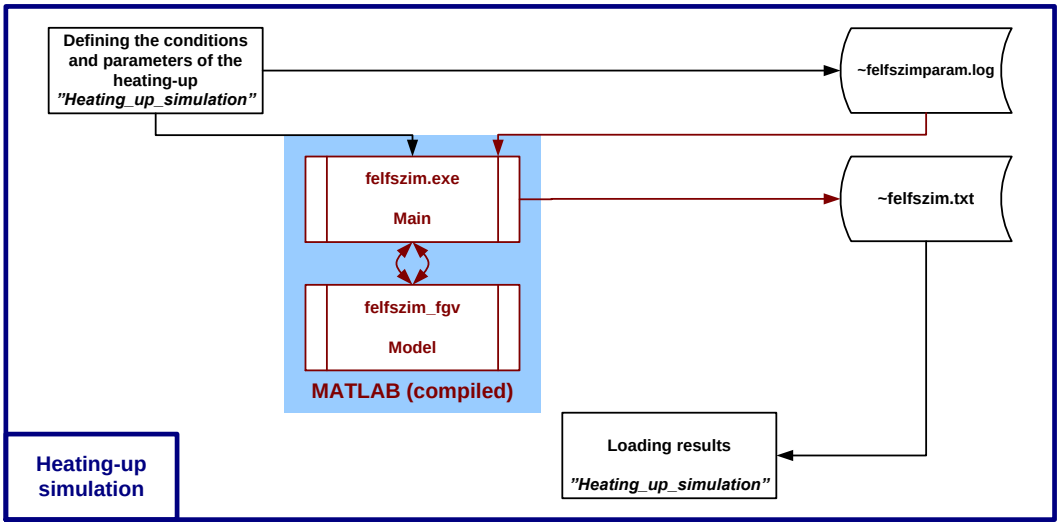

Figure 3.11: The flowsheet of the reactor heating-up simulation

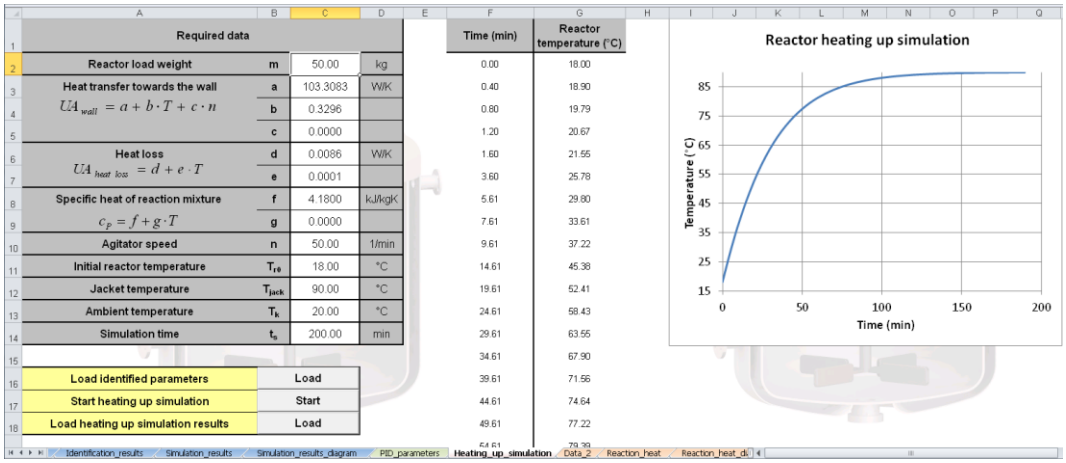

Figure 3.12: The worksheet for the heating-up simulation of the reactor

The necessary thermal parameters can be defined by loading the previous identification results or by entering user-defined values in the worksheet called

"Heating_up_simulation" (Figure 3.12). After running the simulation the results can also be loaded to this worksheet into a table and visualized on a diagram.

Reaction heat flow calculation

The fourth sub-application in the Excel workbook is a reaction heat flow calculating module. This functionality can be used to calculate reaction heat flow from measurement data, where reaction was performed in the reactor. Reaction heat flow can be calculated using the previously identified reactor thermal parameters where measurement data without chemical reaction should be used. Using these parameters in the reactor model on such measurement data where reaction was performed, the reaction heat flow can be derived. This information can be useful in recipe design as well as in the temperature control of the reactor.

All of the previously described model equations remain identical except Equation (3.3), which contains the heat balance of the reactor. As it can be seen in Equation (3.17) it is extended with a $\dot{Q}_{reaction}$ part that represents the heat source tag of the reaction. To solve this model and to derive the reaction heat flow, it has to be discretized, which can be seen in Equation (3.18) and (3.19). On the other hand Equation (3.19) still cannot be solved due to two unknown variables namely $T_{reactor}^{k+1}$ and $\dot{Q}_{reaction}^{k}$. However, with the use of the measurement data with reaction and an inverting rule that can be seen in Equation (3.20), after discretization in Equation (3.21) the reaction heat flow can be derived. The resulting equation for calculating the reaction heat flow can be seen in Equation (3.22). The variable τ_r used in Equation (3.20) is the inverting time constant, which is predefined in the algorithm and cannot be changed by the user.

$$\frac{dT_{reactor}}{dt} = \frac{\dot{Q}_{wall} + \dot{Q}_{heat\,loss} + \dot{Q}_{feed1} + \dot{Q}_{feed2} + \dot{Q}_{cal} + \dot{Q}_{reaction}}{m_{reactor} \cdot c_p^{rm}} \tag{3.17}$$

$$\frac{T_{reactor}^{k+1} - T_{reactor}^{k}}{\Delta t} = f^{k} + \frac{\dot{Q}_{reaction}^{k}}{m_{reactor}^{k} \cdot c_P^{rm\,k}}, \text{ where}$$
$$f^{k} = \frac{\dot{Q}_{wall}^{k} + \dot{Q}_{heat\,loss}^{k} + \dot{Q}_{feed1}^{k} + \dot{Q}_{feed2}^{k} + \dot{Q}_{cal}^{k}}{m_{reactor}^{k} \cdot c_P^{rm\,k}} \tag{3.18}$$

$$T_{reactor}^{k+1} = \left(f^{k} + \frac{\dot{Q}_{reaction}^{k}}{m_{reactor}^{k} \cdot c_P^{rm\,k}} \right) \cdot \Delta t + T_{reactor}^{k} \tag{3.19}$$

$$T_{reactor\_m} = T_{reactor} + \tau_r \cdot \frac{dT_{reactor}}{dt} \tag{3.20}$$

$$T_{reactor\_m}^{k} = T_{reactor}^{k} + \tau_r \cdot \frac{T_{reactor}^{k+1} - T_{reactor}^{k}}{\Delta t} \tag{3.21}$$

$$\dot{Q}_{reaction}^{k} = \left(\frac{T_{reactor\_m}^{k} - T_{reactor}^{k}}{\tau_r} - f^{k} \right) \cdot m_{reactor}^{k} \cdot c_P^{rm\,k} \tag{3.22}$$

The reaction heat flow calculation is performed in every time step when measurement data is available. The calculation process can be visualized by the flowchart in Figure 3.13. The flowsheet of the calculation process in the Excel workbook can be seen in Figure 3.14. The reaction heat flow calculation is implemented in a compiled C++ executable file created in MATLAB and it communicates with the Excel workbook through a text file. The structure of the worksheet "Reaction_heat" is very similar to "Data_assigment", since the data assignment of the measurement data with the reaction has to be done here to produce the input for the calculation. Also the desired time range and the conditions of the measurement have to be defined. The results can be loaded to a table and visualized in a diagram as can be seen in Figure 3.15.

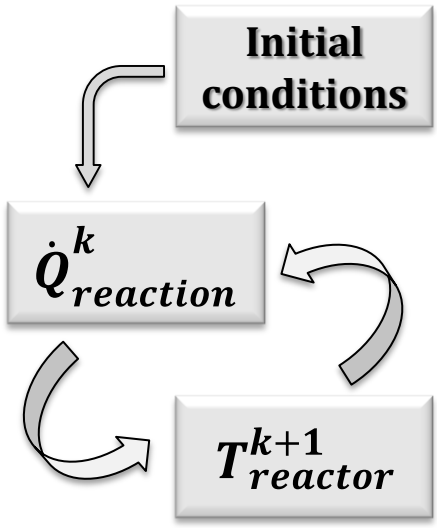

Figure 3.13: The calculation process of the reaction heat flow

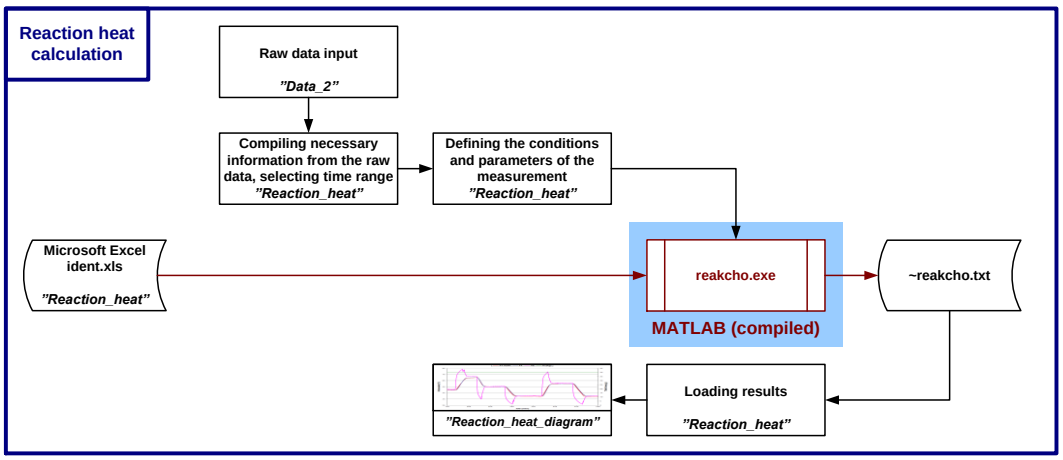

Figure 3.14: The flowsheet of the reaction heat calculation

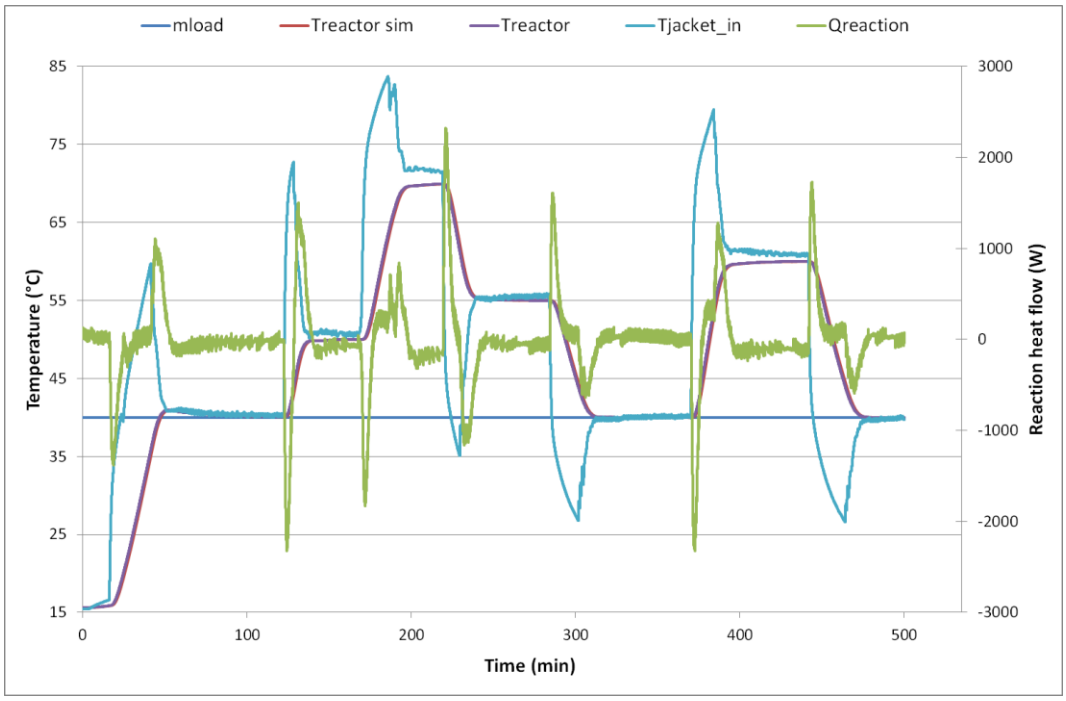

Figure 3.15: Resulting diagram of the reaction heat flow calculation

The measurement used for heat flow calculation was carried out without any chemical reactions in the reactor and also no reaction heat flow was simulated. Thus, it was expected to get zero reaction heat flow as result. However, as it can be seen in Figure 3.15 there are several peak heat flow values that occur in the case of drastic jacket temperature change. The magnitude of these peaks can be compared with the heat flow through the reactor wall. This heat flow can be estimated as we consider the UA_{wall} coefficient constant (120 W/K) and estimate the highest temperature difference between the reactor and the jacket (~30°C) (occurs at the change in the set-point of the reactor). According to Equation (3.4) the heat flow can be estimated ± 3600 W. Consequently, these peak values are comparable with the heat flow through the reactor wall, and thus the modelling error in dynamic sections is quite high. Near-zero reaction heat flow only occurs when no drastic change can be noticed in the jacket temperatures.

In this application as it was described previously in the model equations, only a simplified reactor model was implemented, and there were no thermometer models included. The thermometers of the system have different dynamic behaviour; therefore, accurate heat flow calculations can only be performed with tuned thermometers as it was described in Chapter 2.4. The values of the thermometers can be used in classical temperature control without such problems; however if it is used for advanced calculations, signal conditioning is essential. The effect of including the models of the thermometers in the model of the reactor will be described in the next chapter.

3.2. Detailed process model

If the in-depth analysis of a system is essential to reach our objectives and the accuracy of the simpler models are not enough, detailed process simulators can be useful and user-friendly alternatives for this task. Several different process simulators are available on the market as was described in Chapter 1.2, where general purpose, ones with rich model database, and specialized applications can be found as well. Also, for batch processes several possibilities are available. A dynamic process simulator was chosen for the focus of the analysis that is widely used in the industry, has a wide range of built-in models and has the possibility to implement self-developed models in the simulator. The chosen simulation software was UniSim Design from Honeywell, which is widely used in OTS applications as the process model of the system.

UniSim Design simulation software is mainly used to simulate continuous processes. In the case of batch technologies, it has some limitations. For example, it does not contain a built-in jacketed reactor, and there are difficulties with the online exportation of time-dependent data to third-party software in dynamic mode. Nonetheless, some examples can be found in the literature [53].

In the case of batch technologies, the model building process also differs from the conventional method used at the continuous technologies, where first a steady-state model is created, and from the steady-state operating mode, it is switched to dynamic mode. In a batch processing unit steady state can be difficult to interpret, as steady-state operation is abnormal and can be difficult to perform. Therefore, the model had to be built in dynamic mode, where UniSim Design provided a suitable framework.

If the aim is to build a process model with a dynamic behaviour very similar to the real system, it is a proven method to approximate the results of a test measurement on the real system using a numerical optimisation algorithm. A defined objective function is minimised by modifying the adequate model parameters. This way the parameters affecting the behaviour of the analysed system can be determined. In certain systems, parameters from the literature (e.g., heat transfer and heat loss coefficient) often need corrections.

In such cases when a numerical optimisation algorithm cannot be applied and the parameters are to be determined using engineering intuition, the decomposition-coordination principle can be useful. During decomposition, the complex task is divided into several simpler subtasks, with the estimation of the coordinating parameters. After solving the subtasks, the complex task can be concluded by summing the subtasks using appropriate coordinating parameters.

The problem was solved without using a numerical optimisation algorithm. During the parameter identification, as many parameters as possible were defined by first principle knowledge. Thus, influence of the undefined parameters to the hydrodynamic and thermal behaviour of the system was easier to manage.

First, the parameters affecting the hydrodynamic behaviour of the system were identified in such a way that the monofluid loops in the process model would result in pressure and flow rate values nearly equal to those measured in the real system in both standalone and heating/cooling mode. In the case of the real system, the hydrodynamic behaviour is mainly affected by the resistances and pumps in each loop. The pumps were defined by first principle data (characteristic

curves). Hydrodynamic resistances consist of heat exchangers, pipe segments, and valves. In every loop of the monofluid thermoblock, a throttle valve on the recirculation stream can be found. Its aim is to adjust the flow rate of the jacket recirculation loop feed and the recirculating fluid in heating/cooling mode. The type of this throttle valve was known. However, the value of its hydrodynamic resistance in the process model was not defined by a priori data because all of the unknown resistances in its surroundings (pipe segments, pipe elbows) were incorporated into it. The hydrodynamic resistances of the plate-type heat exchangers and electric heaters located in the monofluid thermoblock loops were unknown. Thus, these were the parameters to be identified, with the aim of obtaining similar simulation results than the measured ones.

The parameters affecting the thermal behaviour of the system were identified after the identification of the hydrodynamic parameters. In the case of the monofluid thermoblock loops, the parameters affecting the thermal behaviour were the heating power of the electric heaters, the overall heat transfer coefficient of the plate heat exchanger, the cooling power of the refrigerator, the heat loss of the tanks, and the liquid level of the tanks. These parameters were initialised using a priori data; then they were modified to approximate the measurements performed for the identification of the thermal parameters.

Since UniSim Design does not contain a built-in module for modelling a jacketed batch reactor, an alternative modelling solution was implemented. First, the vessel of the jacketed batch reactor was modelled by connecting a heat exchanger and a continuous-stirred tank reactor (CSTR) with zero feed and outlet; then a probable, suitable built-in module was analysed that is a separator module extended with a tube bundle. However, little information was available about this module. Using packaged flowsheeting simulation software, little information is usually available about the built-in models. Thus, in some cases, their structure also has to be identified.

The thermal behaviour of the jacket recirculation loop is affected by the heat loss of the reactor and pipe segments as well as by the overall heat transfer coefficient between the reactor and its jacket. Thus, the aim was to find these values during parameter identification for different vessel-modelling solutions for the batch reactor.

Hydrodynamic parameters

At the first step (Figure 3.16), all of the equipment was added and connected with material streams according to the flowsheet shown in Figure 2.1. The detailed defining of the equipment was accomplished based on their technical specifications.

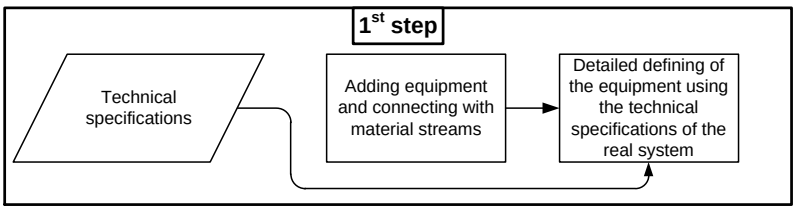

Figure 3.16. First step of building the process model

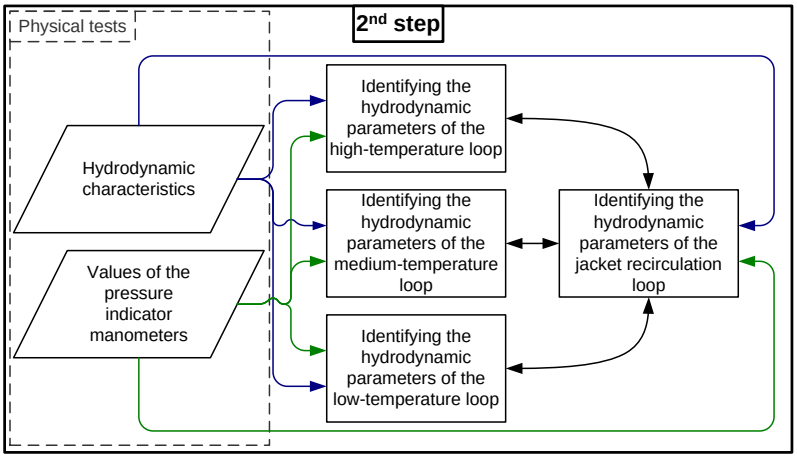

Figure 3.17. Second step of building the process model

At the second step, shown in Figure 3.17, identification of the hydrodynamic parameters of the system, regarding the pumps and the hydrodynamic resistances, were accomplished. The pumps can be defined by their technical specifications (characteristic curves). Thus, the only parameters to be determined are the hydrodynamic resistances, which are partially unknown. For the identification of these parameters, the readings of the local pressure gauges and the flow rate values of the hydrostatic characteristics were used, which were described in Chapter 2.3.

In order to determine the values of the hydrodynamic resistances, the entire system was decomposed into four separate recirculation loops (three monofluid thermoblock loops and one jacket recirculation loop). The hydrodynamic resistances affecting the measured values were also located. The values of the resistances are to be determined in such a way that the decomposed loops would produce the measured values in both standalone and heating/cooling mode. In standalone mode, the measured values can be obtained with several parameter combinations. However, in heating/cooling mode, these have a different effect on the entire system. Thus, during the coordination step, the aim was to find adequate parameter combinations from the previously determined set.

The measured variables (blue) available for the identification of the hydrodynamic parameters of the high temperature monofluid thermoblock loop and the parameters affecting the behaviour of the loop (red) can be seen in Figure 3.18. The hydrodynamic characteristics (flow rate versus control valve position) were measured in three locations per loop (FIT-1 to 3) with a mobile ultrasonic flow meter. The related pressure values were also recorded (PI). The measured flow rate and pressure values depend on the actual position of the control valve. In the process model, the approximation of these values can be achieved by modification of the resistances. The hydrodynamic resistances of the electric heater and the throttle valve after the pressure gauge are unknown. Thus, these are the parameters to be identified. These parameter values also contain the resistances of the surrounding pipe segments, so the identified values are not equal to the hydrodynamic resistance of the physical equipment. The pumps also affect the hydrodynamic behaviour, but they can be defined by their characteristic curves from a priori data.

The standalone operation of the monofluid thermoblock loops can be achieved by the closed position of the control valve (or the ball valves). The

related measured values can be simulated with several different parameter combinations. However, they affect the entire system in heating/cooling mode in different ways.

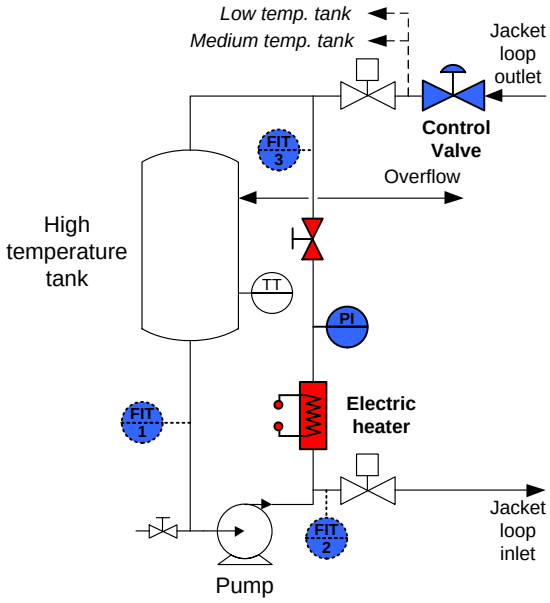

Figure 3.18. Location of measurements (blue) and parameters to be identified (red) in the case of the hydrodynamic parameter identification of the high-temperature loop

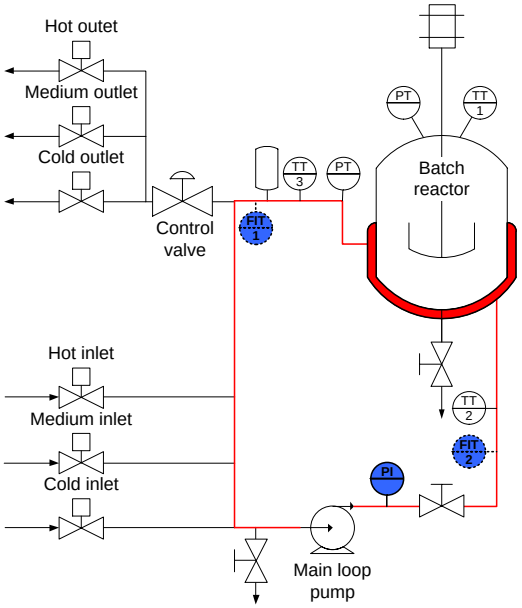

Figure 3.19. Location of measurements (blue) and parameters to be identified (red) in the case of the hydrodynamic parameter identification of the jacket recirculation loop

The parameters of the other two loops of the monofluid thermoblock were identified the same way because their structure and the arrangement of measurements are similar. For the identification of the hydrodynamic parameters of the fourth jacket recirculation loop, the measured variables and the parameters to be identified can be seen in Figure 3.19. Given that the throttle valve is not used

in this loop, the jacket and the built-in pipe segments contain all of the hydrodynamic resistances.

The measured values used for the identification of the high-temperature loop can be seen in Table 3.1. After the identification, the same values were achieved in the process model.

Table 3.1.
Measured values used for the identification of hydrodynamic parameters of the high-temperature loop

	High-temperature loop		**Jacket recirculation**	
	Standalone operation	Heating/cooling mode	Standalone operation	Heating/cooling mode
PI	2.8 bar	2.3 bar	3.5 bar	3.1 bar
FIT 1	1.10 m^3/h	1.86 m^3/h	4.20 m^3/h	4.20 m^3/h
FIT 2	0.00 m^3/h	0.90 m^3/h	4.20 m^3/h	4.20 m^3/h
FIT 3	0.96 m^3/h	0.96 m^3/h		

Since the hydrodynamic behaviour of the system has a great effect on the thermal behaviour, the identification of the hydrodynamic parameters always has to precede the thermal parameter identification. After finding the adequate parameter combinations of the four loops of the system, the process model gives nearly the same values as the measured ones in both standalone and heating/cooling mode. Thus, the thermal parameter identification can be started.

Thermal parameters

The identification of the thermal parameters was accomplished similarly to the hydrodynamic parameters, as seen in Figure 3.20. First, the parameters affecting the measured temperatures had to be found and as many as possible from them had to be defined by a priori data. For the identification of the thermal parameters of the previously described decomposed monofluid thermoblock loops, one experiment per loop was performed on the real system. These test measurements can be approximated properly with several different parameter combinations. However, in the same way as the hydrodynamic parameters, these combinations affect the entire system in heating/cooling mode in different ways.

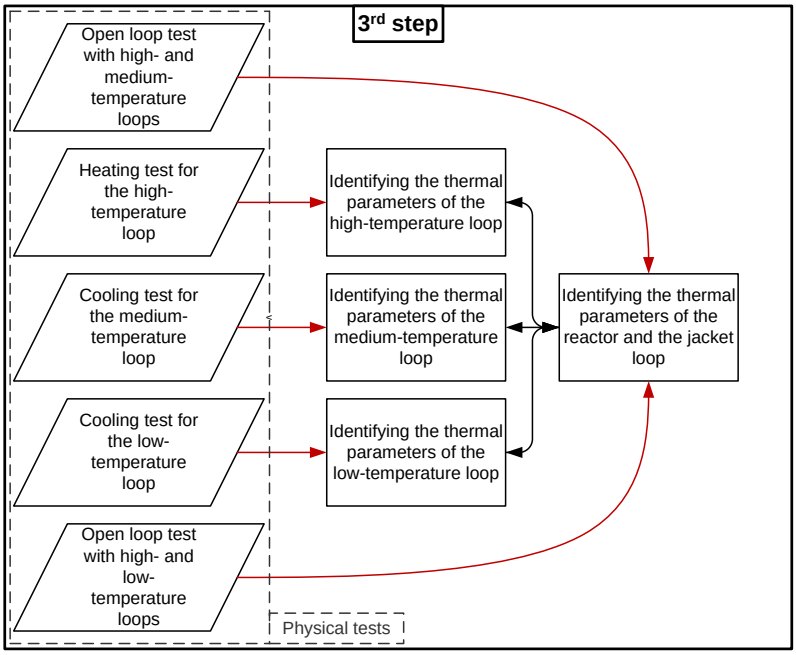

Figure 3.20. Third step of building the process model

Thermal parameters of the monofluid thermoblock loops

In the case of monofluid thermoblock loops, the parameters not defined by a priori data can be seen in Table 3.2. The heat loss coefficient, which was estimated according to the literature data, has a great influence on the behaviour of all three loops. The liquid levels of the tanks, which are unmeasured variables, also have a great effect and can only be estimated from the filling-up status of the system. For the identification of the thermal parameters of the monofluid thermoblock loops, the measured variables and the parameters to be identified can be seen in Figure 3.21 in the case of the high- and low-temperature loop. The structure of the medium-temperature loop is identical to the high-temperature loop.

The maximal heating power of the electric heaters in the high-temperature loop, which is constant in the operation range of the system, can be derived from the heat balance of the tank by using a warming-up test. However, this calculation significantly depends on the liquid level of the tank. As another solution, the power of the electric heaters can be calculated from the electric resistances of the heater filaments. However, the efficiency loss due to fouling has to be considered. Similar values were calculated from both solutions, but both contain uncertainty. Thus, this parameter was left amongst the parameters to be identified.

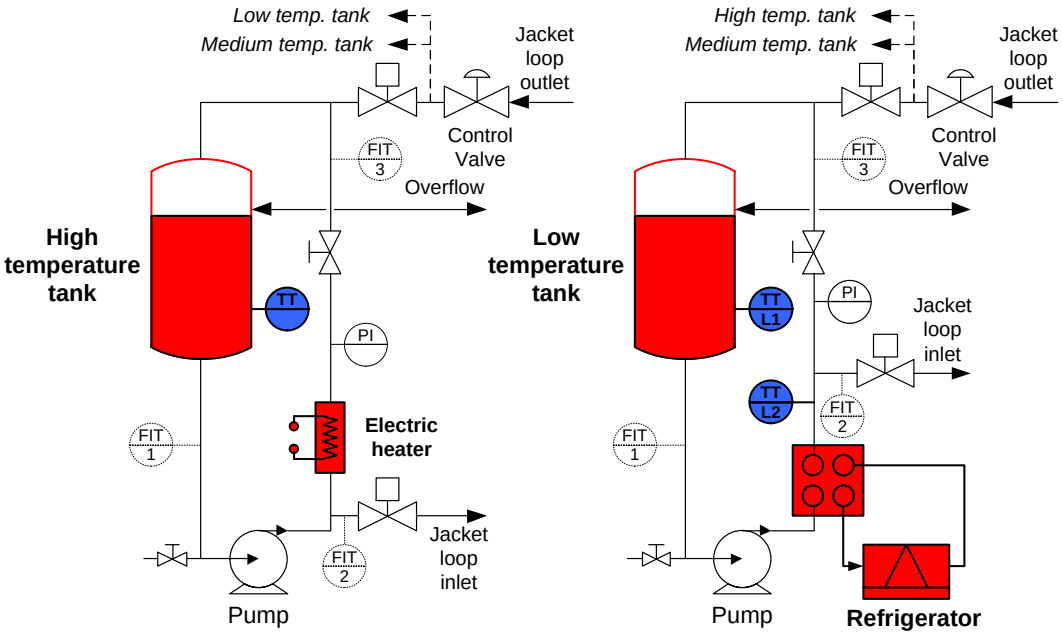

Figure 3.21. Location of measurements (blue) and parameters to be identified (red) in the case of the thermal parameter identification of the high- and low-temperature loop

In UniSim Design, only TEMA-type heat exchangers can be defined. Hence, the technical specification of the plate-type heat exchanger in the medium-temperature loop had to be converted. The heat transfer coefficient for plate-type heat exchangers was defined by data from the literature [54].

The refrigerator of the low-temperature loop was built from its parts, which contains a compressor, a throttle valve and two heat exchangers. The parameters of the parts were defined by a priori data. However, only estimation is available for the pressure and temperature data of the loop. Thus, the accurate cooling performance can be set up by modifying the hydrodynamic resistances of the loop.

Table 3.2.
Identified thermal parameters of the monofluid thermoblock loops

High-temperature loop	**Medium-temperature loop**	**Low-temperature loop**
Heat loss coefficient of the tank	Heat loss coefficient of the tank	Heat loss coefficient of the tank
Heating duty of the electric heaters	Heat transfer coefficient of the plate-type heat exchanger	Cooling duty of the refrigerator
Liquid level of the tank	Liquid level of the tank	Liquid level of the tank

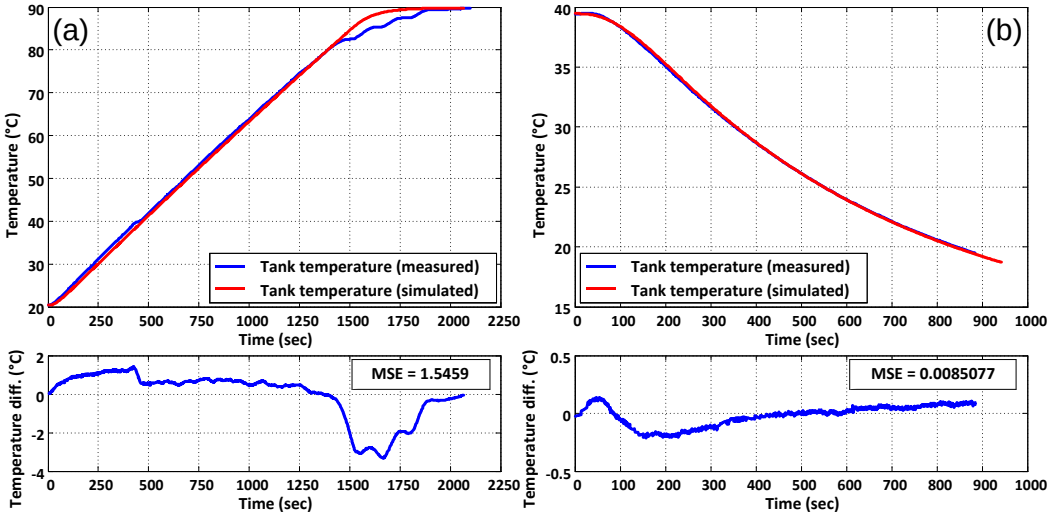

Figure 3.22. Measurement and simulation results for the identification of the thermal parameters of the (a) high- and (b) medium-temperature monofluid thermoblock loops

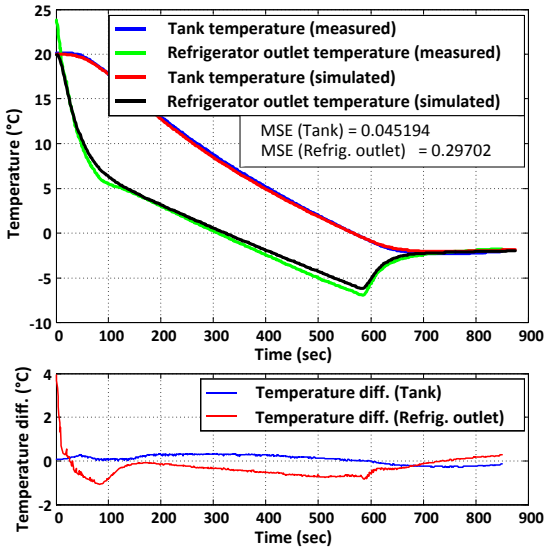

Figure 3.23. Measurement and simulation results for the identification of the thermal parameters of the low-temperature monofluid thermoblock loop

The test measurement used for the identification of the thermal parameters of the high-temperature loop can be seen in Figure 3.22 (a). The simulation approaches the measured values with small error. Difference can only be experienced near the set-point (90 °C) due to the difference of the controllers. For identification of the parameters, only the linear section was used where the electric heaters operate at maximum power.

In the case of the medium-temperature loop, a cooling test measurement was performed. It can be seen in Figure 3.22 (b), together with the result of the simulation that approximates the measurement with little error.

In the low-temperature loop, the data of two thermometers are available for the identification of the parameters. The test measurement results can be seen in

Figure 3.23. The result of the simulation approximates the measured values of both thermometers with small error.

Thermal parameters of the reactor

For the identification of the thermal parameters of the jacket recirculation loop and the batch reactor, the measured data of three thermometers, as shown in Figure 3.24, was available. The identified parameters are the following:

- The heat loss coefficients of the pipe segments in the jacket recirculation loop
- The heat loss coefficients of the reactor
- The overall heat transfer coefficient between the reactor and the jacket
- The parameter sets of the monofluid thermoblock loops

From a thermal point of view test measurement for this loop was only performed in heating/cooling mode because standalone mode provides little information for the identification of thermal parameters. In this case, the liquid level was not modified because a predefined amount of liquid was filled in the reactor during the measurement.

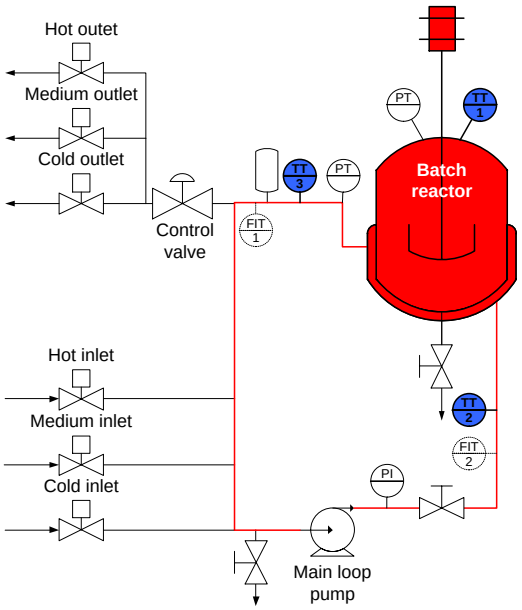

Figure 3.24. Location of measurements (blue) and parameters to be identified (red) in the case of the thermal parameter identification of the jacket recirculation loop and the batch reactor

Since UniSim Design contains no built-in jacketed batch reactor model, the first modelling solution was to build it from its structural elements, namely from a 1-1 pass shell and tube heat exchanger and a CSTR model. From a thermal aspect, the shell side of the heat exchanger represents the jacket and the tube side represents the reactor. The heat flow promoted into the CSTR is set equal to the tube side duty of the heat exchanger. The flow rate on the tube side of the heat exchanger was chosen high, because from a heat transfer aspect, the jacket side is decisive. The geometrical data of the reactor jacket were also converted to match the data of the 1-1 pass TEMA-type heat exchanger available in UniSim Design.

The simulation results with the previously described structural approximation of the reactor can be seen in Figure 3.25. With this construction, the measured values cannot be approximated properly unless the structure of the process model is modified in a way that differs from the real system. Such modification can be, for example, a bypass stream in the recirculation loop of the jacket around the reactor. This can be explained with the unfavourable flow field of the conventional jacket.

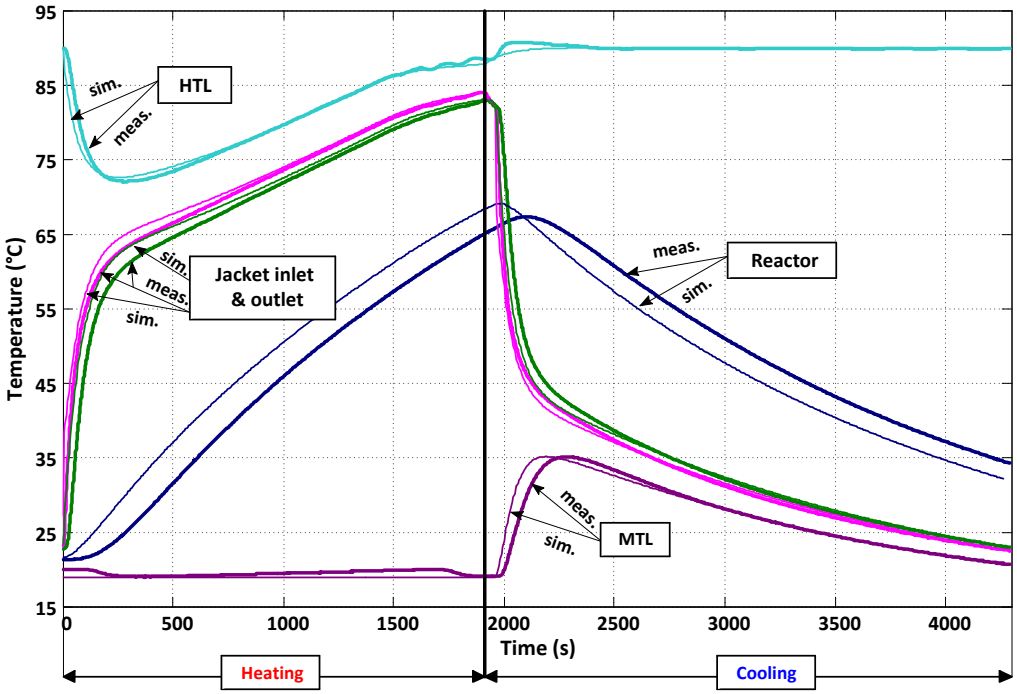

Figure 3.25. Measurement and simulation results (first modelling solution, constant heat transfer coefficient, high and medium temperature levels)

Figure 3.25 shows that the curves representing the results of the simulation of the thermometers have a similar shape as the measured ones. However, their values change sooner. According to the author's prior experience as described in chapter 2.2, in the case of systems where the characteristic time constants are commensurable with the time constants of the measuring instruments, the models of the measuring instruments need to be added to the process model in order to achieve an adequate description [55].

Effect of the thermometer dynamics

In order to achieve proper fitting, it was necessary to add the dynamics of the thermometers to the process model. The dynamics are usually ignored in the case of continuous processes. Simulation results of the process model extended with the thermometer models can be seen in Figure 3.26. The thermometers were modelled with first-order filters using the built-in capability of UniSim Design. The time constants of the thermometer models were determined by estimation and targeted test measurements with disassembled thermometers (Chapter 2.2).

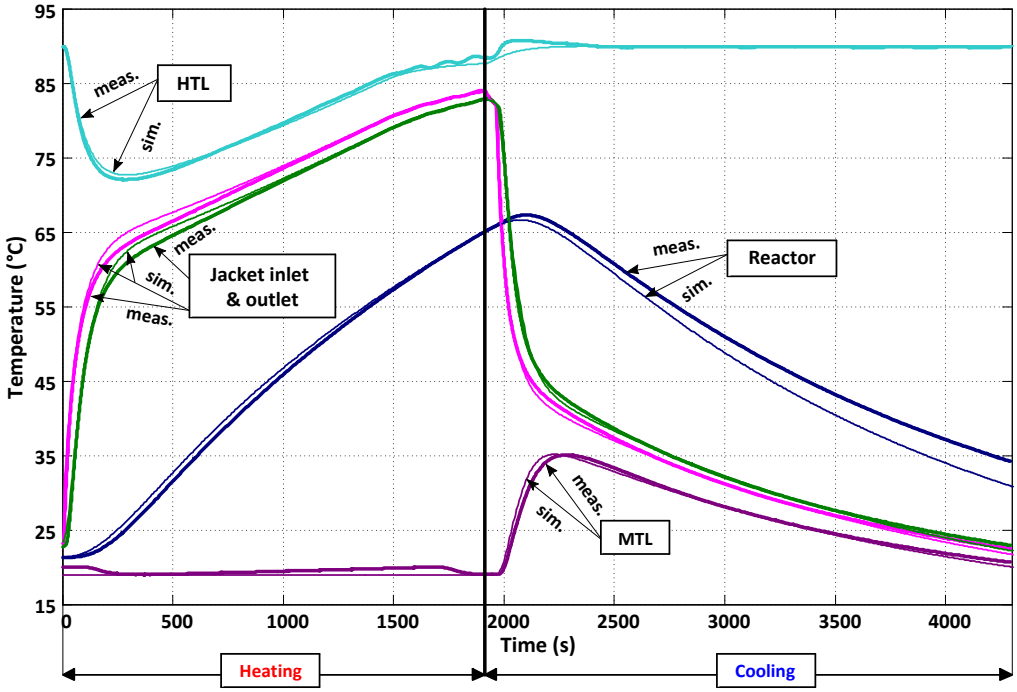

Figure 3.26. Measurement and simulation results using the thermometer models

The behaviour of the process model containing the thermometer models is highly similar to the real system. However, during the cooling step, the jacket side duty is higher compared to the measurement. This can be explained by the significant temperature dependence of the viscosity of the recirculating fluid in the jacket loop (mixture of water and ethylene glycol), which affects the heat transfer coefficient.

Complex heat transfer coefficient calculation

If the properties of the fluid are highly dependent on temperature as can be seen in Figure 2.2, it also affects the heat transfer coefficient. In this study, the viscosity of the water/ethylene glycol mixture varies significantly in the operating temperature range of the system, as seen in Figure 3.27. The data were estimated with UniSim Design using the Peng-Robinson estimation method.

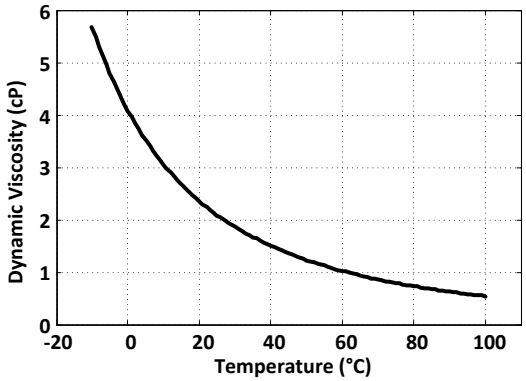

Figure 3.27. Temperature dependency of dynamic viscosity in the case of the water and ethylene glycol mixture

The previously described modelling solution of the reactor vessel was extended with a detailed calculation of the heat transfer coefficient regarding the change of the fluid properties. The Sieder-Tate and Chilton correlation [54] was implemented in a flexible UniSim Design module called “Spreadsheet”, which allows user-defined calculations, where the actual value of the heat transfer coefficient was calculated.

In the coordinating step, the parameters of the fourth loop (jacket recirculation loop and reactor) were identified by selecting the adequate parameter set of the monofluid loops and finding the parameters of the dynamic heat transfer coefficient calculator of the reactor to fit the test measurement results in the heating/cooling mode. The objective function was to reach the temperature values within ±1 °C. Two test measurements were performed in the heating/cooling mode (Figure 3.28 and Figure 3.29), of which the first was used for the identification of the parameters and the second for validation.

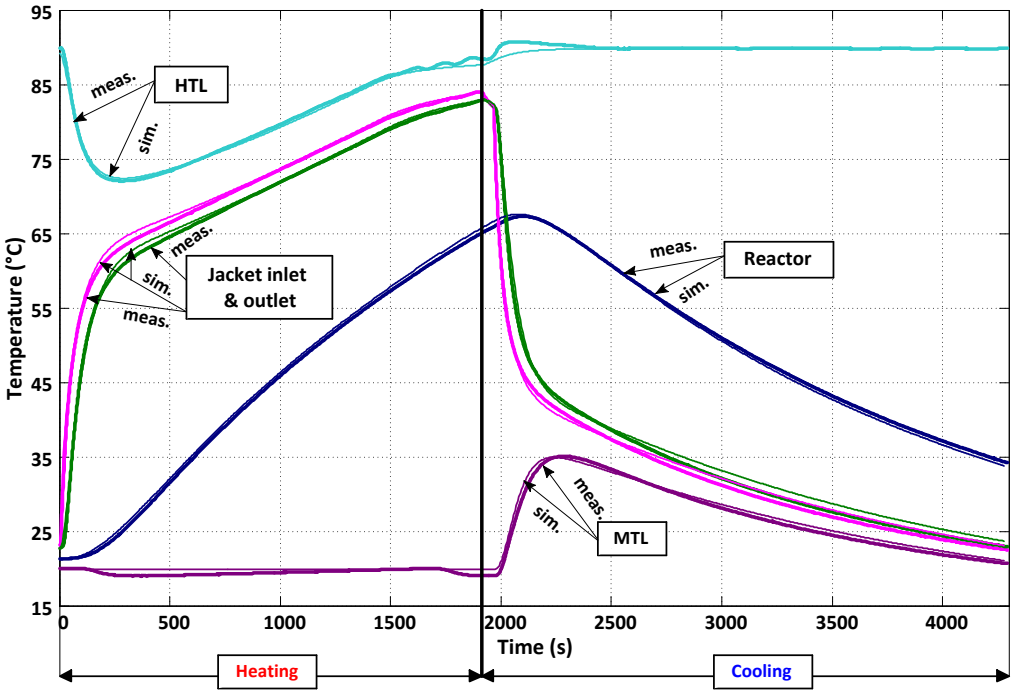

Figure 3.28. Measurement and simulation results (first modelling solution, detailed heat transfer coefficient calculation, high and medium temperature levels)

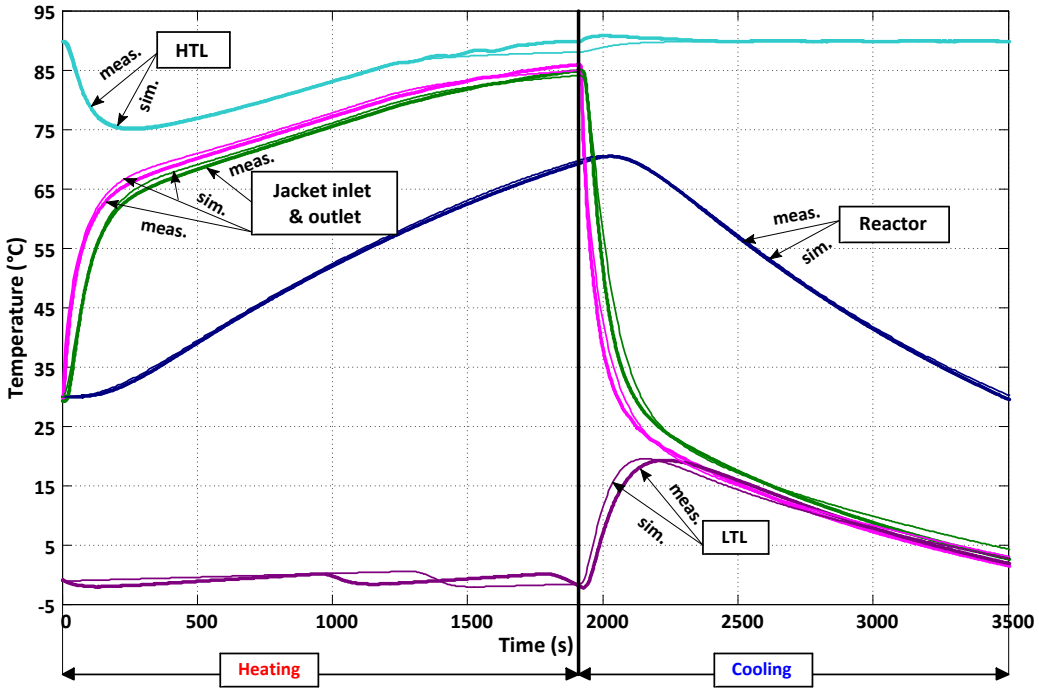

Figure 3.29. Measurement and simulation results (first modelling solution, detailed heat transfer coefficient calculation, high and low temperature levels)

Using the detailed heat transfer coefficient calculator, the approximation error was reduced at the first test measurement (Figure 3.28) using the high- and medium-temperature monofluid loops in the heating/cooling mode compared to the solution where a constant overall heat transfer coefficient was used. Using the parameters identified in the first test measurement, a validating simulation was performed according to Figure 3.29, where the high- and low temperature monofluid loop was used in the heating/cooling mode. As shown, the validation was successful; the simulation approximates the measured data with the preliminary defined acceptable error.

Other modelling solution

In the dynamic mode of UniSim Design, a separator extended with a tube bundle is available. From a modelling point of view, it is very similar to the conventional jacketed reactor. The schematic structure of this type of separator can be seen in Figure 3.30.

With this solution, there is no need to build the vessel of the jacketed batch reactor by connecting two different models. The technical specifications and hydrodynamic parameters of the tube bundle were defined as the parameters of the heat exchanger in the previous solution. In the tube bundle module, vapour and liquid heat transfer coefficients for both sides (tube and separator) can be defined. These parameters were defined using the values of the previously described complex heat transfer calculator. The simulation results with this configuration can be seen in Figure 3.31. The simulated reactor temperature fits well at the heating step. However, at cooling, probably due to the constant heat transfer coefficients, higher cooling duty can be experienced.

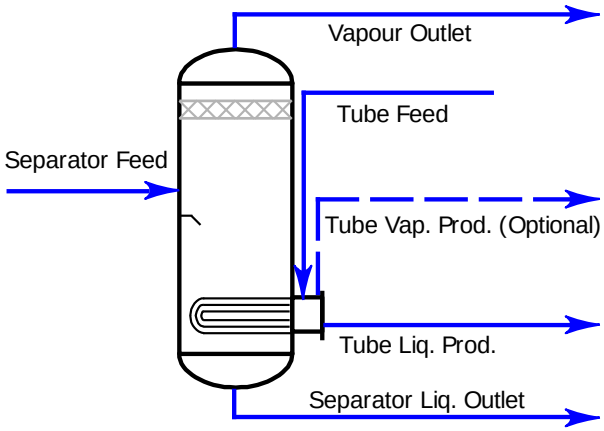

Figure 3.30. Schematic structure of the separator with tube bundle in UniSim Design

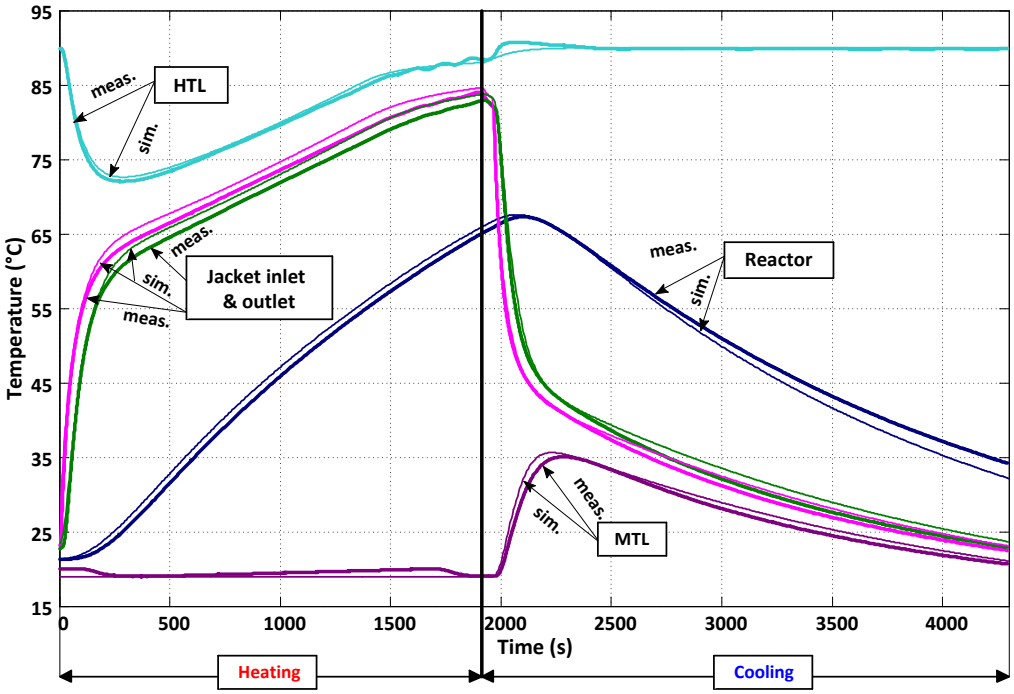

Figure 3.31. Measurement and simulation results (separator with a tube bundle, constant heat transfer coefficient, high- and medium temperature levels)

The built-in separator model with a tube bundle approximates the measured values with small error. However, with the previous modelling solution, where the vessel of the jacketed batch reactor is built from two modules, smaller error can be achieved. This can be explained with the poor information about the structure of the built-in module and the several parameters with partly known effects to be defined.

Conclusion

When building a process simulator with the aim to approximate the real system as well as possible, all the known and relevant phenomena have to be incorporated in the simulator. Knowing the hydrodynamic characteristics of the system is a prerequisite of an accurate simulator. As Figure 3.26 highlighted, the

model of the measuring instruments also are important to be considered and cannot be eliminated.

Boxed process simulation software have some limitations, as UniSim Design in the case of jacketed batch reactors. This limitation was solved by the combination of a CSTR and a heat exchanger model connected by a spreadsheet module. If the properties of the thermal fluid circulating in the jacket depend significantly on temperature (especially their viscosity), which affects the heat transfer between the thermal fluid and the wall of the reactor, the use of a constant heat transfer coefficient brings a lot of error to the simulation. This was the reason why a complex heat transfer coefficient calculation was implemented in the simulator that uses actual fluid properties as an input. With this solution significant improvement was achieved.

In result of this development a simulator was created that is suitable for simulating a jacketed batch reactor and its thermo block with small error. It can be used for trainings, educational use, and testing new control algorithms and parameters.

4. Temperature control

It was described previously in Chapter 1.3.1 that the temperature control of batch reactors is mainly carried out in the industry using PID controllers in cascade structure. It was also mentioned that the quality of the slave control loop (jacket temperature control) fundamentally restricts the quality of complex control solutions; hence, in this chapter the analysis of this loop is performed.

4.1. The control structure

For the slave loop controller a constrained PI controller was chosen [56]. The structure of the PI controller can be seen in Figure 4.1.

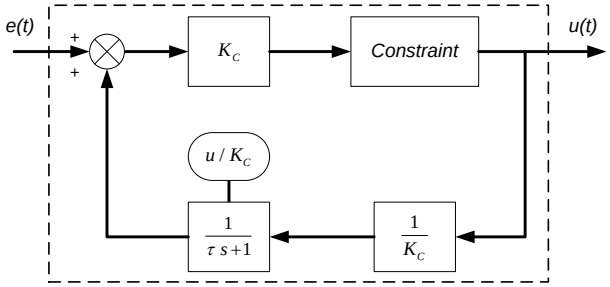

Figure 4.1. The structure of the constrained PI controller

The split-range controller is preferred in industrial control engineering in the slave loop of the cascade control to operate two actuators with different effects at the same time. Thus, the split-range controller is a single-input two-output (SI2O) controller that contains a splitter block splitting the output of the PID. The splitter block is shown in Figure 4.2, where the input of the block is the output of the slave loop controller. In the case of the temperature control of the jacket, one of its outputs is the valve opening of the control valve (the set-point to the actuator of the control valve) and the other is the desired operating mode of the thermoblock.

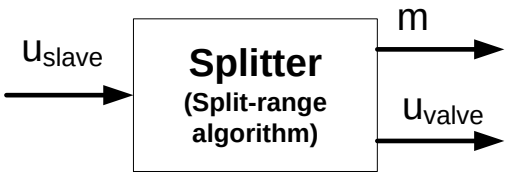

Figure 4.2. The splitter block in case of reactor temperature control

If the controller handles two modes of operation, mainly proportional splitting is used, which can be seen in Figure 1.8 . The desired position of the control valve can be calculated from the linear correlation shown in the figure.

The values of each manipulated variable can be calculated by means of the correlation built in the splitter. Thus, in terms of the PID controller, the two actuators can be considered as one manipulated variable and the split-range algorithm as part of the controlled system. The main role of the split-range algorithm is to maintain the sign of the gain of the controlled object unchanged.

If three operating modes are to be handled with the split-range algorithm, the control becomes more complicated. To keep the sign of the gain of the controlled virtual object is not as trivial as it was with two operating modes.

However, due to the advantages of thermoblocks with three different temperature levels the research efforts on controllers handling such systems are becoming more important. The aim of the research was to analyse different model-based split-range solutions and to find a solution that could be implemented in the conventional cascade temperature control structure of batch reactors (using PID controllers) without restructuring or using advanced control solutions.

4.2. Model-based split-range algorithms

One of the aims of this research was to develop a split-range algorithm more specific to the jacket configuration commonly used in the industry, which provides better control performance compared to other more universal solutions.

From a modelling point of view, the jacket recirculation loop can be separated into the jacket of the reactor and a mixer, as seen in Figure 4.3. If the temperature change of the jacket inlet caused by the reactor differs significantly from the temperature change caused by the thermal fluid feed, which is mainly relevant in the case of systems located in the industry but not valid for small-scale laboratory reactors, then the jacket recirculation loop can be satisfactorily described with a so-called mixer model. In this case, the reactor is treated as an unmeasured load disturbance. If the dynamics of the two effects are commensurable, then the model can be extended with the model of the jacket that contains the temperature of the reactor. In this case, the temperature of the reactor is treated as a measured disturbance.

The inlet temperature of the jacket can be modified by the fluid entering the jacket recirculation loop from the monofluid thermoblock. The heating or cooling effect of the actual inlet fluid can be determined unequivocally from the model of the recirculation loop, the structure of which can be seen on Figure 4.3.

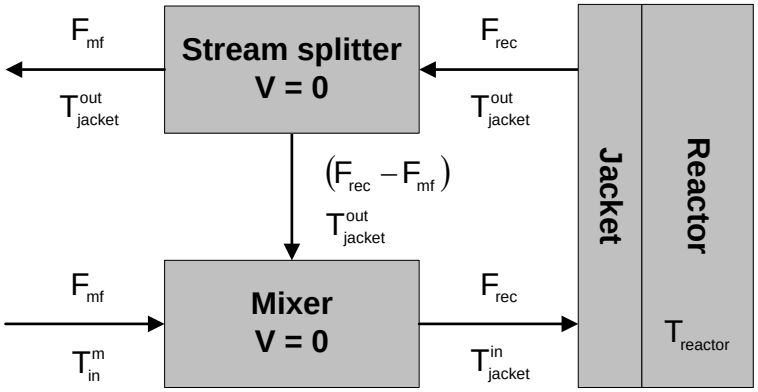

Figure 4.3. The structure of the jacket recirculation loop

The temperature dependence of the thermal fluid shown in Chapter 2 was ignored in the models used in the split-range algorithms. Since small temperature difference occurs on the jacket this effect can be ignored, and furthermore the resulting equations are significantly simpler, which is quite important in control applications.

4.2.1. Mixer model-based split-range algorithm

As the first modelling solution the jacket recirculation loop can be described by a mixer model. The steady-state model of the mixer can be expressed with following equation:

$$\begin{aligned} &F_{rec} \cdot \rho_{mf} \cdot c_p^{mf} \cdot T_{jacket}^{in} = \\ &= \left(F_{rec} - F_{mf}\right) \cdot \rho_{mf} \cdot c_p^{mf} \cdot T_{jacket}^{out} + F_{mf} \cdot \rho_{mf} \cdot c_p^{mf} \cdot T_{in}^{m} \end{aligned} \tag{4.1}$$

The correlation for the inlet heat flow of the monofluid feed entering the jacket recirculation loop follows:

$$F_{mf} \cdot \rho_{mf} \cdot c_p^{mf} \cdot \left(T_{in}^{m} - T_{jacket}^{out}\right) \tag{4.2}$$

According to equation (4.2), the heating or cooling effect of the actual inlet fluid only depends on the relation of the jacket outlet (T_{jacket}^{out}) and the feed temperature of the recirculation loop (T_{in}^{m}). For example, a heating effect can be achieved if the feed temperature of the recirculation loop is higher than the jacket outlet temperature.

Ascertaining the heating or cooling effect of the inlet fluid is important because during the operation of the reactor, the medium temperature level of the monofluid thermoblock can be either a heater or cooler fluid depending on the jacket outlet temperature. In addition the other two temperature levels can become heater or cooler media, although this is uncommon in practice; it can only occur in the case of highly exothermic or endothermic reactions. This effect has to be considered in the split-range algorithm, since the splitter establishes a connection between the slave loop controller, the actual position of the control valve, and the actual mode of operation. Thus, with a proper algorithm implemented in the splitter, the gain of the controlled object will not change sign.

Considering the aforementioned model (Equation (4.1)), the gain of the slave loop object (jacket recirculation loop) can be evaluated from the following equation, where the valve is taken into account with linear characteristics (as it is in the physical system):

$$T_{jacket}^{in} = T_{jacket}^{out} + \frac{F_{max}}{F_{rec}} \cdot \frac{u_{valve}}{100} \cdot \left(T_{in}^{m} - T_{jacket}^{out}\right) \tag{4.3}$$

$$K_{sl\_o} = \frac{\partial T_{jacket}^{in}}{\partial u_{valve}} = \frac{F_{max}}{F_{rec}} \cdot \frac{1}{100} \left(T_{in}^{m} - T_{jacket}^{out}\right) \tag{4.4}$$

The resulting gain values that depend on the jacket temperature in the case of all three modes of operation can be seen in Figure 4.4. The sign of the gain changes depending on the jacket outlet temperature in all three modes of operation. Only highly exothermic/endothermic reactions can cause the jacket temperature (through the wall of the reactor) to be higher/lower than the highest available heating/lowest cooling media. Thus, the reactor operates in most of its operation time between the highest and lowest-available temperature levels. When using two modes of operation, the split-range algorithm in Figure 1.8 satisfies the needs during most of the operation time to keep the sign of the gain of the controlled object unchanged. However, as Figure 4.4 reveals, when using three

modes of operation in the case of the medium temperature level, the sign of the gain can change during normal operation. Consequently, it has to be considered in the split-range algorithm. From the aspect of the slave loop controller, the split-range algorithm can be considered to be part of the controlled object; it has the role of keeping the sign of the gain of the controlled object unchanged and managing the two manipulated variables (mode of operation and position of the control valve) of the slave loop object.

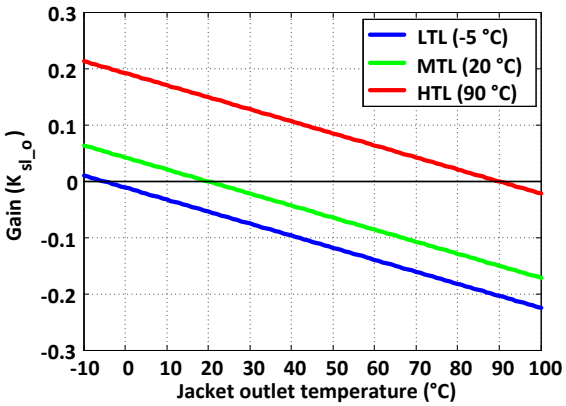

Figure 4.4. The gain of the slave loop object in the case of the mixer model

The first algorithm

According to these considerations as can be seen in Figure 4.5, four different split-range characteristics can be defined.

The range of the PID controller output was divided into three equal parts according to the consideration that all of the temperature levels can be heating or cooling media. Other considerations can be also used in splitting the range of the PID controller output.

If the split-range algorithm is considered as the part of the controlled object, the gain of this composite object can be calculated with equation (4.5):

$$K_{c\_o} = \frac{\partial T_{jacket}^{in}}{\partial u_{slave}} = \frac{F_{max}}{F_{rec}} \cdot \frac{s_m}{100}\left(T_{in}^{m} - T_{jacket}^{out}\right) \tag{4.5}$$

The gain of the controlled object can be seen in Figure 4.6 as a function of the jacket outlet temperature. With this solution, the sign of the gain remains unchanged.

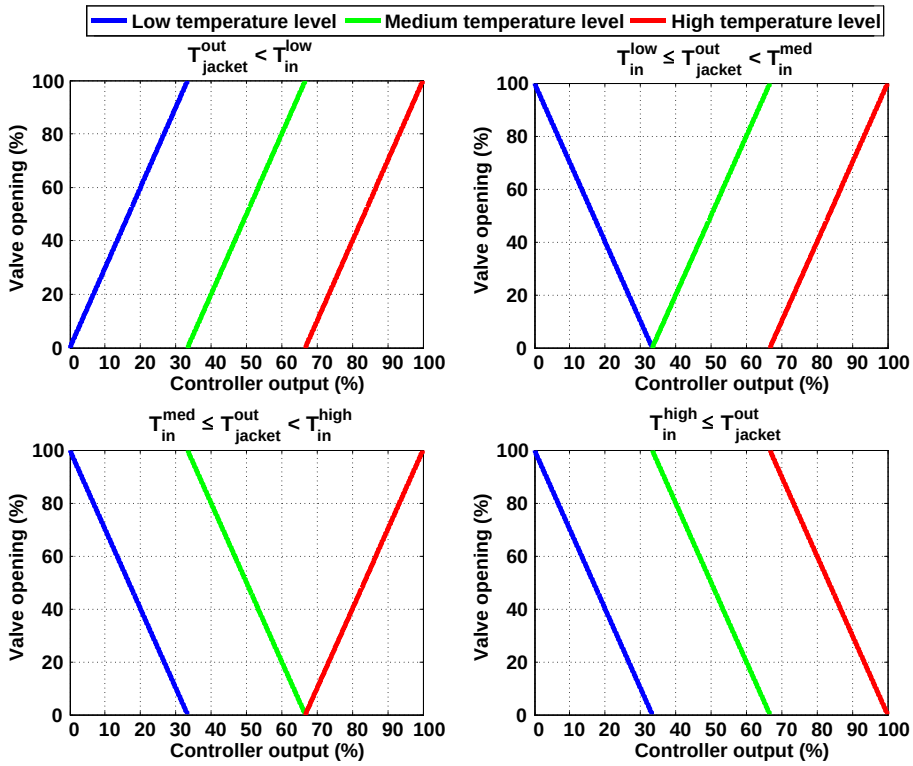

Figure 4.5. The resulting split-range characteristics in the case of the first, mixer model-based split-range algorithm

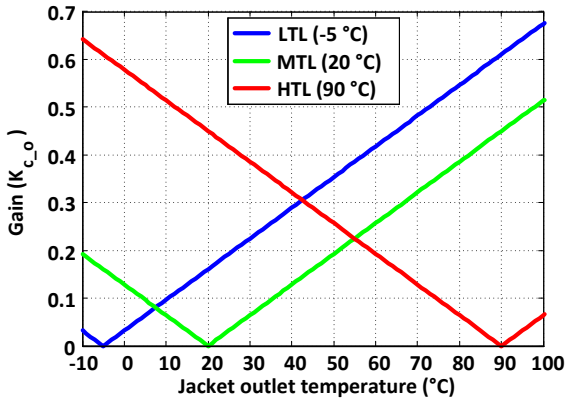

Figure 4.6. The gain of the controlled composite object in the case of the first, mixer model-based split-range algorithm

If only one split-range characteristic is implemented in the splitter then the split-range characteristic would not depend on the actual jacket outlet temperature, and this could lead to instability. For example, if only the third characteristic is implemented, the gain of the controlled object would change according to Figure 4.7. In that case, when the jacket outlet temperature is lower than the medium temperature level and the system is using this mode of operation, the system becomes instable due to the wrong sign of the gain. The change in the PID controller output results in the opposite effect as expected. The instability causes the controller to change mode of operation, thus stabilizing it. However, it cannot utilize all three modes of operation, especially the medium one with lower energy consumption.

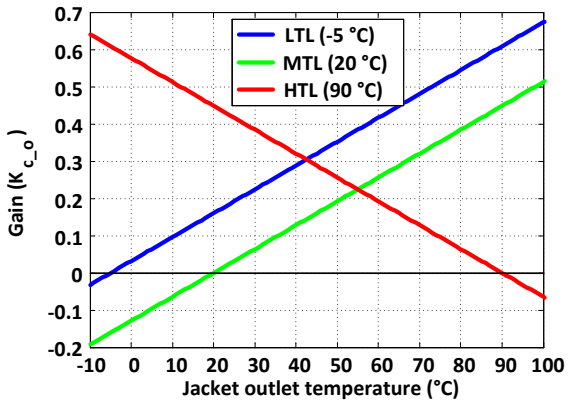

Figure 4.7. The gain of the controlled object in the slave loop containing only the third split-range characteristic

The aforementioned split-range solution is able to handle the change in the sign of the gain of the controlled object in the range of the highest and lowest temperature levels. However, it also works universally outside this temperature range.

The second algorithm

The split-range algorithm can be considered part of the controlled object from the aspect of the slave loop controller, which has the role of keeping the sign of the gain of the controlled object unchanged by managing the two manipulated variables (mode of operation and the control valve); in addition to this role, an adequate split-range algorithm can also compensate for the varying of the gain both in the case of jacket temperature and a change in the mode of operation.

In the first step of this algorithm, the maximal possible steady-state jacket inlet temperatures at maximal control valve opening are calculated at all three temperature levels. The jacket inlet temperatures at maximal valve opening can be calculated by Equation (4.6).

$$T_s^m = T_{jacket}^{out} + \frac{F_{max}}{F_{rec}} \cdot \left(T_{in}^m - T_{jacket}^{out}\right) \tag{4.6}$$

The output of the slave loop PID controller is converted to temperature range according to Equation (4.7). With this conversion, the output of the PID controller can be handled as a desired steady-state temperature for the jacket inlet temperature.

$$u_{slave}^T = T_{jacket}^{in\_min} + \left(T_{jacket}^{in\_max} - T_{jacket}^{in\_min}\right) \cdot \frac{u_{slave}}{100} \tag{4.7}$$

The minimal and maximal possible steady-state jacket inlet temperatures (Equation (4.8) and Equation (4.9)) are derived from the previously calculated T_s^m (Equation (4.7)) and the actual jacket temperature.

$$T_{jacket}^{in\_min} = min\left(T_s^{low}, T_{jacket}^{out}\right) \tag{4.8}$$

$$T_{jacket}^{in\_max} = max\left(T_s^{high}, T_{jacket}^{out}\right) \tag{4.9}$$

When choosing the adequate mode of operation, the possible steady-state jacket inlet temperatures are first arranged in ascending order. These values can be seen in Table 4.1.

Table 4.1. Ordering the possible steady-state temperatures in different cases in the algorithm based on the mixer model

Temperature Range	Temperature Order
$T_{jacket}^{out} < T_{in}^{low}$	$P = \left[T_{jacket}^{out}, T_s^{low}, T_s^{med}, T_s^{high}\right]$
$T_{in}^{low} \le T_{jacket}^{out} < T_{in}^{med}$	$P = \left[T_s^{low}, T_{jacket}^{out}, T_s^{med}, T_s^{high}\right]$
$T_{in}^{med} \le T_{jacket}^{out} < T_{in}^{high}$	$P = \left[T_s^{low}, T_s^{med}, T_{jacket}^{out}, T_s^{high}\right]$
$T_{in}^{high} \le T_{jacket}^{out}$	$P = \left[T_s^{low}, T_s^{med}, T_s^{high}, T_{jacket}^{out}\right]$

Using the previously created P vector, the adequate mode of operation can be chosen in the function of the temperature ranged controller output. The different cases can be seen in Table 4.2.

Table 4.2. Choosing the adequate mode of operation

Temperature Range	Mode of Operation
$u_{slave}^{T} \le P(2)$	$m = 'low'$
$P(2) < u_{slave}^{T} \le P(3)$	$m = 'medium'$
$P(3) < u_{slave}^{T}$	$m = 'high'$

The valve opening can be calculated from the steady-state model of the slave loop object (Equation (4.3)) as it can be seen in Equation (4.10).

$$u_{valve} = \frac{u_{slave}^{T} - T_{jacket}^{out}}{\frac{F_{max}}{F_{rec}} \cdot \left(T_{in}^{m} - T_{jacket}^{out}\right)} \cdot 100 \tag{4.10}$$

The previously described split-range algorithm can result in several different split-range characteristics that depend on the actual temperature of the jacket and the temperature levels of the monofluid thermoblock. Some example characteristics at different jacket temperatures can be seen in Figure 4.8. For example, at 50 °C according to Equation (4.7), the PID output percentage where the medium and high temperature levels have zero valve opening represent the jacket temperature on the basis of the PID output. The heating/cooling capacities are also continuous when more than one heating/cooling media is available.

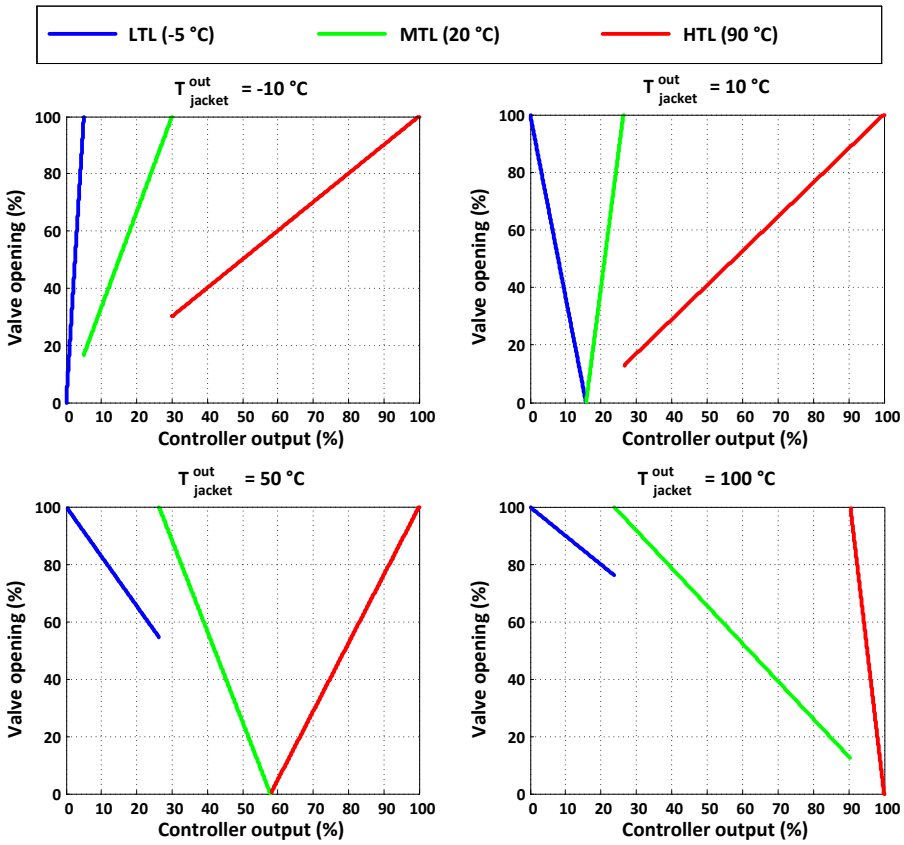

Figure 4.8. Example of split-range characteristics at different jacket temperature values for the second, mixer model-based split-range algorithm

If the split-range algorithm is considered part of the controlled object, the gain of this virtual object can be calculated with Equation (4.5). With this split-range algorithm, it is possible to conclude that the sign of the gain does not change in the whole operation range. Moreover, the gain is kept constant in the normal operation temperature range and is also independent of the actual mode of operation. Therefore, as an outcome, the change in the mode of operation does not result in a drastic change in the output of the PID controller. The gain values can be seen in Figure 4.9.

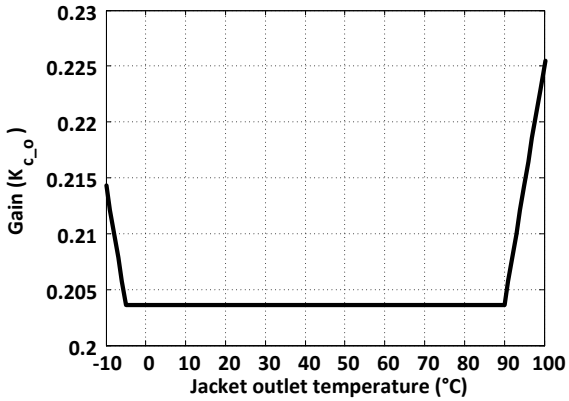

Figure 4.9. The gain of the controlled composite object in the case of the second, mixer model-based split-range algorithm

Using the previously described split-range algorithm, the varying of the gain of the slave loop object, which is a function of several variables, can be compensated. The only dependence left in the gain of the virtual object is the varying temperatures of the monofluid thermoblock loops; however, this can be compensated with the PID controller.

4.2.2. Jacket recirculation loop model-based split-range algorithm

If the dynamics of the heat transfer between the jacket and the reactor is comparable with the dynamics of the temperature change caused by the convectional heat flow of the thermal fluid entering the jacket recirculation loop from the monofluid thermoblock, the model of the slave loop object can be described with the following two equations. The temperature of the jacket is equal to the jacket outlet as the jacket was considered with lumped model.

$$V_{jacket} \cdot \rho_{mf} \cdot c_p^{mf} \cdot \frac{dT_{jacket}^{out}}{dt} = \\ = F_{rec} \cdot \rho_{mf} \cdot c_p^{mf} \cdot \left(T_{jacket}^{in} - T_{jacket}^{out}\right) + UA_{wall} \cdot \left(T_{reactor} - T_{jacket}^{out}\right) \tag{4.11}$$

$$F_{rec} \cdot \rho_{mf} \cdot c_p^{mf} \cdot T_{jacket}^{in} = \\ = \left(F_{rec} - F_{mf}\right) \cdot \rho_{mf} \cdot c_p^{mf} \cdot T_{jacket}^{out} + F_{mf} \cdot \rho_{mf} \cdot c_p^{mf} \cdot T_{in}^{m} \tag{4.12}$$

In steady state, the jacket inlet temperature can be derived from the previous equations as follows:

$$T_{jacket}^{in} = \frac{a \cdot T_{reactor} + \frac{F_{max}}{F_{rec}} \cdot \frac{u_{valve}}{100} \cdot \left[(1+a) \cdot T_{in}^{m} - a \cdot T_{reactor}\right]}{a + \frac{F_{max}}{F_{rec}} \cdot \frac{u_{valve}}{100}} \\ a = \frac{UA_{wall}}{F_{rec} \cdot \rho_{mf} \cdot c_p^{mf}} \tag{4.13}$$

The gain of the resulting object can be calculated by Equation (4.14) where the gain is a function of the valve opening, the temperature of the reactor, and the actual jacket recirculation loop inlet temperature.

$$K_{sl\_o} = \frac{\partial T_{jacket}^{in}}{\partial u_{valve}} = \frac{a \cdot \frac{F_{max}}{F_{rec}}(1+a)}{\left(a + \frac{F_{max}}{F_{rec}} \cdot \frac{u_{valve}}{100}\right)^2} \cdot \frac{\left(T_{in}^{m} - T_{reactor}\right)}{100} \tag{4.14}$$

The gain values of the object containing the mixer and the jacket model can be seen in Figure 4.10. In all three modes of operation, the values of the gain as well as the sign changes in the function of both the reactor temperature and the valve opening.

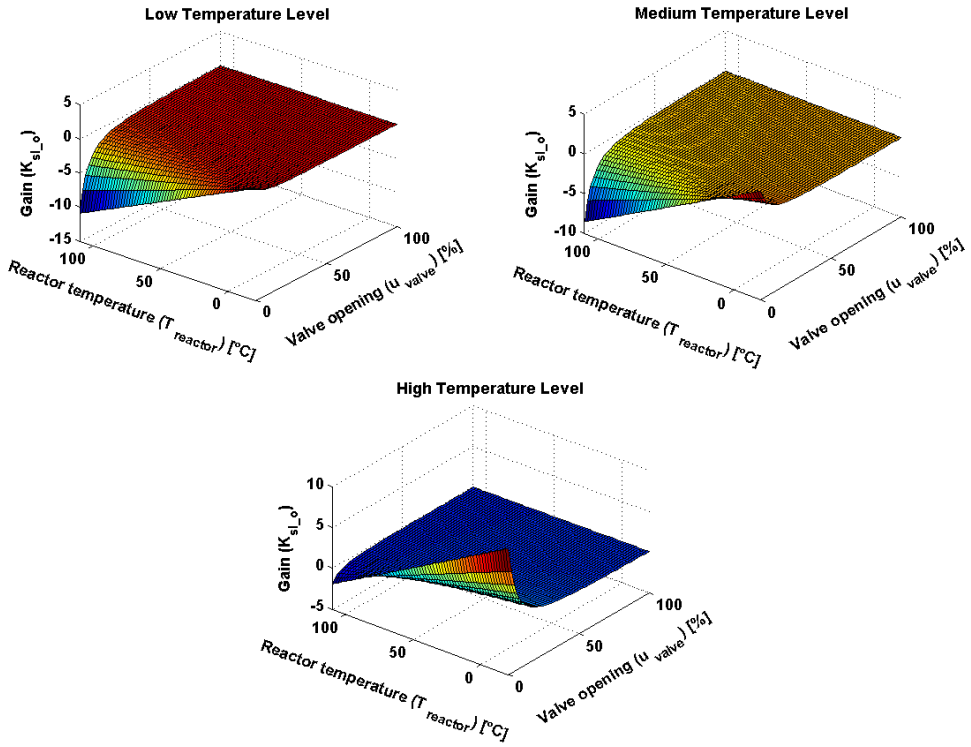

Figure 4.10. The gain of the slave loop object in the case of the jacket recirculation loop model

The algorithm

The algorithm is identical to the solution described in "The second algorithm" in Chapter 4.2.1. The differences are caused by the different model used in the algorithm.

In the first step, the maximal possible steady-state jacket inlet temperatures at maximal control valve opening are calculated at all three temperature levels. The jacket inlet temperatures at maximal valve opening can be calculated by Equation (4.15).

$$T_s^m = \frac{a \cdot T_{reactor} + \frac{F_{max}}{F_{rec}} \cdot \left[(1+a) \cdot T_{in}^m - a \cdot T_{reactor} \right]}{a + \frac{F_{max}}{F_{rec}}} \tag{4.15}$$

The output of the slave loop PID controller is converted to temperature range according to Equation (4.7). With this conversion, the output of the PID controller can be handled as a desired steady-state temperature for the jacket inlet temperature.

The minimal and maximal possible steady-state jacket inlet temperatures (Equation (4.16) and Equation (4.17)) are derived from the previously calculated T_s^m (Equation (4.7)) and the actual jacket temperature.

$$T_{jacket}^{in\_min} = min\left(T_s^{low}, T_{reactor}\right) \tag{4.16}$$

$$T_{jacket}^{in\_max} = max\left(T_s^{high}, T_{reactor}\right) \tag{4.17}$$

When choosing the adequate mode of operation, the possible steady-state jacket inlet temperatures are first arranged in ascending order. These values can be seen in Table 4.3.

Table 4.3. Ordering the possible steady-state temperatures in different cases in the algorithm based on the jacket recirculation loop model

Temperature Range	Temperature Order
$T_{reactor} < T_{in}^{low}$	$P = \left[T_{reactor}, T_s^{low}, T_s^{med}, T_s^{high}\right]$
$T_{in}^{low} \le T_{reactor} < T_{in}^{med}$	$P = \left[T_s^{low}, T_{reactor}, T_s^{med}, T_s^{high}\right]$
$T_{in}^{med} \le T_{reactor} < T_{in}^{high}$	$P = \left[T_s^{low}, T_s^{med}, T_{reactor}, T_s^{high}\right]$
$T_{in}^{high} \le T_{reactor}$	$P = \left[T_s^{low}, T_s^{med}, T_s^{high}, T_{reactor}\right]$

Using the previously created P vector, the adequate mode of operation can be chosen in the function of the temperature range controller output. The different cases can be seen in Table 4.2.

The valve opening can be calculated from the steady-state model of the slave loop object (Equation (4.11)) as it can be seen in Equation (4.18).

$$u_{valve} = \frac{a \cdot F_{rec}}{F_{max}} \cdot \frac{T_{reactor} - u_{slave}^{T}}{a \cdot \left(T_{reactor} - T_{in}^{m}\right) + \left(u_{slave}^{T} - T_{in}^{m}\right)} \cdot 100 \tag{4.18}$$

Some resulting characteristics can be seen in Figure 4.11. These characteristics are similar to the ones in Figure 4.8; the differences arise only from differences of the models.

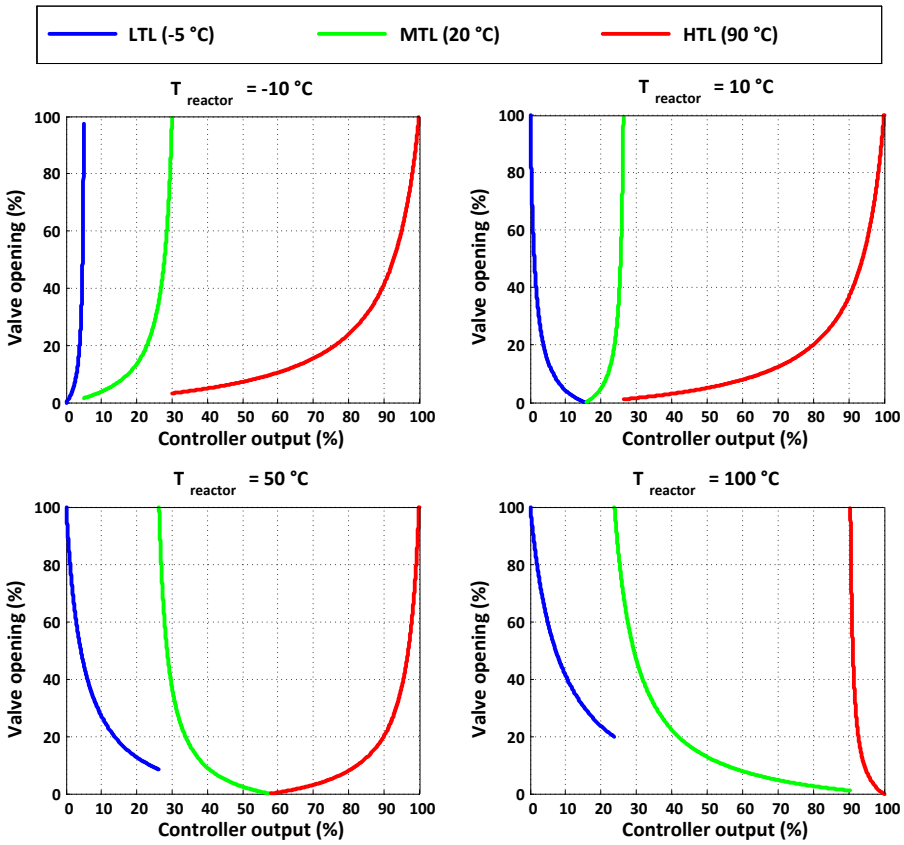

Figure 4.11. Example of split-range characteristics at different jacket temperature values for the jacket recirculation loop model-based split-range algorithm

If the split-range algorithm is considered part of the controlled object, the gain of this virtual object can be calculated with Equation (4.5). The resulting gain values can be seen in Figure 4.12

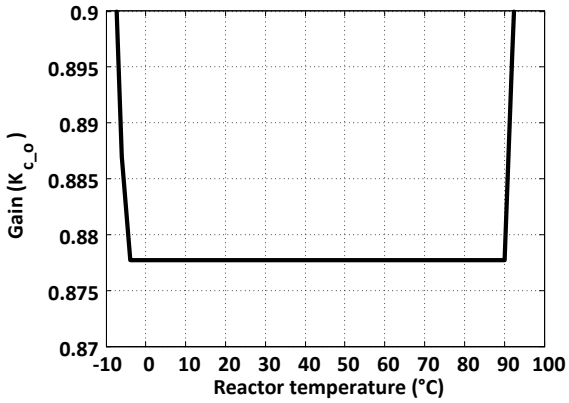

Figure 4.12. The gain of the controlled composite object in the case of the jacket recirculation loop model-based split-range algorithm

Also with this split-range algorithm as with the solution in "The second algorithm" in Chapter 4.2.1, it is possible to keep the sign of the gain unchanged in the whole operation range. Moreover, the gain is kept constant in the normal operation temperature range and is also independent of the actual mode of operation. This solution has similar advantages as the previously described algorithm. Despite the change in the mode of operation, the resulting output of the

PID controller remains smooth, since the heating/cooling effect changes without discontinuity. This algorithm, based on the model of the jacket recirculation loop, can be advantageous if the dynamics of the heat transfer between the jacket and the reactor is comparable with the dynamics of the temperature change caused by the convectional heat flow of the thermal fluid entering the jacket recirculation loop.

4.2.3. Simulation results

Before testing the split-range algorithms on the pilot plant, simulation tests were performed to ascertain the proper operation of the algorithms and determine the parameters of the slave loop PI controller. For this purpose the previously described UniSim Design–based simulator (Chapter 3.2) was planned to be used. However due to its limitations regarding interfaces towards third-party software it could not be used. According to these difficulties a simulator created in MATLAB Simulink was used, which was simplified compared to the UniSim Design–based simulator. The model equations describing the reactor and the jacket recirculation loop was identical to the ones in Chapter 4.2.2.

The model of the pilot plant was implemented in MATLAB Simulink (Figure 4.13), since this software package provides a flexible environment to test algorithms and to solve ordinary and differential equations and their sets. In addition, with the use of its OPC toolbox, the model of the pilot plant can be replaced with the real process using OPC connections. This can ensure that the conditions, parameters, and created algorithms are the same during both the simulation tests and the test measurements. The simulator includes the following parts:

- Reaction mixture: lumped model
- Reactor body as an extra heat capacity: lumped model
- Jacket of the reactor: lumped model
- Recirculation loop of the jacket: according to Figure 4.3 and Equation (4.11)
- Heat transfer establishes a connection between the reaction mixture, the reactor body, and the jacket

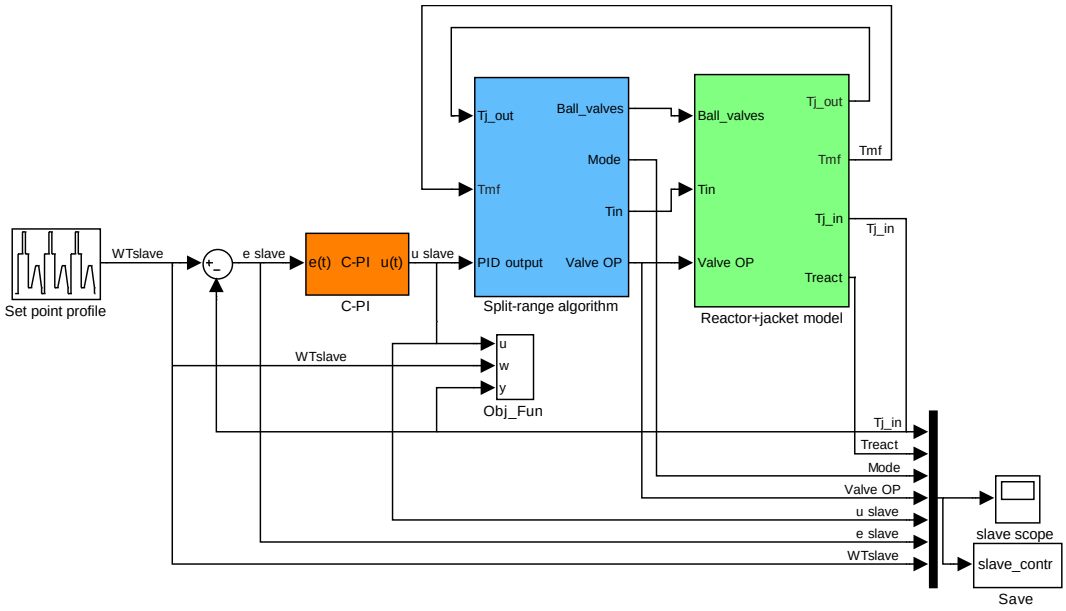

Figure 4.13: The structure of the MATLAB Simulink model for the simulation tests

The temperature levels of the monofluid thermoblock were constant in the simulator implemented in Simulink.

Constant heat transfer coefficient was used between the jacket and the reactor that was equal with the value implemented in the jacket recirculation loop model-based split-range algorithm. As the heat transfer coefficient depends on the temperature, an average value was chosen. In terms of the jacket temperature control the reactor is a load-type disturbance with high time constant, thus the reactor temperature in the simulator does not need to be so accurate as it was an important criteria in Chapter 3.2. This is the reason why in the simulation tests without reaction, the temperature of the reactor differs from the test measurement values. The heat transfer value is slightly under-estimated during this test, thus the temperature of the reactor is lower compared with the test measurement values. In the case of tests with reaction, due to the higher initial temperatures, the heat transfer coefficient is more accurate, which causes the slight difference in reactor temperature between simulation and test measurement.

The thermometer models were also implemented in the simulator, since the dynamics of the thermometers are comparable to the process dynamics. Thus, the reactor, jacket inlet, and outlet thermometer were modelled with a first order plus dead time transfer function.

The parameters used in the constrained PI controller were determined by numerical optimization. The Covariant Matrix Adaptation Evolutionary Strategy (CMA-ES) algorithm was used as the numerical optimization method, and besides the integrated square error, the overshoot and oscillation of the controlled variable was considered by penalty terms in the objective function. The optimization resulted several different parameter combinations for each split-range solutions when using different penalty terms.

The set-point profile was compiled to cover the whole temperature range and to contain ramped and constant sections as well as drastic changes in set-point.

Two types of simulation test were carried out that differ in the initial conditions of the reactor and the in the reaction heat flow introduced. In the first type of test the reaction mixture, the wall of the reactor and the temperature of the jacket was initialized with 20 °C as a cold start of the reactor (Table 4.4). No chemical reactions were performed in this test; the reaction mixture in the reactor was water.

In the second type of test the initial conditions were different, as can be seen in Table 4.4; the reaction mixture was 55 °C; the wall and the jacket of the reactor was 30 °C at the beginning of the test. These initial values were chosen to simulate the conditions of the reactor after the preheating of the reactor. Also reaction heat was introduced to the reaction mixture as a constant (2.3 kW) heat flow. It was chosen to simulate the most important disturbance in the control of the reactor, and with this method the same effect could be easily reproduced in the test measurements with the reaction heat simulation loop of the reactor. The introduced heat flow is equal to the power of two filaments of the three available for reaction heat simulation.

Table 4.4: The conditions for the different simulation tests performed

	Without reaction	**With reaction**
Initial reaction mixture temperature	20 °C	30 °C
Initial reactor wall temperature	20 °C	30 °C
Initial jacket temperature	20 °C	55 °C
Reaction heat flow	0 kW	2.3 kW

In the following simulations and test measurements results the modes of operation are coded as the following, concerning temperature levels: 1 – high, 2 – medium, 3 – low.

Industrial solution

The solution used in the industry for thermoblocks with three different temperature levels was also tested with simulation. In this split-range solution only one characteristic is used that is suitable for most of the operating range, but it can make the controller instable when the gain of the controlled composite object changes sign. The tested split-range characteristic can be seen in Figure 4.14. The PID output is divided unequally in this solution that can be originated from the split-range solution used for two temperature levels (Figure 1.8). This solution can be stabile only if the medium temperature level is always a cooling media.

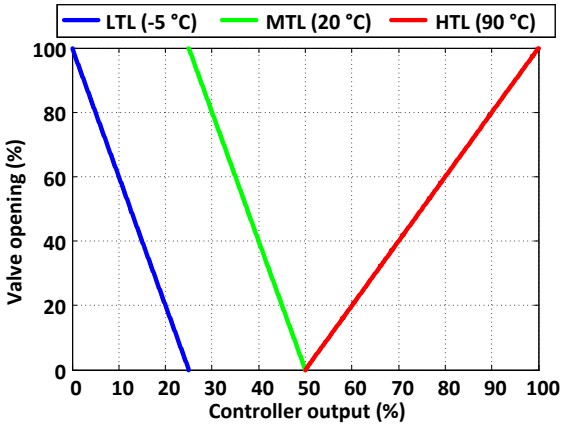

Figure 4.14: Split-range characteristic used in the industry

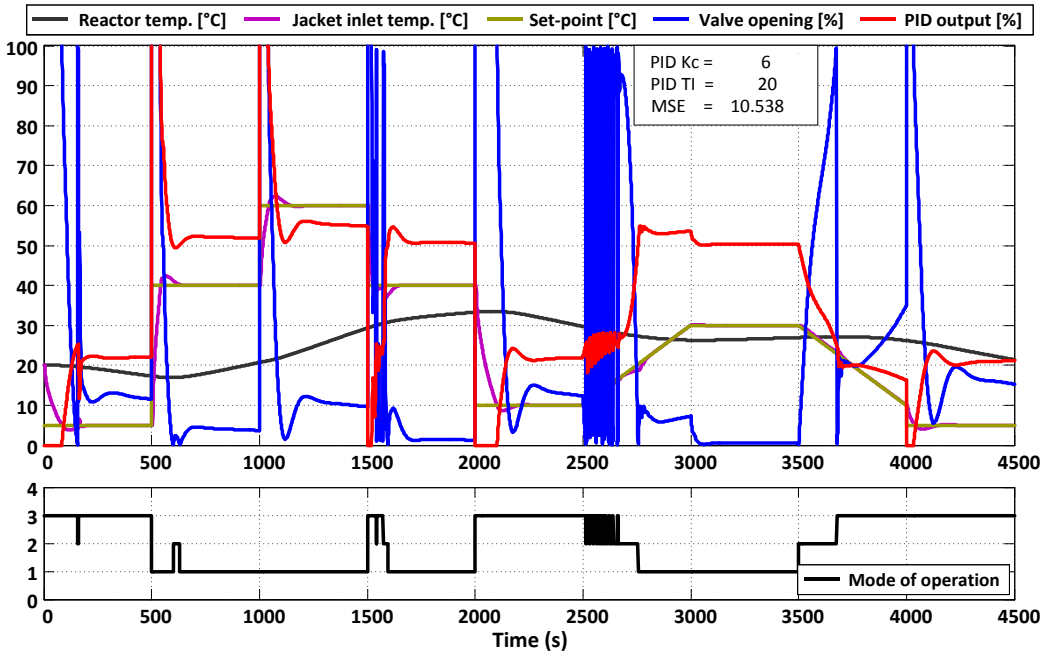

Figure 4.15: Simulation results of the slave control loop in the case of the industrial split-range solution (without reaction heat flow)

As it can be seen in Figure 4.15 the split-range algorithm performs well in almost the entire analysed temperature range, except at 2500 seconds when the temperature of the jacket is lower than the medium temperature level. In this case the sign of the gain of the composite controlled object changes, since the medium temperature level is a heating media at this point. This makes the control to become instable, resulting in an operating mode change. Thus, the medium temperature level cannot be utilised at lower temperatures as would be desirable.

Mixer model-based algorithm, first solution

The results of the first simulation test performed on the slave control loop using the first mixer model based split-range solution can be seen in Figure 4.16. In this test no reaction was performed in the reactor. The controlled variable reaches the set-point with a slight overshoot and low settling time; oscillation in the controlled variable and frequent changes in the mode of operation cannot be

discovered. The only unfavourable effect appears at approximately 2700 seconds, where during the ramping of the set-point, the jacket inlet temperature reaches the inlet temperature of the jacket recirculation loop. After the change in the mode of operation, a slight oscillation appears in the output of the PI controller. The controller is too dynamic for set-point ramping with a high driving force. However, this has a minimal effect on the controlled variable.

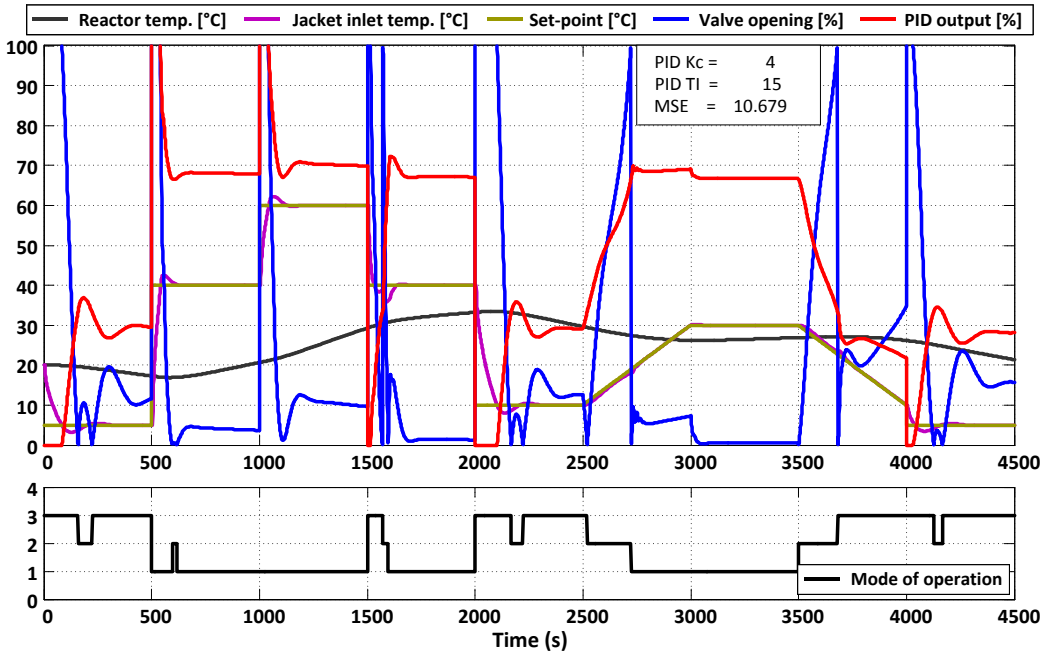

Figure 4.16. Simulation results of the slave control loop in the case of the first split-range algorithm based on the mixer model (without reaction heat flow)

The simulation test results containing constant reaction heat flow and different initial conditions can be seen in Figure 4.17. The same PI parameters were used in the PI controller, since the results of the PI parameter identification were similar. Good control performance was achieved similarly to the previous simulation test and no oscillation occurred during the test. The Mean Square Error (MSE) of this test is slightly lower. The difference between the two simulation tests regarding the output of the PI controller is caused by the different temperatures of the reactor, which generates different amount of heat flow between the reactor and the jacket.

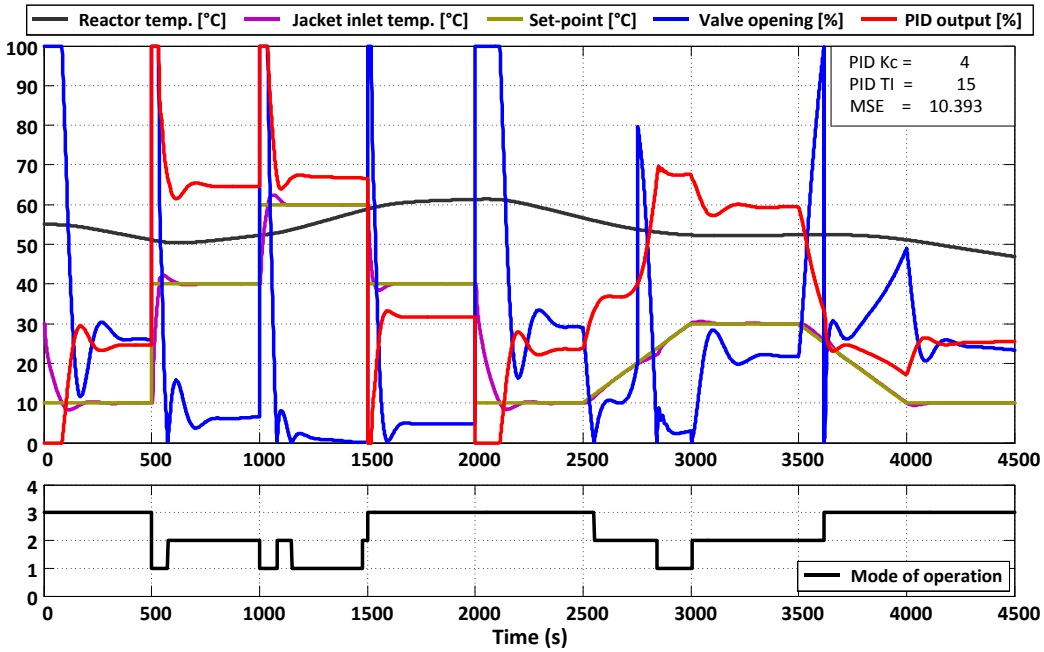

Figure 4.17. Simulation results of the slave control loop in the case of the first split-range algorithm based on the mixer model (with reaction heat flow)

Mixer model based algorithm, second solution

The results of the first simulation test using the second mixer model based split-range solution can be seen in Figure 4.18. With this solution, better results can be achieved, and no oscillation or fluctuation is experienced. Besides identifying the parameters of the PID controller for this composite controlled object by numerical optimisation, satisfactory parameters can also be determined by trial and error. This can promote the use of this solution in industrial applications where control engineers have significant PID controller-tuning experience. The used PI parameters are different from the ones used for the first mixer model based solution, since the composite controlled object is different. This results in different optimal PI parameters.

The results of the second simulation test can be seen in Figure 4.19, where a constant reaction heat flow was used. The controller performs as well as in the test without reaction. A slight decrease can be noticed in the MSE value between the two tests. Compared with the previous solution both of the MSE values are better, which means that control error is lower when using this solution.

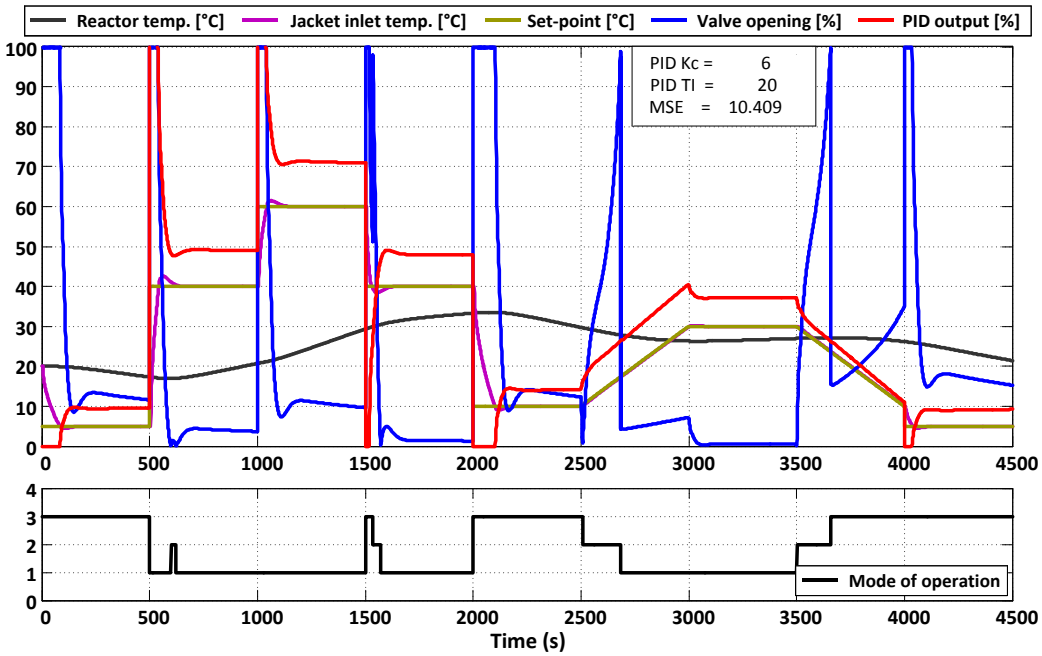

Figure 4.18. Simulation results of the slave control loop in the case of the second split-range algorithm based on the mixer model (without reaction heat flow)

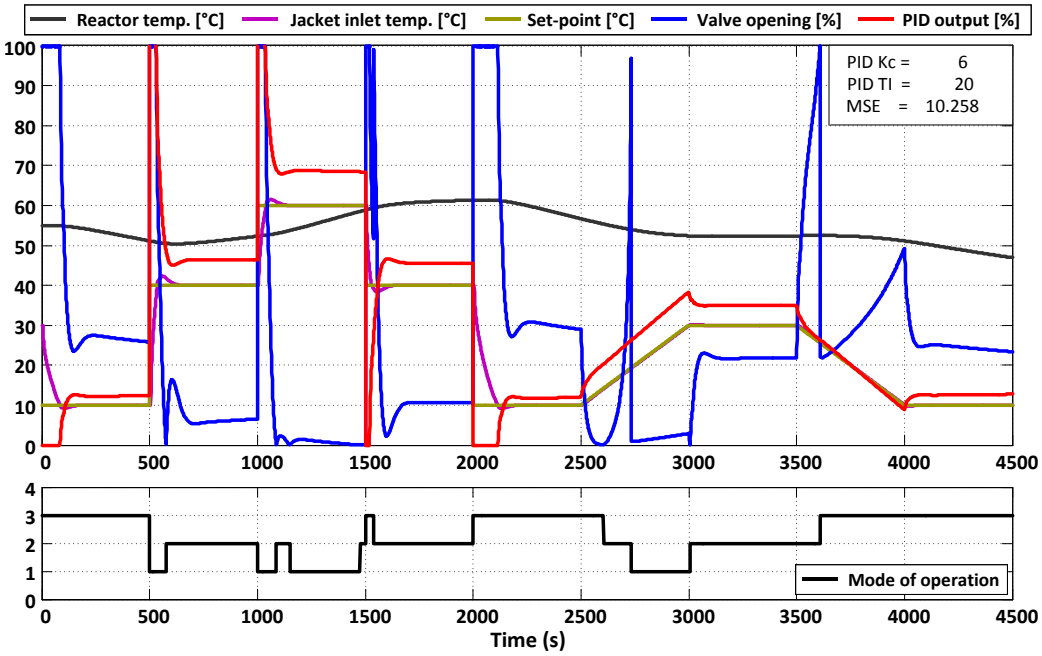

Figure 4.19. Simulation results of the slave control loop in the case of the second split-range algorithm based on the mixer model (with reaction heat flow)

Jacket recirculation loop model based algorithm

The same set-point profile was also used for the test of this split-range algorithm. The simulation results in the first test can be seen in Figure 4.20. The behaviour of the PID output is relatively fluctuating, which is a disadvantageous property of this solution. The parameters used in the model of this split-range

solution were exactly the same as used in the simulation model. Thus, the modelling error was eliminated. The identification of the PI parameters for this solution resulted significantly different values compared with the previous ones. This can be explained with the different composite controlled object.

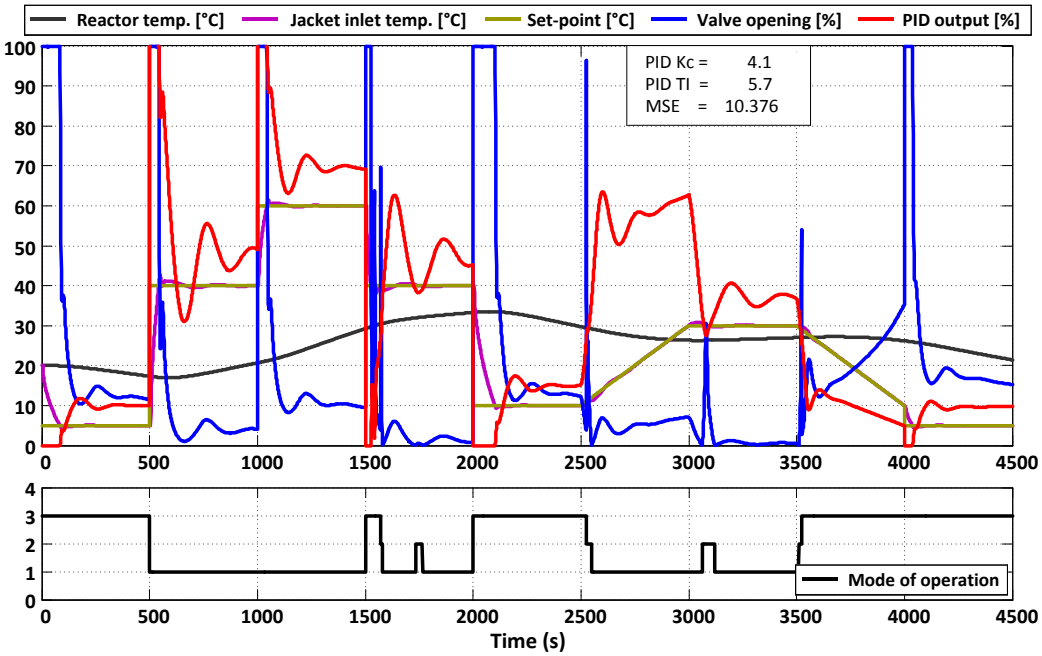

Figure 4.20. Simulation results of the slave control loop in the case of the split-range algorithm based on the jacket recirculation loop model (without reaction heat flow)

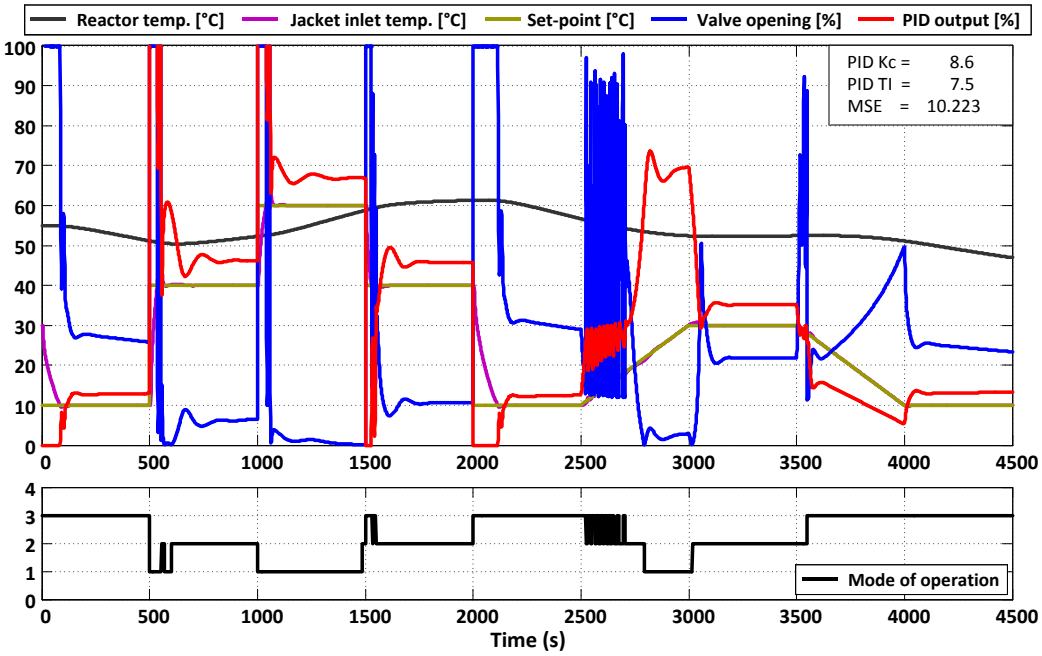

Figure 4.21. Simulation results of the slave control loop in the case of the split-range algorithm based on the jacket recirculation loop model (with reaction heat flow)

In the second simulation test that can be seen in Figure 4.21 different PI parameters were used according to the identification results. If the same PI parameters would have been used, high oscillation and fluctuation could have been noticed. The parameters used for the first test would have been too dynamic for the second test. The oscillation effect from 2500 seconds is caused by the inadequate sign of the gain used by the split-range algorithm; however, in a system where the dynamics of the jacket and the recirculation loop is similar (for example, in small-scale laboratory reactors), this effect does not occur.

The summary of the simulation tests can be found in Table 4.5. According to the MSE values the jacket recirculation loop model based split-range solution was proved to be the best choice. However, if the movement of the controller output is also considered then the second mixer model based solution performs better.

According to the experience in simulation tests, the second mixer model based split-range solution appeared to be the better modelling approach. It is more robust than the solution containing the jacket recirculation loop model, which results in the slave loop being less sensitive to the PID parameters. However, the main advantage of both mixer model based split-range solutions is the simplicity of the model. It only contains such parameters that can be measured easily in the real system (for example: flow rate, temperature). There is no need to identify the heat transfer coefficient, heat transfer area, etc., of the reactor. Thus, it is not as sensitive to modelling error and is more suitable for different kinds of jacket configurations. Due to its simplicity, it can be easily implemented in industrial controllers without serious changes in the configuration. Comparing the two mixer model based split-range algorithms, the second solution obviously performs better, as it maintains not only the sign of the gain of the composite controlled object unchanged but also keeps the gain on a constant value. This makes the composite controlled object easier to control for the PID controller.

Table 4.5: The summary of the different simulation tests performed

Split-range type	Figure Number	Reaction heat flow	P	I	MSE
Industrial	Figure 4.15	OFF	6	20	10.538
Mixer model based, first solution	Figure 4.16	OFF	4	15	10.679
Mixer model based, first solution	Figure 4.17	ON	4	15	10.393
Mixer model based, second solution	Figure 4.18	OFF	6	20	10.409
Mixer model based, second solution	Figure 4.19	ON	6	20	10.258
Jacket recirculation loop model based	Figure 4.20	OFF	4.1	5.7	10.376
Jacket recirculation loop model based	Figure 4.21	ON	8.6	7.5	10.223

Utility cost calculation

Not just only the MSE can be a good measure to compare the different split-range solutions but also the calculated utility costs for each simulation and test measurements. The different temperature levels have different production costs due to the distinct equipment controlling their temperature.

The high temperature level consumes in its electric heaters only electric energy. As it was described in Chapter 2.1 the sum electric energy consumption of the two electric heaters are 12 kW. The efficiency of resistance immersion heaters for fluid heating is very high as the produced heat only can be transferred to the surrounding fluid. The efficiency was estimated 98% and thus the effective heat flow is 11.8 kW as can be seen in Table 4.7.

The medium temperature level is controlled by cooling water through a plate heat exchanger. The cooling capacity of the plate heat exchanger was calculated from measurement data with an average of 7.4 kW as it can be seen in Table 4.7. For cooling, a constant 1.18 m^3/h cooling water is consumed if the solenoid valve is open.

The low temperature level is controlled by a refrigerator through a plate heat exchanger. The cooling capacity of this system also can be calculated from measurement data. As can be seen in Table 4.7, this occurred at an average of 10 kW. The nominal power of the compressor in the refrigerator is 5.5 kW, thus this is the energy consumed to produce the previously described cooling performance.

To calculate the energy specific prices of each temperature level, the prices of the consumed utilities are necessary. These prices can be seen in Table 4.6. By applying these energy specific prices the cost of each simulation and test measurement can be calculated and compared.

The operating cost of each temperature level can be calculated as the product of the consumed electric energy or utility and its price (Equation (4.19)). The energy specific price of each temperature level can be calculated using Equation (4.20). These specific energy prices can be seen in the bottom row of Table 4.7. As it is expected the cheapest temperature level is the medium temperature level.

$$C_{op} = c_{ut} \cdot E_{cons} \tag{4.19}$$

$$c_{mf} = C_{op} \Big/ \dot{Q}_{eff} \tag{4.20}$$

Table 4.6: Utility prices

Energy type	Price	Unit
Electric energy	40	HUF/kWh
Cooling water	10	HUF/m^3

As the energy specific price of each temperature level is known, the cost of the tests can be calculated with the following equation:

$$C_m = \int_0^{t_{end}} F_{max} \cdot \frac{u_{valve}(t)}{100} \cdot \rho_{mf} \cdot c_p^{mf} \cdot \left| T_{in}^{m}(t) - T_{jacket}^{out}(t) \right| dt \tag{4.21}$$

Table 4.7: The calculation of the prices of the different temperature levels

	LTL	**MTL**	**HTL**
Heating/cooling capacity (kW)	10.0	7.4	11.8
Heating/cooling capacity (MJ/h)	36.0	26.6	42.3
Electric energy consumption (kW)	5.5		12.0
Cooling water consumption (m3/h)		1.18	
Operating cost (HUF/h)	220	11.8	480
Energy specific price (HUF/MJ)	6.11	0.44	11.34

The cost of each simulation test presented previously can be seen in Table 4.8. Only the simulation tests that had the same conditions can be compared, namely the reaction heat flow was turned on or off. Considering the MSE values the jacket recirculation loop based solution slightly has the lowest MSE values in both type of simulation tests. This means that from a control point of view, the lowest control error occurs in the case of this solution. However, analysing the cost values the mixer model based second solution eventuates the lowest values, which means that it uses the medium temperature level more often than the other ones. From an operating cost point of view, the mixer model based second solution appears to be the best split-range solution of the analysed ones.

Table 4.8: The utility cost of the different simulation tests

Split-range type	**Figure Number**	**Reaction heat flow**	**Cost**
Industrial	Figure 4.15	OFF	179.4 HUF
Mixer model based, first solution	Figure 4.16	OFF	181.7 HUF
Mixer model based, first solution	Figure 4.17	ON	168.5 HUF
Mixer model based, second solution	Figure 4.18	OFF	177.1 HUF
Mixer model based, second solution	Figure 4.19	ON	160.1 HUF
Jacket recirculation loop model based	Figure 4.20	OFF	186.7 HUF
Jacket recirculation loop model based	Figure 4.21	ON	164.1 HUF

4.2.4. Test measurement results

The model of the pilot plant in Simulink was replaced with an object containing the necessary OPC inputs and outputs of the pilot plant as it can be seen in Figure 4.22. Thus, the pilot plant was inserted into the slave control loop using an OPC connection. The same set-point profile was used in the test measurements; however, the PI parameters previously identified by numerical optimization had to be changed in some cases due to the disturbance that were not included in the model. The changing of the PI parameters was performed by the experience during the test measurement.

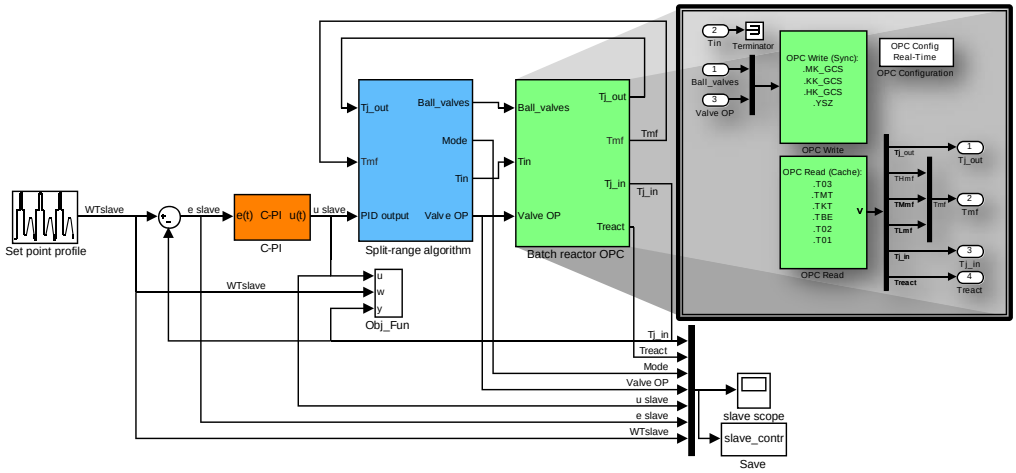

Figure 4.22: The structure of the MATLAB Simulink model for the test measurements

The summary of the performed test measurements can be seen in Table 4.9. In the case of jacket recirculation loop based split-range algorithm and the industrial solution, test measurement was only performed without reaction as the results of the simulation test were unfavourable.

Table 4.9: The summary of the different test measurements performed

Split-range type	Figure Number	Reaction heat flow	P	I	MSE
Mixer model based, first solution	Figure 4.23	OFF	4	15	21.414
Mixer model based, first solution	Figure 4.24	ON	7	30	20.621
Mixer model based, second solution	Figure 4.25	OFF	6	20	19.477
Mixer model based, second solution	Figure 4.26	ON	7	30	20.406
Jacket recirculation loop model based	Figure 4.27	OFF	4	15	21.365

The accuracy of the measuring instruments was described in detail in Chapter 2.2. Raw data is displayed in all figures, which were collected from the OPC server of the Siemens SoftPLC.

Mixer model based algorithm, first solution

The results of the first test measurement for the first split-range algorithm based on the mixer model can be seen in Figure 4.23. In this measurement no reaction heat flow was introduced to the reaction mixture and the initial conditions were similar to the first simulation test described previously. The results are also similar to the previously presented simulation results. This means that the simulator approximates the variables of the real technology properly and is thus suitable for identification of the controller parameters. In the behaviour of the PI controller output in the section of 0-1500 seconds, the varying temperature of the inlet monofluid temperature level can be discovered, which was considered constant in the simulator. In sections of 1500-2000 and 3000-3500 seconds, oscillation can be noticed both in the controlled variable and controller output. This is caused by the frequent change in the mode of operation. This effect appears when the temperature of the jacket and the reactor are almost the same. In this case, no or a small amount of heat is transferred through the wall of the reactor. Due to the proper insulation of the jacket recirculation loop, no heat loss occurs. Thus, a valve opening near zero would be needed. However, due to the mechanical design of the system and the lag of the control valve, this effect cannot be eliminated with control; only the amplitude and frequency of the oscillation can be modified.

Despite the aforementioned effect, the controlled variable, similarly to the simulation results, follows the set-point appropriately both at constant and ramped set-points.

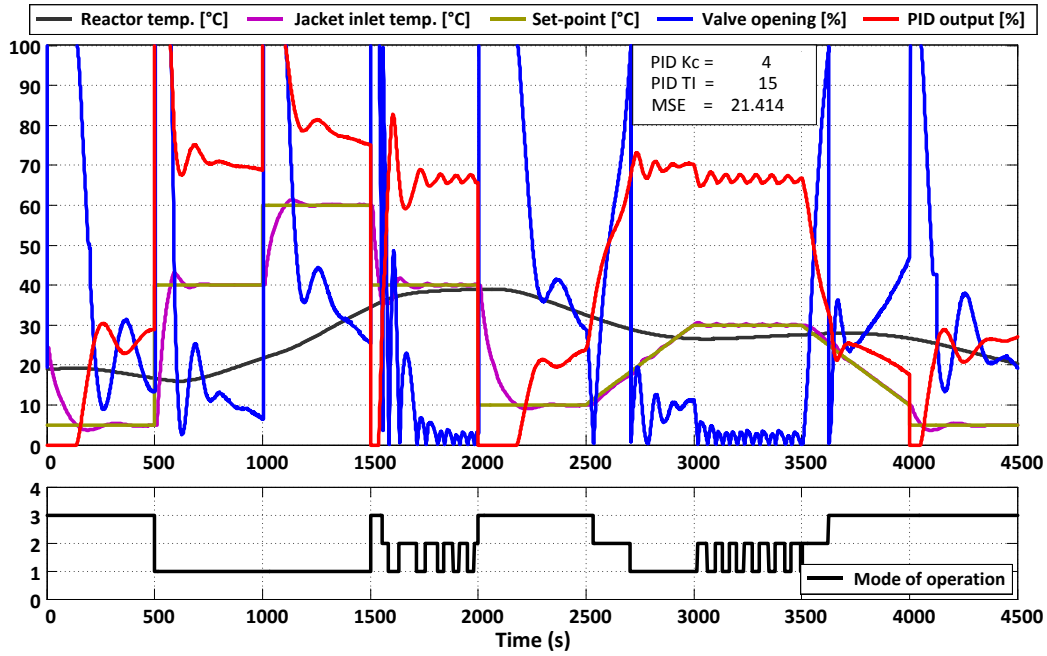

Figure 4.23. Test measurement results of the slave control loop in the case of the first split-range algorithm based on the mixer model (without reaction heat flow)

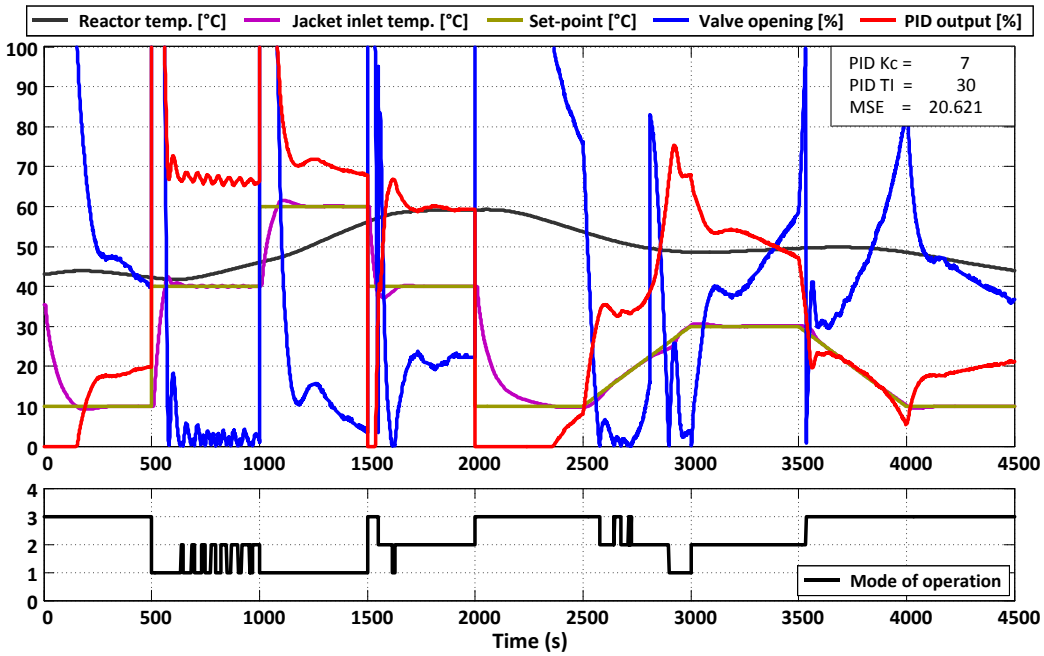

Figure 4.24. Test measurement results of the slave control loop in the case of the first split-range algorithm based on the mixer model (with reaction heat flow)

Also in the second test measurement the initial conditions were similar to the simulation test. A constant heat flow was introduced to the reaction mixture of the reactor with the reaction heat flow simulation loop. Two of the three filaments were turned on that resulted a 2.3 kW heat flow to the reactor. The results can be seen in Figure 4.24, where compared with the first test measurement just slight oscillation can be discovered. This can be explained with the previously described cause of the oscillation. Due to the higher reactor temperature and the constant reaction heat flow, the heat flow to be transferred to the jacket side is never close to zero. Thus, the control valve is almost always in the range where it performs without any lagging. The MSE value of the second test measurement is slightly better; however, it is hard to compare these values as the conditions were not exactly the same as they were in the simulation tests.

Mixer model based algorithm, second solution

The results of the first test measurement for the second mixer model based split-range algorithm can be seen in Figure 4.25. Similarly to the previous test measurements in this first test no reaction heat flow was introduced. The similar oscillation can be noticed as in the previous split-range solution in sections of 1500-2000 and 3000-3500 seconds. The most notable differences between the simulation and test measurement result are caused by the varying temperatures of the monofluid loops of the thermoblock, especially between 1000 and 1500 seconds. The constantly changing PID output in this section is the compensation of the increasing temperature of the high temperature level.

The results of the second test measurement can be seen in Figure 4.26. Similarly to the simulation, constant reaction heat was introduced to the reactor. The oscillation only occurs between 500 and 1000 seconds, where a near-zero valve opening would be needed.

The MSE values of this solution are only slightly better than the ones at the previous split-range solution. However, some progress can be seen in the movement of the PID controller output.

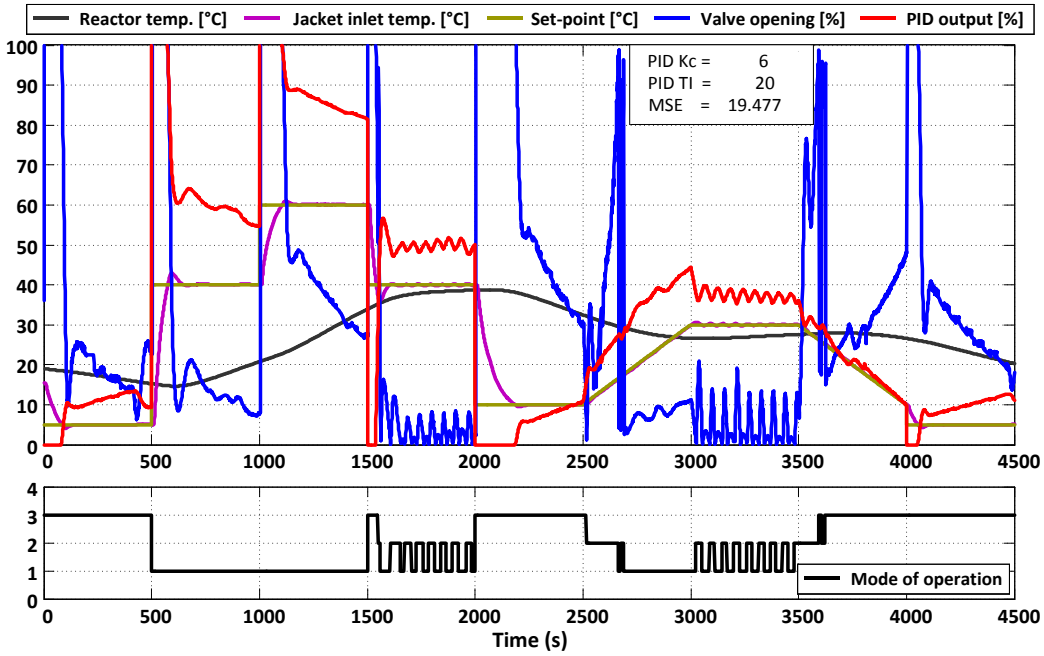

Figure 4.25. Test measurement results of the slave control loop in the case of the second split-range algorithm based on the mixer model (without reaction heat flow)

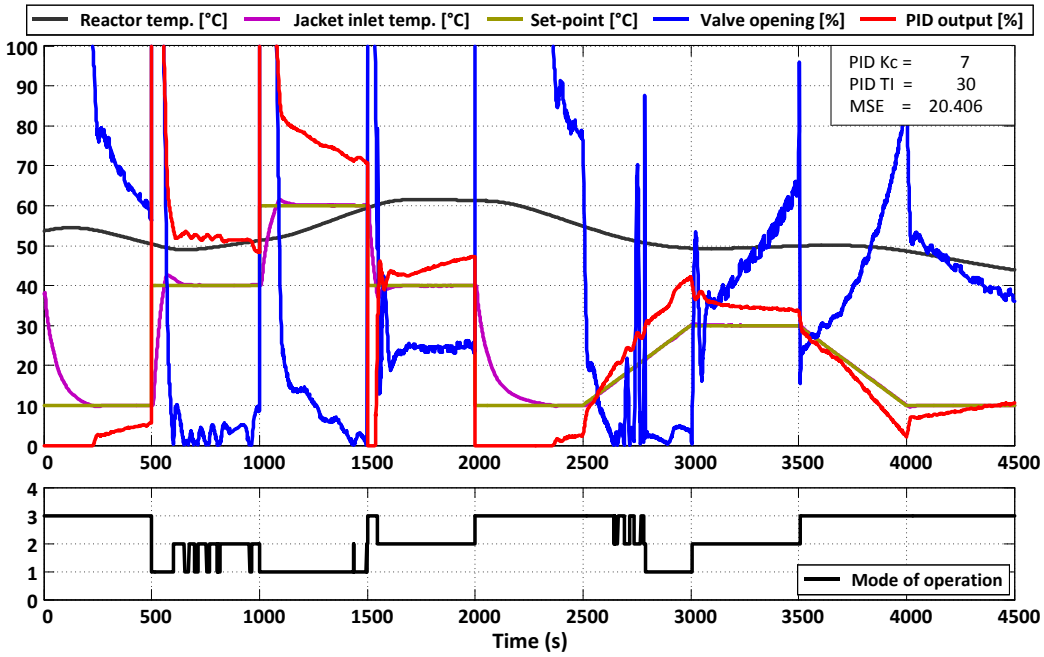

Figure 4.26. Test measurement results of the slave control loop in the case of the second split-range algorithm based on the mixer model (with reaction heat flow)

Jacket recirculation loop model based algorithm

After the simulation tests of the jacket recirculation loop based split-range algorithm on the simulator of the pilot batch reactor, high performance was expected from this solution. The results of the test measurement can be seen in Figure 4.27, where no reaction heat flow was introduced to the reactor. The PI parameters identified during the simulation tests were too dynamic for the real system test, thus less dynamic ones were implemented. The significant change needed in the PI parameters denotes that the model used in the split-range algorithm has a high modelling error. Despite the feedback control this structure cannot compensate the modelling error; hence this solution does not perform well in the test measurements. As it can be seen in the figure it controls the jacket temperature well during steps in the set-point; however during the ramped sections the controlled variable fluctuates around the set-point and never reaches as it should. This can be also noticed in the output of the PID controller. Also the MSE value is higher than the most of the previous test measurements.

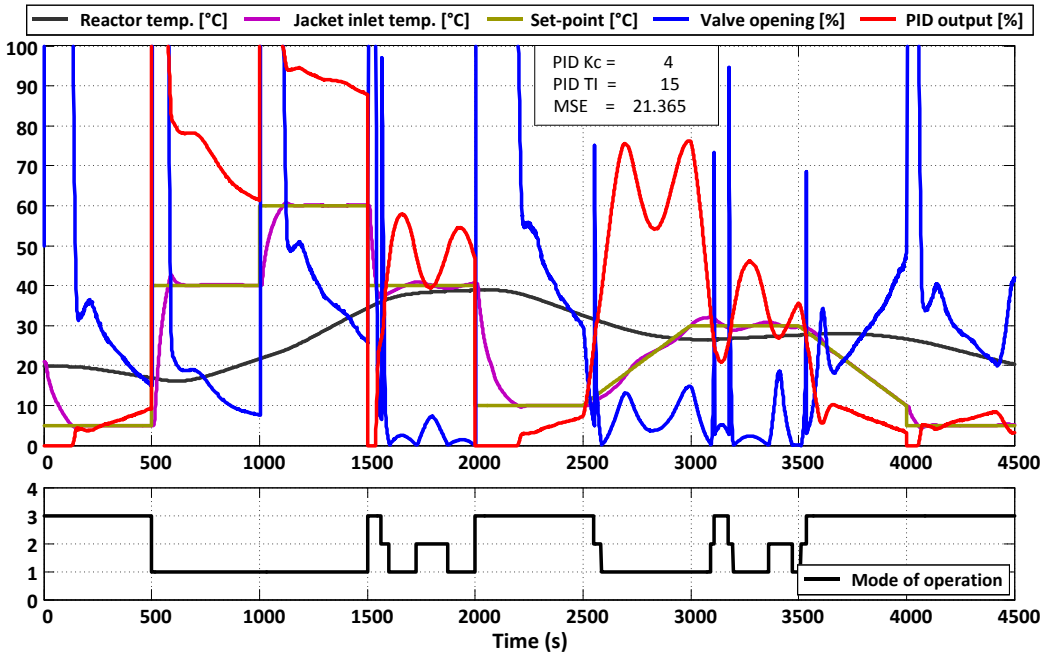

Figure 4.27. Test measurement results of the slave control loop in the case of the split-range algorithm based on the jacket recirculation loop model (without reaction heat flow)

Utility cost calculation

According to the equations in Chapter 4.2.3 the same utility cost calculations were performed for the test measurements. The cost of each test measurement can be seen in Table 4.10. Similarly to the simulation tests the lowest utility cost occurs at the mixer model based second solution in both type of test measurements. Therefore the test measurements confirmed the results gained during the simulation tests.

Table 4.10: The utility cost of the different test measurements

Split-range type	Figure Number	Reaction heat flow	Cost
Mixer model based, first solution	Figure 4.23	OFF	304.8 HUF
Mixer model based, first solution	Figure 4.24	ON	337.4 HUF
Mixer model based, second solution	Figure 4.25	OFF	286.5 HUF
Mixer model based, second solution	Figure 4.26	ON	345.4 HUF
Jacket recirculation loop model based	Figure 4.27	OFF	289.8 HUF

Conclusion

Concluding the experiences of the simulations and test measurements it can be stated that split-range solutions based on the mixer model perform better in both tests and due to their simpler construction they are not so sensitive to modelling error. They only contain such parameters that can be measured easily in the real system (for example: flow rate, temperature). There is no need to identify the heat transfer coefficient, heat transfer area, etc., of the reactor.

From the two mixer model based solutions the second is the more preferable as it keeps not only the sign of the gain of the composite controlled object unchanged but the value of the gain remains constant in the operating range of the batch processing unit. This makes the composite controlled object simpler to be controlled for the slave loop controller.

By analysing the utility costs of each simulation and test measurement to compare the utilising of the cheap medium temperature level, it can be stated that the mixer model based second solution uses the most amount of medium temperature level, thus, from an operating point of view it is the most favourable solution.

5. Summary and Theses

In high-value-added manufacturing processes the temperature of the reaction mixture has a high relevance, as a small difference in the temperature of the reactor might cause great difference in the final product. Thus, in pharmaceutical-, food-, polymer- and fine-chemical industries where the heatable, coolable and stirred autoclaves dominate, the adequate temperature control is an essential issue. While the realization of the control system is supported by the S88 standard, the implementation of control algorithms at different hierarchy levels are encumbered by theoretical and mechanical issues. Scientific research mainly focuses on the more complex problems of the higher hierarchy levels, e.g., optimization, scheduling, etc. However, the unsolved control problems of the lower hierarchy levels make the realization of the higher hierarchy solutions impossible.

During the mechanical design and construction of chemical manufacturing systems, the location and implementation of measuring instruments are commonly driven by aesthetic and practical principles. If classical control solutions are used (e.g., PID controller) these errors rarely cause poor control quality. However, in the case of advanced and model based control algorithms the control performance is significantly affected. In Chapter 2 different thermometer installation errors are described, which can cause unwanted effects preventing the better performance of advanced control algorithms. These effects were discovered during the development of the pilot batch processing unit located in the laboratory of the author's department. One of the most important issues is the location of the thermometers in the technology. If the measured value is preferred to be used in calculations, the adequate location must be found. The thermometer installation directions in pipe bends also have significant effects on control; however it is not considered important during design and construction. The thermowell of the thermometer also has a great effect on the response time of the measured value. And yet, in active operating technologies the replacement of these instruments are costly, and due to the requirements of the environment a better solution might not be installable. Therefore, if no replacement is performed, at least the response time should be identified, which can improve the performance of model based control solutions.

It can be concluded that without the detailed analysis and tuning of the measuring instruments and the technology itself, better control performance cannot be achieved with model based solutions (or just worse) compared to classical control solutions, as the calculations that use the measuring instruments as input have significant uncertainty.

In the industry an increasing number of heating/cooling systems utilizing three different temperature levels can be found, which are advantageous from an economic point of view; however, it makes the control more complicated. The temperature of the reactor is controlled through its jacket, thus, the control quality of the jacket temperature controller mainly restricts the quality of the reactor temperature controller.

A pilot batch processing unit can be found in the laboratory of the author's department that has a monofluid thermoblock containing three different temperature levels. It was used to test different control solutions feasible for

handling such systems. In this thermoblock the medium temperature level can also be a heating or cooling media depending on the actual state of the reactor. The classical split-range solution handling two modes of operation are not suitable for such systems, thus development of new solutions were needed.

Besides handling three temperature levels, the aim of the split-range algorithm development was to find a solution that can be easily attached to existing PID-based control structures. For this purpose two split-range algorithms were developed and two different models were used to describe the jacket recirculation loop of the reactor. This resulted in three different split-range solutions.

The first split-range algorithm considers the actual temperature value of the jacket and the inlet thermal fluid. According to the mixer model describing the jacket recirculation loop it switches between a set of predefined splitting characteristics with the aim to avoid the change in the sign of the gain of the controlled object. With this solution the adequate utilization of all the three temperature levels by the jacket temperature controller can be achieved.

A second split-range algorithm was also developed. Its aim was to compensate not only the changes in the sign of the gain of the controlled object but also to keep the value of the gain constant in the whole operating range. In this algorithm two different modelling considerations were used to describe the jacket recirculation loop. In the first modelling consideration the jacket recirculation loop was described by a mixer model that was also used in the previous split-range algorithm. This model resulted in a simple split-range solution compared to the second one, which results less modelling error due to the less parameters and it is also easier to implement in industrial applications. The simulation and measurement tests proved the quality of this solution. In the second solution the model of the whole jacket recirculation loop was used. This model involved the temperature of the reactor as the most significant disturbing effect on the jacket. This solution performed worse compared with the mixer model based ones, which can be explained with the significant difference in the response time of the jacket and the reactor and also with the higher modelling error.

The testing and analysis of the different split-range solutions were not only performed by MATLAB based simulations but also by test measurements on the pilot batch processing unit. The first split-range algorithm performed well, both in simulation and measurement tests. However, it cannot compete in control quality with the mixer model based second split-range algorithm as the second algorithm compensates not only the sign of the gain of the controlled object but also the value of the gain. The jacket recirculation model based second algorithm had the worst results due to its high modelling error and as it is not feasible for this system. The results of both simulation and test measurements were compared not only with control error but with the utility cost of the tests.

It can be concluded that according to the simulation and measurement test results the best control performance can be achieved with the second split-range algorithm based on the mixer model. Not just the control performance makes it favourable but also the simplicity that promotes its implementation in industrial applications.

5.1. Theses

1. **The measurements of a batch processing unit can be used in engineering calculations and model based control solutions limitedly without the analysis of the measuring instruments and the mechanical construction and also the adequate tuning of the system is necessary.**
    a. It was proven by test measurements that the dynamics of the thermometers significantly depend on the way of their installation, which effect has to be considered in the related calculations.
    b. An application was developed that uses measurement data to identify the main thermal parameters of the reactor, and therefore it provides the opportunity to calculate the PID parameters of the reactor temperature controller. The application also can be used to determine the reaction heat flow offline from usual measurement possibilities.
    c. A methodology was developed wherewith batch technologies can be implemented into simulation software designed for continuous technologies. A method, based on a more detailed model, was developed for calculating the heat transfer coefficient with the aim to improve the accuracy of the heat flow calculation between the reactor and the jacket.

    Related publications: 1, 4, 5, 6, 7, 8, 9, 11, 12, 13, 14

2. **A split-range algorithm was developed for the jacket temperature control of batch reactors that is able to handle a thermoblock containing three different temperature levels.**
    a. It was ascertained that the classical split-range solutions cannot be used in the temperature control of the jacket in the case of a thermoblock with three different temperature levels.
    b. It was proven that by reason of the change in the sign of the gain of the slave loop controlled object, caused by the temperature change of the jacket and the thermoblock loops, the slave loop controller cannot utilize properly all three temperature levels if only one split-range characteristic is used.
    c. A split-range algorithm was developed that allows the normal utilization of all three temperature levels, which can be used along with the classical PID controllers and easily installed in industrial applications.

    Related publications: 2, 15

3. **Split-range algorithms were developed based on the model of the jacketed batch reactor that can be parameterized by the geometrical and thermal properties of the reactor, can handle a thermoblock with three temperature levels and compensate the changes in the gain of the slave loop controlled object.**
    a. A split-range algorithm was developed based on the model of a mixer that can compensate not only the changes in the sign of the gain of the controlled object but also the changes in its value.
    b. Split-range algorithm was developed based on the model of the jacket, which can be used in the case of reactors where the dynamics of the jacket can be compared with the dynamics of the reactor temperature. It can compensate the disturbing, dynamically comparable, and nonlinear effect of the reactor temperature on the control of the jacket temperature and therefore keep the gain of the controlled object constant.
    c. The modelling inaccuracies of the jacketed reactor significantly influence the gain compensating effect of the split-range algorithm. Despite that the split-range algorithm based on the jacket model has a more detailed model compared to the mixer model based solution, it performs worse on the pilot system as it has more input parameters that can be loaded with error.

Related publications: 3, 10, 15, 16

5.2. Tézisek

1. **Igazoltam, hogy egy szakaszos gyártócella mérései - a gépészeti megoldásainak valamint mérőműszereinek részletes vizsgálata, ezen felül a rendszer megfelelő beállítása nélkül – a mérnöki számításokban illetve modell-alapú szabályozási megoldásokban csak korlátozottan alkalmazhatóak.**
    a. Mérésekkel igazoltam, hogy a köpenyes reaktor hőmérőinek dinamikája jelentősen függ azok beépítési módjától, mely hatást a rájuk épülő számításokban figyelembe kell venni.
    b. Kifejlesztettem egy alkalmazást, amely mérési adatok felhasználásával meghatározza a reaktor legfontosabb hőtani paramétereit, és ezáltal, lehetőséget biztosít a reaktor PID hőmérsékletszabályozó paramétereinek számítására. Az alkalmazással, a szokásos mérési lehetőségek mellett, offline meghatározható a hőáramforrás (reakcióhő) is.
    c. Kidolgoztam egy módszert, amellyel a szakaszos gyártócella folyamatos technológiákra kialakított szimulációs eszközökbe is implementálható. A hőátszármaztatási tényező számítására egy részletesebb modellen alapuló módszert dolgoztam ki, amely növeli a reaktor és a köpeny közötti hőáram számításának pontosságát.

    Kapcsolódó publikáció: 1, 4, 5, 6, 7, 8, 9, 11, 12, 13, 14

2. **Kifejlesztettem egy a szakaszos reaktorok köpeny-hőmérsékletének szabályozásához kapcsolódó split-range algoritmust, amely képes három különböző hőmérsékleti szinttel rendelkező hűtő/fűtő blokk kezelésére.**
    a. Megállapítottam, hogy a klasszikus split-range megoldások nem alkalmazhatóak három különböző hőmérsékleti szinttel rendelkező hűtő/fűtő rendszer esetén a köpenyhőmérséklet szabályozásában.
    b. Igazoltam, hogy a köpeny- valamint a hűtő/fűtő közegek hőmérsékletváltozása által okozott, a slave köri objektum erősítésének előjelében történő váltás miatt, a slave-köri szabályozó nem tudja megfelelően kihasználni mindhárom hőmérsékleti szintet egyetlen beépített split-range karakterisztikával.
    c. Olyan split-range algoritmust fejlesztettem ki, amely mindhárom közeg üzemszerű használatát lehetővé teszi, a klasszikus PID szabályzókkal együtt alkalmazható, és ipari rendszerekbe is könnyen telepíthető.

    Kapcsolódó publikáció: 2, 15

3. **Köpenyes reaktor modelljére alapozott split-range algoritmusokat fejlesztettem ki, amelyek a reaktor geometriai és hőtani tulajdonságaival paraméterezhetőek, három különböző hőmérsékleti szinttel rendelkező hűtő/fűtő rendszer kezelésére is alkalmasak, valamint képesek kompenzálni a szabályozott objektum erősítésének változásait.**
    a. Keverő modellre épülő split-range algoritmust fejlesztettem ki, amely nem csak a szabályozott objektum erősítésében jelentkező előjelváltásokat, hanem értékének változását is képes kompenzálni.
    b. A reaktor köpeny modelljére épülő split-range algoritmust fejlesztettem ki, amely azon reaktorok esetén alkalmazható, ahol a köpenyhőmérséklet változásának dinamikája összemérhető a reaktor hőmérséklet változásának dinamikájával. A reaktor hőmérsékletének a köpenyszabályozásra gyakorolt zavaró, dinamikában összemérhető, nemlineáris hatását képes kompenzálni és így a szabályozott objektum erősítését állandó értéken tartani.
    c. Megállapítottam, hogy a köpenyes reaktort leíró modell pontatlanságai nagyban befolyásolják a split-range algoritmus erősítés kompenzáló hatását. A köpeny modellre alapozott split-range algoritmus annak ellenére, hogy részletesebb modellt tartalmaz, mint a keverő modell alapú megoldás, a valós rendszeren rosszabbul teljesít, mivel több bemeneti paraméterrel rendelkezik, amelyek hibával terheltek.

Kapcsolódó publikáció: 3, 10, 15, 16

6. Publications related to theses

Articles in international journals

1. M. G. Balaton, L. Nagy and F. Szeifert, "Operator Training Simulator Process Model Implementation of a Batch Processing Unit in a Packaged Simulation Software", *Computers & Chemical Engineering*, vol. 48, pp. 335-344, 2013.

2. M. G. Balaton, L. Nagy and F. Szeifert, "Jacket Temperature Control of a Batch Reactor Using Three Different Temperature Levels", *Industrial & Engineering Chemistry Research*, vol. 52, no. 5, pp. 1939–1946, 2013.

3. M. G. Balaton, L. Nagy and F. Szeifert, "Model-Based Split-Range Algorithm for the Temperature Control of a Batch Reactor", *Engineering*, vol. 4, no. 9, pp. 515-525, 2012.

Articles in Hungarian journals

4. Balaton M. G., Nagy L., Szeifert F,: "Szakaszos gyártócella szimulációja", *Acta Agria Kaposvariensis*, vol. 15, no 3, pp. 257-269, 2011.

Refereed presentations

5. Balaton M. G., Nagy L., "Szakaszos gyártócella szimulációja", *Műszaki Kémiai Napok*, Veszprém, 2009, pp. 117-122.

6. Balaton M. G., Nagy L., Szeifert F., "Szakaszos gyártócella szimulációja", *Informatika Korszerű Technikái*, Dunaújváros, 2010.

7. M. G. Balaton, L. R. Tóth, L. Nagy and F. Szeifert, "Reaction heat flow control by dynamically calibrated thermometers", in *proceedings of 11th International PhD Workshop on Systems and Control*, Veszprém, 2010, pp. 80-85.

8. M. G. Balaton, L. R. Tóth, L. Nagy and F. Szeifert, "Optimal Temperature Control of Partially Simulated Batch Reactor", in *Proceedings of 1st International Scientific Workshop on DCS*, Lillafüred, 2010, pp. 15-23.

9. M. G. Balaton, L. Nagy and F. Szeifert, "OTS System Development for a Batch Process Unit", in *Proceedings of 2nd International Scientific Workshop on DCS*, Lillafüred, 2011, pp. 13-20.

10. M. G. Balaton, L. Nagy and F. Szeifert, "Model Based Temperature Control of Batch Reactors", in *Proceedings of 5th International Interdisciplinary Technical Conference of Young Scientists*, Poznan, Poland, 2012, pp. 21-26.

11. M. G. Balaton, L. Nagy and F. Szeifert, "Simulation of a batch reactor and its monofluid heating-cooling system", *19th International Congress of Chemical and Process Engineering CHISA 2010* [CD-ROM], Prague, Czech Republic, 2010.

Non-refereed presentations

12. Balaton M. G., Nagy L., Szeifert F., "Szakaszos gyártócella szimulációja", *VIII. Alkalmazott Informatika Konferencia*, Kaposvár, 2010.

13. M. G. Balaton, L. Nagy and F. Szeifert, "Simulation of a batch reactor and its monofluid heating-cooling system", *8th Meeting of Young Chemical Engineers*, Zagreb, Croatia, 2010.

14. M. G. Balaton, L. Nagy and F. Szeifert, "Simulation of a batch reactor and its monofluid heating-cooling system", *APS Forum*, Balatonfüred, 2010.

15. M. G. Balaton, L. Nagy and F. Szeifert, "Controlling the jacket side temperature of a batch reactor", *9th Meeting of Young Chemical Engineers*, Zagreb, Croatia, 2012.

16. M. G. Balaton, L. Nagy and F. Szeifert, "Controlling the jacket side temperature of a batch reactor using a thermoblock with three different temperature levels", *CAPE Forum 2012 Computer Aided Process Engineering*, Veszprém, 2012.

References

[1] D. W. Green and R. H. Perry, *Perry's Chemical Engineers' Handbook*, 7th edition, McGraw-Hill, 1997.

[2] P. Sawyer, *Computer-Controlled Batch Processing*, IChemE, 1993.

[3] D. Bonvin, "Optimal operation of batch reactors – a personal view", *Journal of Process Control*, vol. 8, no. 5 6, pp. 355-368, 1998.

[4] S. Erdoğan, M. Alpbaz and A. R. Karagöz, "The effect of operational conditions on the performance of batch polymerization reactor control", *Chemical Engineering Journal*, vol. 86, no. 3, pp. 259-268, 2002.

[5] M. Friedrich and R. Perne, "Design and Control of Batch Reactors – An Industrial Viewpoint", *Computers & Chemical Engineering*, vol. 19, pp. S357-S368, 1995.

[6] J. E. Edwards, "Dynamic modelling of batch reactors & batch distillation", Paper presented at the Batch Reactor Systems Technology Symposium, Teesside, October 2001.

[7] Z. Louleh, M. Cabassud and M. V. Le Lann, "A new strategy for temperature control of batch reactors: experimental application", *Chemical Engineering Journal*, vol. 75, no. 1, pp. 11-20, 1999.

[8] Aningas S.A., "Monofluid System Heating/Cooling + 360°C/-30°C", 2012, Available at: www.aningas.com/ing/monofluido.html [Accessed 5 May, 2012]

[9] NOXMAN, S.A, "Thermal Fluids Flowtherm", 2014, Available at: http://noxman.com/en/heat-transfer-tluids-flowtherm.html [Accessed 31 January, 2014]

[10] J. Madár, F. Szeifert, L. Nagy, T. Chován and J. Abonyi, "Tendency model-based improvement of the slave loop in cascade temperature control of batch process units", *Computers & Chemical Engineering*, Vol. 28, Issue 5, pp. 737–744, 2004.

[11] Z. Louleh, M. Cabassud, M. V. Le Lann, A. Chamayou and G. Casamatta, "A new heating-cooling system to improve controllability of batch reactors", *Chemical Engineering Science*, vol. 51, no. 11, pp. 3163-3168, 1996.

[12] H. Bouhenchir, M. Cabassud, M.V. Le Lann and G. Casamatta, "A heating-cooling management to improve controllability of batch reactor equipped with a mono-fluid heating-cooling system", *Computer Aided Chemical Engineering*, vol. 8, pp. 601-606, 2000.

[13] D. R. Lewin, W. D. Seider and J. D. Seader, "Integrated process design instruction", *Computers and Chemical Engineering*, vol. 26, pp. 295–306, 2002.

[14] I. T. Cameron and D. R. Lewin, "Curricular and pedagogical challenges for enhanced graduate attributes in CAPE", *Computers & Chemical Engineering*, vol. 33, no. 10, pp. 1781-1792, 2009.

[15] T. F. Edgar, B. A. Ogunnaike and K. R. Muske, "A global view of graduate process control education", *Computers & Chemical Engineering*, vol. 30, no. 10-12, pp. 1743-1774, 2006.

[16] D. Mahoney, B. Young and W. Svrcek, "A completely real time approach to process control education for process systems engineering students and practitioners", *Computers & Chemical Engineering*, vol. 24, no. 2-7, 1481-1484, 2000.

[17] S. Sundquist, J. Ilme, L. Määttä and I. Turunen, "Using models in different stages of process life-cycle", *Computers & Chemical Engineering*, vol. 24, no. 2-7, pp. 1253-1259, 2000.
[18] J. M. Zaldívar, H. Hernández and C. Barcons, "Development of a mathematical model and a simulator for the analysis and optimisation of batch reactors: Experimental model characterisation using a reaction calorimeter", *Thermochimica Acta*, vol. 289, pp. 267-302, 1996.
[19] B. Bradu, P. Gayet and S.-I. Niculescu, "A process and control simulator for large scale cryogenic plants", *Control Engineering Practice*, vol. 17, pp. 1388–1397, 2009.
[20] Á. Fürcht, T. Kovács and I. Rabi, "Implementation of Operator Training System in the MOL Danube Refinery", *MOL Group Scientific Magazine*, 2008 / 2.
[21] F. Rey, P. Thiabaud and J. Tourdjman, "Operator Training Simulator: Payback and Risk Mitigation" in *Gastech 2008*, Bangkok, Thailand, 2008.
[22] S. H. Yang, L. Yang and C. H. He, "Improve Safety of Industrial Processing Using Dynamic Operator Training Simulators", *Transactions of the Institution of Chemical Engineers*, vol. 79, Part B, pp. 329-338, 2001.
[23] P. W. Seccombe, "The Benefits of Using Dynamic Simulation & Training Systems for Expanding Operator Knowledge and Understanding", White Paper, Invensys Systems Inc., 2010.
[24] D. Petrides, A. Koulouris, C. Siletti, J. O. Jiménez and P. T. Lagonikos, "The Role of Simulation and Scheduling Tools in the Development and Manufacturing of Active Pharmaceutical Ingredients", *Chemical Engineering in the Pharmaceutical Industry*: *R&D to Manufacturing*, New Jersey: John Wiley & Sons, 2010.
[25] A. A. Linninger, S. Chowdhry, V. Bahl, H. Krendl and H. Pinger, "A systems approach to mathematical modeling of industrial processes", *Computers and Chemical Engineering*, vol. 24, pp. 591-598, 2000.
[26] D. P. Petrides, A. Koulouris and P. T. Lagonikos, "The Role of Process Simulation in Pharmaceutical Process Development and Product Commercialization", *Pharmaceutical Engineering*, vol. 22, no. 1, pp. 56-65, 2002.
[27] ProSim Inc., "BatchReactor, Simulation of Batch Chemical Reactors – ProSim – Software Solution", 2011, Available at: http://www.prosim.net/en/batch/kinetic.html [Accessed 11 October, 2011]
[28] T. Chován, "Kinetic modelling for batch process development", Ph.D dissertation, Department of Process Engineering, University of Pannonia, Veszprém, Hungary, 2006.
[29] *UniSim® Design, Operations Guide*, R400 Release, Honeywell International Inc., Canada, 2010.
[30] *UniSim® Design Dynamic Modelling, Reference Guide*, R400 Release, Honeywell International Inc., Canada, 2010.
[31] D. Vasanthi, B. Pranavamoorthy and N. Pappa, "Design of a self-tuning regulator for temperature control of a polymerization reactor", *ISA Transactions*, vol. 51, no. 1, pp. 22–29, 2012.

[32] Control Station Inc., “A Cascade Control Architecture for the Jacketed Stirred Reactor”, 2012, Available at: http://www.controlstation.com/page/187-a-cascade-control-architecture-for-the-jacketed-stirred-reactor [Accessed 30 September, 2012]
[33] B. W. Bequette, S. Holihan and S. Bacher, “Automation and control issues in the design of a pharmaceutical pilot plant”, *Control Engineering Practice*, Vol. 12, Issue 7, pp. 901–908, 2004.
[34] H. Bouhenchir, M. Cabassud and M. V. Le Lann, “Predictive functional control for the temperature control of a chemical batch reactor”, *Computers & Chemical Engineering*, vol. 30, no. 6-7, pp. 1141–1154, 2006.
[35] M. Huzmezan, B. Gough and S. Kovac, “Advanced control of batch reactor temperature”, in *Proceedings of the American Control Conference*, vol. 2, pp. 1156-1161, 2002.
[36] F. Szeifert, L. Nagy and T. Chovan, “PID és modell alapú szabályozó algoritmusok a DCS folyamatirányító rendszerekben”, Presented in *DCS Distributed Control Systems 7th Meeting*, Lillafüred, Hungary, 2001.
[37] K .J. Åström, T. Hägglund, C. C. Hang and W. K. Ho, “Automatic Tuning and Adaption for PID Controllers – A Survey”, *Control Eng. Practice*, vol. 1, no. 4, pp. 699-714, 1993.
[38] A. I. Dounis, P. Kofinas, C. Alafodimos and D. Tseles, “Adaptive fuzzy gain scheduling PID controller for maximum power point tracking of photovoltaic system”, *Renewable Energy*, vol. 60, pp. 202-214, 2013.
[39] C.-H. Lee and C.-C. Teng, “Calculation of PID controller parameters by using a fuzzy neural network”, *ISA Transactions*, vol. 42, pp. 391–400, 2003.
[40] G. Karer, I. Škrjanc, B. Zupančič, “Self-adaptive predictive functional control of the temperature in an exothermic batch reactor”, *Chemical Engineering and Processing: Process Intensification*, vol. 47, no. 12, pp. 2379-2385, 2008.
[41] C. T. Chen and S. T. Peng, “A Simple Adaptive Control Strategy for Temperature Trajectory Tracking in Batch Processes”, *The Canadian Journal of Chemical Engineering*, vol. 76, pp. 1118-1126, 1998.
[42] W. Cho, T. F. Edgar and J. Lee, “Iterative Learning Dual-Mode Control of Exothermic Batch Reactors”, in *Proceedings of 5th Asian Control Conference*, Melbourne, Australia, 2004.
[43] E. Ekpo and I. Mujtaba, “Performance Analysis of Three Controllers for the Polymerisation of Styrene in a Batch Reactor”, *Chemical Product and Process Modeling*, vol. 2, no.1, 2007.
[44] *Profit Design Studio – Product Information Note*, Honeywell International Inc., 2010, Available at: https://www.honeywellprocess.com/library/marketing/notes/ProfitDesignStudioPIN2010eop.pdf [Accessed: 9 December, 2013]
[45] M. A. Hussain and L. S. Kershenbaum, “Implementation of an Inverse-Model-Based Control Strategy Using Neural Networks on a Partially Simulated Exothermic Reactor”, *Chemical Engineering Research and Design*, vol. 78, no. 2, pp. 299-311, 2000.

[46] X. Zhao, S. Xu and H. Zhou, “A New Strategy For Batch Reactor’s Temperature Control”, in *Proceedings of World Congress on Computer Science and Information Engineering*, vol. 5, pp. 56-61, Los Angeles, California, 2009.
[47] T. Xie, T. Gong, T. Ye, D. Huang, “Intelligent hybrid temperature control of the BSTR based on the SIMATIC PCS7”, in *Proceedings of the 7th World Congress on Intelligent Control and Automation*, pp. 7931-7935, Chongqing, China, 2008.
[48] A. Egedy, T. Varga and T. Chován, “Examination of temperature probe setup using computational fluid dynamics simulators”, in *Proceedings of Conference of Chemical Engineering 2012*, Veszprém, Hungary, pp. 78-84, 2012.
[49] A. E. Eiben and J.E. Smith, *Introduction to Evolutionary Computing*, 2nd printing, SpringerVerlag, 2007.
[50] N. Hansen, “Invariance, self-adaptation and correlated mutations in evolution strategies”, in *Proceedings of the 6th International Conference on Parallel Problem Solving from Nature*, Paris, France, 2000, pp. 355-364.
[51] N. Hansen, “References to CMA-ES applications”, Available at: https://www.lri.fr/~hansen/ [Accessed 31 January, 2014]
[52] T. Varga, F. Szeifert and J. Abonyi, “Evolutionary Strategy for Feeding Trajectory Optimization of Fed-batch Reactors”, *Acta Polytechnica Hungarica*, vol. 4, no. 4, pp. 121-131, 2007.
[53] A. Aspelund, T. Gundersen, J. Myklebust, M. P Nowak and A. Tomasgard, “An optimization-simulation model for a simple LNG process”, *Computers & Chemical Engineering*, vol. 34, no. 10, pp. 1606-1617, 2010.
[54] J. M. Coulson and J. F. Richardson, *Chemical Engineering*, vol. 1, Fluid Flow, Heat Transfer and Mass Transfer, Oxford: Pergamon Press, 1990.
[55] M. G. Balaton, L. Nagy and F. Szeifert, “OTS System Development for a Batch Process Unit”, in *Proceedings of 2nd International Scientific Workshop on DCS*, Lillafüred, Hungary, 2011, pp. 13-20.
[56] F. Szeifert, F. Nagy, T. Chován and J. Abonyi, “Constrained PI(D) algorithms (C-PID)”, *Hungarian Journal of Industrial Chemistry,* , vol. 33, no. 1-2, pp. 81-88, 2005.